Heterogeneity of Photosystem II as it Occurs in Domain Specific Regions of the Thylakoid Membrane of Spinach (*Spinacia oleracia L.*)

Michael D. McConnell B.Sc. (Hon)
Department of Biological Sciences

Submitted to the Department of Biological Sciences
in partial fulfillment of the requirements of the degree of
Master of Science

Brock University
St. Catharines, Ontario

The end is apparent in every beginning, yet, only by knowing the whole story do we come to understand it. This is the pleasure of life.

David Weaver, 2000.

I. Abstract

Thylakoid membrane fractions were prepared from specific regions of thylakoid membranes of spinach (*Spinacia oleracea*). These fractions, which include grana (B3), stroma (T3), grana core (BS), margins (Ma) and purified stroma (Y100) were prepared using a non-detergent method including a mild sonication and aqueous two-phase partitioning.

The significance of PSIIα and PSIIβ centres have been described extensively in the literature. Previous work has characterized two types of PSII centres which are proposed to exist in different regions of the thylakoid membrane. α-centres are suggested to aggregate in stacked regions of grana whereas β-centres are located in unstacked regions of stroma lamellae.

The goal of this study is to characterize photosystem II from the isolated membrane vesicles representing different regions of the higher plant thylakoid membrane. The low temperature absorption spectra have been deconvoluted via Gaussian decomposition to estimate the relative sub-components that contribute to each fractions signature absorption spectrum. The relative sizes of the functional PSII antenna and the fluorescence induction kinetics were measured and used to determine the relative contributions of PSIIα and PSIIβ to each fraction. Picosecond chlorophyll fluorescence decay kinetics were collected for each fraction to characterize and gain insight into excitation energy transfer and primary electron transport in PSIIα and PSIIβ centres.

The results presented here clearly illustrate the widely held notions of PSII/PSI and PSIIα/PSIIβ spatial separation. This study suggests that chlorophyll fluorescence decay lifetimes of PSIIβ centres are shorter than those of PSIIα centres and, at F_M, the longer lived of the two PSII components renders a larger yield in PSIIα-rich fractions, but smaller in PSIIβ-rich fractions.

II. Acknowledgments

There are a number of people present at Brock University who deserve many thanks. The Brock Electronic and Machine Shops have been a constant source solutions for the Bruce lab. This project was enhanced greatly for having their assistance. The same sort of thanks are deserved by my lab mates. To do no one any injustice, I will leave out all of their names. None off them are insignificant by any means however, as soon as I begin to list them I become flustered because they all deserve to be mentioned first and foremost. They are well aware of who they are, and I hope they are also aware of how important they have been for the last two years. I thank my examiners (both internal and external) and advisors for their time and guidance during this project.

There are also a small group of people outside of Brock, some I have never met, that made this project possible. The Photosynthesis Group at Lunds Universitet, Lund, Sweden do this amazing thing with Spinach that you'll have to read further to find out about. Fikret Mamedov, Ravi Danielsson and Stenbjorn Styring provided not only the special spinach thylakoids for this project, but loads of enthusiasm and kindness to help its success.

I can never be able to pay my parents back for their decision to have me stay around for the last two years to complete this very important job.

There are three more people that are involved in this project that pushed it towards the checkered flag. The first is not even aware that she is part of this project. Christine Dobbin now knows more about photosynthesis than any other person outside the field, and she doesn't even know it! That poor girl put up with my random babbling about reaction centres, antennae, and broken down β-centres and appeared to enjoy it. She is bright and beautiful, a deadly combination!

The other two are of course Doug Bruce and Sergej Vasil'ev. In an effort to supervise a successful master's degree candidate, these two men have manage somehow helped put me in a position to become one of them. Scary? Not really. I admire them for their wisdom, enthusiasm, generosity and most of all their positive role in my life, to help me figure out my own way in this exciting field of intriguing pursuits and bold discoveries.

III. Table of Contents

IV. List of Figures

V. List of Tables

VI. List of Abbreviations

α-DM - *n*-dodecyl-α,D-maltoside
a.u. - arbitrary units
B3 - grana thylakoid membrane fraction
BBY - photosystem II-enriched preparation made according to Berthold *et al.*, 1981
BChl - bacteriochlorophyll
BS - grana core thylakoid membrane fraction
CCI - core complex I
CCII - core complex II
CF_0 - a coupling factor
CF_1 - a coupling factor
Chl *a* - chlorophyll *a*
Chl *b* - chlorophyll *b*
Chl_z - accessory reaction centre Chl *a*, bound to a tyrosine residue
cyt b_6/f - cytochrome b_6-cytochrome *f* complex
DAS - decay associated spectra
DCMU - 3-(3,4,-dichlorophenly)-1,1-dimethlyurea
F_0 - minimal level of fluorescence
F_M - maximal level of fluorescence
F_{SAT} - fluorescence yield after a single saturation flash
F_V - variable fluorescence (F_M - F_0)
Fd - ferredoxin
FNR - ferredoxin-$NADP^+$ reductase
HEPES - *N*-2-hydroxyethylpiperazine-*N*'-ethanesulfonic acid
LHCI - light-harvesting complex I
LHCII - light-harvesting complex II
Ma - grana margins thylakoid membrane fraction
OEE - oxygen-evolution enhancer
P680 - photosystem II reaction centre
P700 - photosystem I reaction centre
PC - plastocyanin
Pheo - pheophytin
PMF - proton motive force
PQ - plastoquinone
PSI- photosystem I
PSIα - photosystem I alpha centre
PSIβ - photosystem I beta centre
PSII - photosystem II
PSIIα - photosystem II alpha
PSIIβ - photosystem II beta
Q_A - first bound plastoquinone acceptor
Q_B - second semi-bound plastoquinone acceptor
qE - energy-dependent quenching
qI - photoinhibitory quenching
qN - nonphotochemical quenching
qP - photochemical quenching
qT - state transitions
R_0 - critical distance for Förster transfer measured in Å
rubisco - ribulose bisphosphate carboxylase/oxygenase
T3 - stroma lamellae thylakoid membrane fraction
Y100 - purified stroma lamellae thylakoid membrane fraction

1. Introduction

Chloroplasts are the energy converting organelles of higher plants. Chloroplasts not only contain the earth's most abundant soluble enzyme, ribulose bisphosphate carboxylase/oxygenase (rubisco), but also the most abundant biological membrane, the photosynthetic membrane known as the thylakoid. Thylakoid membranes, like all biological membranes, are fluid-mosaic structures in which lipid bilayers act as two-dimensional fluids (Singer and Nicolson 1972). Proteins and protein complexes may diffuse freely within its structure, both rotationally and laterally. The light reactions of photosynthesis take place in and across the thylakoid membrane, The word thylakoid comes from the Greek, "ΘΨΛΑΚΟΕΙΔΗΣ", meaning sac-like. The sac-like grana region in higher plants occur in stacked, or appressed membrane regions joined by unstacked, or unappressed stroma lamellae. Four major components of the plant thylakoid membrane are the light-driven photosystems I and II (PSI and PSII), a cytochrome b_6/f (cyt b_6-f) complex and an ATP synthase. Each of these components are intimately involved, in series, in the light reactions of electron transport and proton pumping in cooperation with mobile carriers to liberate electrons from water, which ultimately reduce $NADP^+$, to form NADPH, stored chemical energy (Albertsson 2001; Barber 1990; Menke 1962).

Some contemporary insights into thylakoid membrane biomass have estimated that 1 μg of chlorophyll corresponds to 16.7 cm^2 of plant surface. This value may be highly variable and is indeed species specific (Barber 1990). The thylakoid membranes employed in a typical leaf occupy a total surface area 600 to 1000 times greater than this area . Barber states, "I think there is little doubt that the thylakoid membrane is the most abundant biologically active lipo-protein structure on our planet!" (Barber 1990).

Upon examination of the dynamic architecture of the thylakoid membrane, its mystery begins to reveal itself. About twenty years ago it was first noted that the two light driven pigment-protein complexes are spatially separated within thylakoid membranes of higher plants (Anderson and Melis 1983). This regional segregation surprised many researchers since these photosystems operated in series (Hill 1937; Hill and Bendall 1960).

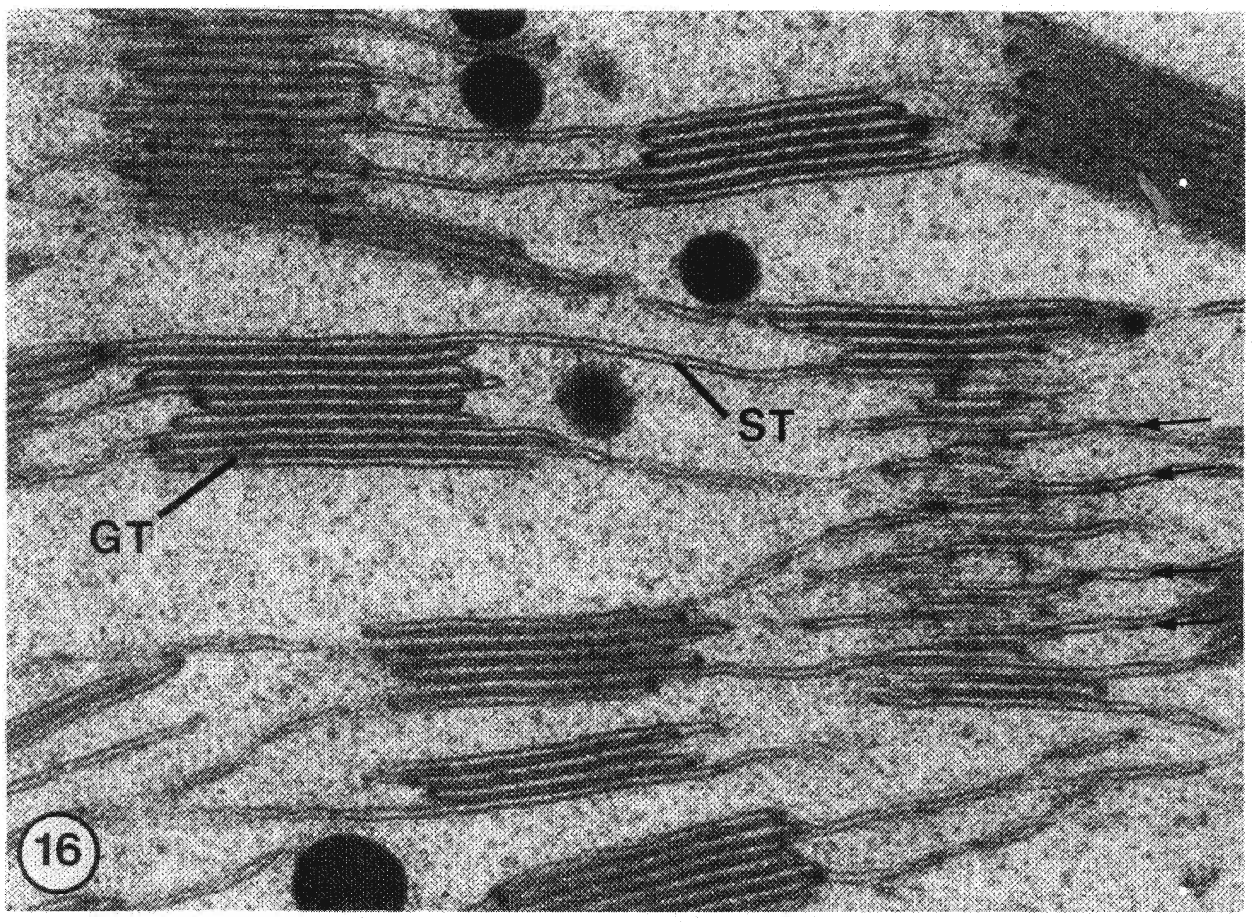

Figure 1 - Electron micrograph of thylakoid membranes (80,000x). Grana appears as flattened stacked discs (GT), connected by unstacked stroma lamellae (ST) (Staehelin 1986).

Clearly, thylakoid membranes of green plants are some of the most complex and dynamic membrane systems in biology (Staehelin and van der Staay 1996).

Photosynthetic systems and assemblies are most commonly studied by one of three preparation types. Intact systems offer insight into real processes that may occur under physiological conditions. Commonly, these experiments employ cyanobacteria, green algae or intact chloroplasts. Intact chloroplasts may be within the leaf, in protoplasts or carefully isolated from the other plant material. These organisms are well suited for photosynthesis research on multiple levels because of the extensive homology that exists among cyanobacteria, green algae and higher plants. These similarities are likely the results of evolutionary endosymbiosis several millions of years ago.

Semi-intact systems are the most widely used preparations for biophysical studies of higher plants. Intact thylakoid membranes can very easily be harvested from whole leaves and assayed for photosynthetic activity in ways very similar to those employed in experiments utilizing intact systems. The variable fluorescence yield, a commonly measured character, collected from isolated thylakoid membranes may be somewhat smaller in magnitude, but nonetheless, the data obtained from this very abundant source of plant material remains tremendously valuable.

The third, and most labour intensive preparation type used to study photosynthesis involves the further dissection of semi-intact systems to their individual components. Some decades ago, researchers began to design specialized isolation procedures to effectively zoom in on specific pigment-protein complexes, or individual proteins, derived from intact thylakoid membranes, harvested from the chloroplasts of higher plants or cyanobacteria. The use of such systems is widespread in the field. These localized components have allowed investigators to answer very specific questions surrounding the activities, or inactivities of countless components essential to light-driven electron transport and chemical energy accumulation. In combination with recombinant DNA techniques, the knowledge of photosynthetic systems has met with unparalleled growth. Random knock-outs and site-directed mutagenesis have allowed researchers to probe specific genes that are intimately involved in photosynthetic processes. It is now possible to assay the

biophysical characteristics of photosynthesis in the absence and/or up-regulation of a wide variety of genes in model organisms such as *Synechocystis* sp. PCC 6803, a commonly used cyanobacterium (Kaneko *et al.* 1996; Tabata and Ikeuchi 2001; Vermaas 1998), *Chlamydomonas reinhardtii*, a single celled eukaryotic green alga, (Kindle 1998; Nedelcu and Lee 1998; Silflow 1998) and *Arabidopsis thaliana*, a higher plant (Arabidopsis Genome Initiative 2000; Barkan 1998; Jansson 1999; Wakasugi *et al.* 2001), where the entire genomes (including the chloroplasts genome where appropriate, see Hiratsuka *et al.* 1989 for example) has been sequenced and mapped.

This study involves a thorough biophysical study of the photosynthetic apparatus of the higher plant *Spinacia oleracea* L., commonly referred to as spinach. The method employs an advanced separation technique whereby chloroplast derived thylakoid membranes are subjected to a mild sonication followed by an aqueous two-layer partitioning (Albertsson 1986; Albertsson *et al.* 1994; Åkerlund and Albertsson 1994). The uniqueness of this technique lies in its detergent free nature. In the past, thylakoid fractions rich in one pigment-protein complex or another were prepared solely by detergent dependent isolations (Berthold *et al.* 1981). Certainty that the complexes of interest are maintained in their native form is reduced upon the introduction of detergents. Thylakoid membranes from *Nicotiana tabacum* (tobacco) chloroplasts (Gadjieva *et al.* 1999) and the green algae *Dunaliella salina* (Stefánsson *et al.* 1997) have also been successfully fractionated using the relatively non-invasive detergent-free technique. This exciting method is not limited to thylakoid membranes. It has also proven to be useful in the specific domain isolation of plasma membrane and smooth endoplasmic reticulum from mammalian liver cells (Gierow 1994; López-Pérez *et al.* 1981).

This study employed five unique thylakoid membrane fractions. These included grana, stroma lamellae, grana core, grana margins and a special purified stroma lamellae. The spatial distribution of different types of PSII reaction centres, hereon referred to as PSIIα and PSIIβ centres (the foci of this study), is well documented. PSIIα centres are reported to aggregate within the stacked regions of grana, whereas PSIIβ centres are located within the unstacked stroma

lamellae (Albertsson *et al.* 1990b; Albertsson *et al.* 1991; Albertsson *et al.* 1994). This allows, with considerable certainty, measurements to be obtained from functional PSII centres of either α- or β-variety separately and clearly.

This study is a multifaceted and comprehensive pursuit of the characterisation of PSII heterogeneity. It is unique in that the plant material employed in these experiments has been mechanically derived from the thylakoid membranes of spinach without using detergents (Albertsson 1986; Albertsson *et al.* 1990b; Albertsson and Svensson 1988; Svensson *et al.* 1990). This is one of the key elements to this study. The detergent free isolation procedure offers confidence in the native state of the preparations. For the first time, PSIIα from appressed grana regions and PSIIβ from unappressed stroma exposed regions of higher plant thylakoid membranes are studied using the techniques described here. Spatial separation of the two PSI and PSII, as well as PSIIα and PSIIβ will be demonstrated using a variety of biophysical techniques including: absorption spectroscopy, 77K fluorescence emission spectroscopy, fluorescence induction kinetics and PSII absorbance cross section analyses. The picosecond chlorophyll fluorescence decay kinetics and their global analysis provide insight into primary processes of photosynthesis with respect to PSII heterogeneity.

2. Literature Review

2.1. Photosynthesis

Photosynthesis is the process by which sunlight fuels a series of redox reactions to produce stored chemical energy where breathable oxygen is a byproduct. A very simplified summary of the entire process is demonstrated in Saussure's equation (1).

$$6CO_2 + 6H_2O \xrightarrow{h\nu} C_6H_{12}O_6 + 6O_2 \quad (1)$$

The sunlight available to plants is approximately 2 $mE \cdot m^{-2} \cdot s^{-1}$ considering only radiation involved actively in photosynthesis, a considerably small amount relative to the gross amount of solar radiation that is cast towards the earth (Mauzerall and Greenbaum 1989). The portion of this light employed by any given plant, or photosynthetic bacteria, is dependent upon the type(s) of pigments they harbour. Since each pigment type may preferentially absorb from different regions of the spectrum, an organism that employs a wider range of pigments may, hypothetically, make use of a larger portion of the radiant energy available.

2.1.1. The Light Reactions

Water is split by a light-catalysed process which occurs in the lumen of the thylakoid membrane. The liberation of an electron from water, coupled with the evolution of O_2 by the Mn-cluster (Kok *et al.* 1970) is the primary step in oxygenic photosynthesis. The instability of the PSII reaction centre in its oxidized excited state offers it a unique ability. Simply put, PSII's ability to oxidize water is a direct consequence of the high oxidizing potential of the oxidized reaction centre special pair, $P680^+$ (Durrant *et al.* 1995). To reach $P680^+$, the electron is passed by one other intermediate carrier, Y_z (a tyrosine radical), the primary donor. The special pair of chlorophylls, P680, is the terminal acceptor of absorbed excitation energy by the PSII-antenna in higher plants. It is here that the electron is excited. Excited $P680^*$ performs a charge separation ($P680^+ \bullet Pheo^- \bullet Q_A$) upon reduction of pheophytin (Pheo), a pigment molecule similar to Chl *a*, without the central Mg atom;

$$P680 + Pheo + h\nu \xrightarrow{3ps} P680^+ + Pheo^- \quad (2)$$

followed by a charge stabilization, ($P680^+ \bullet Pheo \bullet Q_A^-$). Charge stabilization is achieved by the further movement one electron at a time to Q_A. Both charge separation and charge stabilization are energetically favourable reactions however Q_A reduction is more stable (or less reversible) since the movement of the electron is further removed from $P680^+$ (Hara *et al.* 1997). The two-electron gate allows Q_B to be reduced to the semiquinone in one step, then to plastoquinol on the second:

$$2H_2O + 4photons + 2PQ + 4H^+ \longrightarrow O_2 + 4H^+ + 2PQH_2 \quad (3)$$

The Q_B site must stabilize the semiquinone since it is usually very unstable and reactive. Upon reduction by PQH_2, the cytochrome b_6 (also called *cyt b563*) - cytochrome *f* (for *frons* or leaf) complex, abbreviated *cyt* b_6-*f*, is then able to reduce a small copper-containing protein, plastocyanin (PC), a mobile carrier,

$$2PQH_2 + 4PC(Cu^{2+}) \longrightarrow 2PQ + 4PC(Cu^+) + 4H^+ \quad (4)$$

which is subsequently oxidized by the P700 reaction centre within the lumen of the thylakoid.

LHCI, the major antenna system of PSI, delivers absorbed excitation energy by inductive resonance from its 100 chlorophylls to the P700 reaction centre. Excited P700 reduces A_0, a Chl *a* molecule;

$$P700 + Chla + h\nu \longrightarrow P700^+ + Chla^- \quad (5)$$

followed by the reduction of A_1, phylloquinone (vitamin K_1). F_X, an iron-sulphur group (with a 4Fe-4S centre similar to the 2Fe-2S group of *cyt* b_6-*f*) is able only to pick up a single electron at a time, even though four centres are present. Electrons are transferred to a soluble form of Fe-S protein, ferredoxin (Fd):

$$h\nu + 4PC(Cu^+) + 4Fd(Fe^{3+}) \longrightarrow 4PC(Cu^{2+}) + 4Fd(Fe^{2+}) \quad (6)$$

In the stroma ferredoxin-$NADP^+$ reductase (FNR) catalyses the oxidation of mobile ferredoxin by NADP to form NADPH:

$$4Fd(Fe^{2+}) + 2NADP^{+} + 2H^{+} \longrightarrow 4Fd(Fe^{3+}) + 2NADPH \qquad (7)$$

ADP (+ *Pi*) is converted to ATP and H_2O by the coupling factor, ATPase. The CF_0 subunit extends through the hydrophobic region of the thylakoid and the CF_1 subunit is attached on the stromal side. Protons generated by the hydrolysis of H_2O and the oxidation of PQH_2 are pumped out of the lumen through CF_0, towards CF_1 where ADP is phosphorylated in the stroma. These reactions are summarized in the z-scheme diagram in figure 3 (Salisbury and Ross 1992). NADPH and ATP produced during these reactions are used to reduce CO_2 to carbohydrates in the subsequent dark reactions (figure 2).

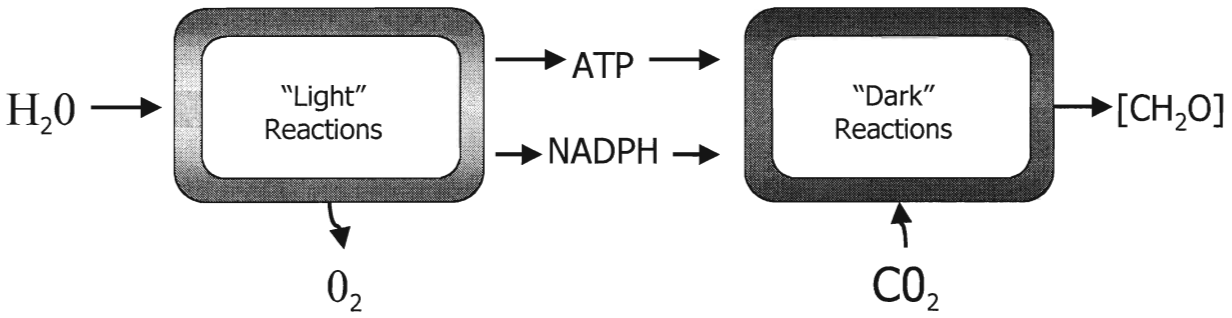

Figure 2 - The relationship between the "light" reactions and the "dark" reactions of photosynthesis.

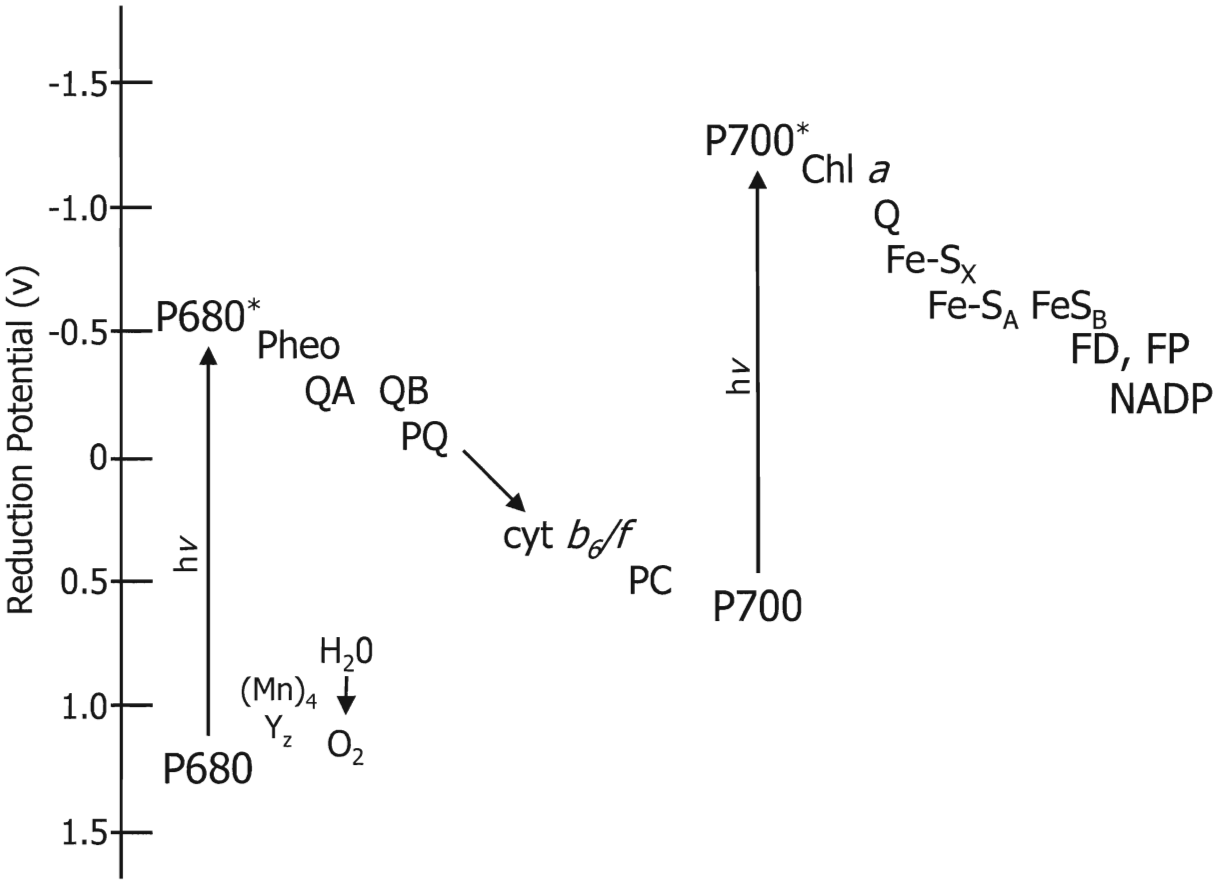

Figure 3 - Summary of the light-driven electron transport events within thylakoid membranes, commonly called the z-scheme. The reduction potential of each carrier indicates a higher affinity for electrons as it becomes increasingly positive (Zubay 1993).

2.2. Thylakoid Membrane Architecture

The thylakoid membranes within the chloroplasts of higher plants are functionally similar to those of cyanobacteria, which are suspected to be their ancestors via endosymbiosis many millions of years ago. Chloroplasts typically measure 5 μm in diameter and are 1 to 2 μm thick. In mature leaf cells these green photosynthetically active plastids occupy only 20% of the cellular volume but they may occupy up to 70% of the surface area (Ellis and Leech 1985). Like mitochondria, these organelles contain their own circular genome, however many of the genes coding for photosynthetic proteins have been translocated to the nucleus. Much of what is left functions primarily in fatty acid synthesis (Waller *et al.* 1998). Chloroplasts divide by binary fission, a process that closely resembles bacterial cell division morphologically and genetically (Leech 1976; Whatley 1988). The principal determinant leading to the number of chloroplasts that may occur in a leaf mesophyll cell is its size (Dean and Leech 1982). Furthermore, evidence suggests that chloroplasts may only appear once a critical cell size in attained (Ellis *et al.* 1983). A recent study with respect to chloroplast size revealed that employment of many small chloroplasts may be more advantageous to mature higher plants than fewer large ones. Small chloroplasts are more mobile within the cell than large chloroplasts. Movement within the cytoplasm of leaf cells offers 1) a means of protection from photodamage to the photosynthetic apparatus under excess light conditions and 2) enhances efficient utilization of low-incident photon flux densities (Jeong *et al.* 2002). Chloroplast movement, with respect to light conditions, is a process known as phototaxis.

Many components of the thylakoid membranes have been remarkably conserved between cyanobacteria and higher plants through evolution with respect to their structure and function. For this reason many studies regarding the biophysical and photochemical properties of the process of photosynthesis apply to both prokaryotic and eukaryotic systems, regardless of the organism used in the laboratory. The main difference lies in the relative organization of their macrodomains. Whereas many cyanobacteria arrange concentric layers of thylakoid membranes within their prokaryotic cellular interior, the thylakoid membranes within the chloroplasts of most eukaryotic higher plants are arranged in regions of stacked (or appressed) grana and unstacked (or

unappressed) stroma lamellae. The ratio of stacked to unstacked membrane regions is variable and depends primarily upon growth conditions (Staehelin 1986). Under low light conditions, grana have larger diameters and make up a larger proportion of the thylakoid membrane area. For example, it is reported that at higher light intensities, *Zea mays* mesophyll chloroplasts contain 61% stacked regions and an average granum diameter of 0.35 μm, however at lower light intensities the stacked regions make up 73% of the thylakoid architecture and grana measure 0.43 μm on average (Staehelin 1986).

The formation of grana has been well documented. Thylakoid membrane appressions occur between regions of the membrane where the Coulombic repulsive forces between two adjacent membrane surfaces are decreased (Dahlin *et al.* 1990). Coulomb's law states that the magnitude of the electrostatic force exerted by one point charge on the other point charge is directly proportional to the magnitudes of the charges and inversely proportional to the square of the distant between them. At high salt concentrations (>5 mM) the electrostatic screening of surface negative charges is improved so reduced coulombic repulsion permits thylakoid membrane stacking and a concomitant phase separation of membrane complexes based on differential surface charge densities (Barber 1990). The method of thylakoid membrane vesicle separation used in this study takes advantage of this fundamental property of appressed grana and nonappressed stroma lamellae. Since one photosystem (and its associated antenna) has a greater net surface charge density than the other it is believed that the phenomenon of spatial separation may rest on this parameter. Reversible changes in the degree of stacking are induced by changes in cation concentration. Trivalent cations are more effective than divalent cations which are more effective than monovalent cations (Horton 1999). These changes greatly influence the chlorophyll fluorescence yield, even when photochemical activity is blocked by presence of a herbicide. At low salt levels, where the electrostatic screening is lowest, a reduction of the fluorescence yield occurs since lateral intermixing of all complexes allows efficient energy transfer between the photosystems (Armond *et al.* 1976; Barber 1990; Newell *et al.* 1987).

Membrane appression occurs not only among the stroma exposed surface of the grana

partition, but also within the lumen of the thylakoid membranes therein. Attractive forces between two opposing inner surfaces keep them within close contact (Albertsson 1982). This space is loaded with proteins, including lumenally exposed portions of intrinsic membrane proteins and soluble ones as well (Bricker *et al.* 2001; Kieselbach *et al.* 1998). The functional role of grana stacking is not completely understood. Some early studies suggested that formation of grana may be required to activate photosystem II (PSII) (Arnzten and Briantais 1975). Evidence contrary to these ideas was revealed when algal mutants, deficient in grana, where shown to be photochemically competent (Goodenough *et al.* 1969; Goodenough and Staehelin 1971) and with mutants of higher plants which demonstrated high PSII activity while maintaining relatively few appressed membrane regions (Highkin *et al.* 1969; Keck *et al.* 1970; Armond *et al.* 1976). It is suggested however, that the formation and maintenance of grana offer the thylakoid membranes within chloroplasts functional flexibility in terms of a) maximizing the absorption cross-section by densely packing Chl *a* and *b* in large numbers, b) ability to modify the cross-section in both short term (Allen 1992), and long term, acclimation, situations and c) rapidly alter energy quenching upon exposure to excess light to prevent photodamage (Aro *et al.* 1993; Horton 1999).

More than thirty years ago spatial separation of PSI and PSII was described within the thylakoid membranes of higher plants (Anderson and Boardman 1966; Boardman and Anderson 1964). Functional PSII complexes are found predominantly in the appressed membrane regions of grana, where the PSI complex occurs at its lowest frequency. The margins of the grana surrounding the PSII-rich core houses a large proportion of PSI (Anderson and Goodchild 1987). The unappressed stroma regions house different species of PSI and PSII. This special organization of two photosystems is a universal feature of all granal chloroplasts (Arvidsson and Sundby 1999; Garab and Mustárdy 1999; Gunning and Schwartz 1999; Horton 1999; Mehta *et al.* 1999) in spite of the relatively low viscosity of the glycero-lipid phase of the thylakoid membrane which one may suspect may confer a homogenous mixture of all thylakoid components (Graan and Ort 1984; Voet and Voet 1995). The ATP synthase is restricted to stroma exposed regions of the thylakoid membrane (Miller and Staehelin 1976). The size of the CF_1 subunit makes it virtually

impossible for this large coupling factor to squeeze within the appressed membranes of stacked grana (Allen and Forsberg 2001). The advantages and disadvantages of spatial separation of the photosystems will be addressed in section 2.2.3.

2.2.1. Photosystem I - the FeS type reaction centre

Photosystem I (PSI) is an evolutionary product of anoxygenic green photosynthetic bacteria based on bacteriochlorophyll (BChl). The BChl antennae of green bacteria are substantially larger than that of the purple bacteria and their reaction centres perform electron transport in a slightly different way (figure 4). Not until the late 1980s were the fundamental differences revealed among the purple, green and the newly discovered heliobacteria. The reaction centres of both the green sulphur bacteria and the heliobacteria are less complex homodimeric homologs of PSI from higher plants and cyanobacteria (Baymann *et al.* 2001). PSI centres in higher plants do not aggregate into trimers, which they do in cyanobacteria. The PsaL (and possibly PsaI) gene product, which manages this trimerization in cyanobacteria (Schluchter *et al.* 1996), may rather be part of light-harvesting complex I (LHCI) stabilization. This is only one of the key differences surrounding PSI structure between higher plants and cyanobacteria. The structure of PSI will not be discussed in such great detail here (relative to that of PSII, section 2.2.2.), however several important features are described below.

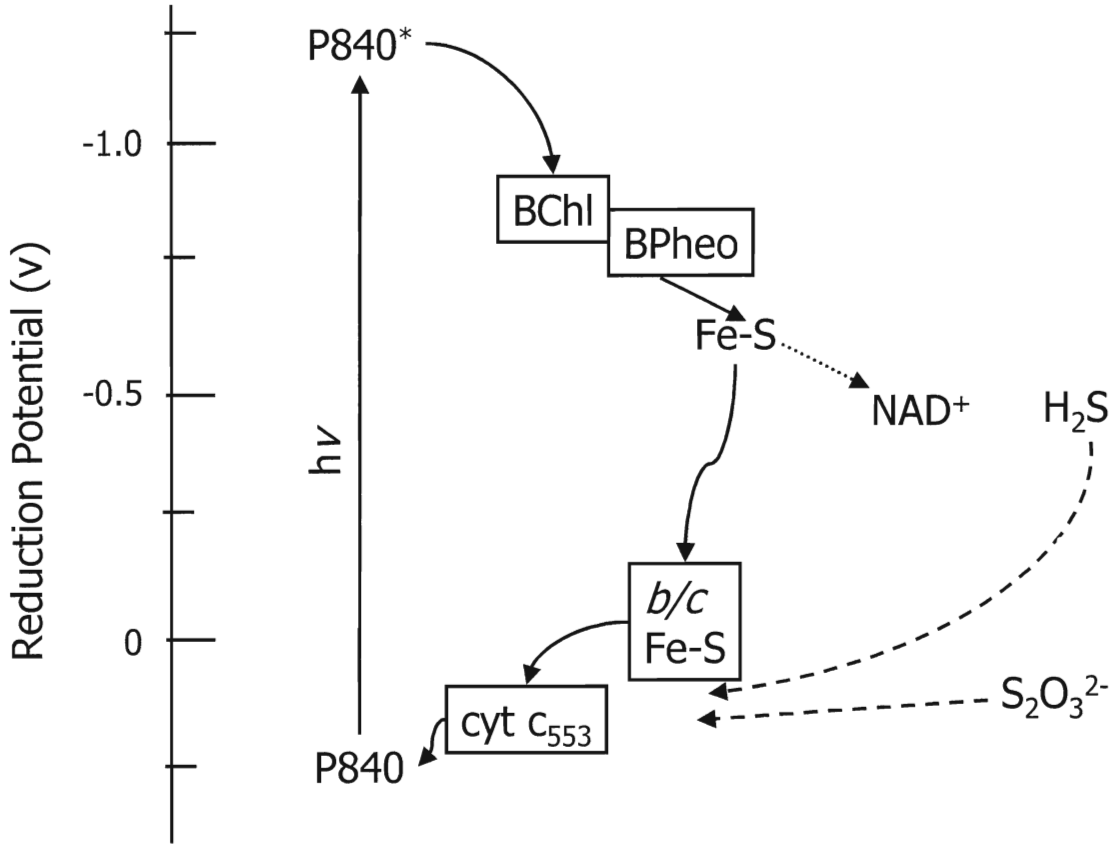

Figure 4 - Green sulphur bacterial photosynthesis. Electrons, originating from sulphur donors are used to reduce NAD+ via light driven ATP cyclic photophosphorylation.

Table 1 - Composition of core complex I and inner antenna of higher plants (Scheller *et al.* 2001).

Gene	Subunit (cofactors)	Mass (kDa)	Function
PsaA	PsaA (~96 Chl *a*, ~22 β-carotene, P700, A_0	83.2	Light-harvesting
PsaB	PsaB (A_1, F_x)	82.4	Charge separation, e^- transport
PsaC	PsaC (F_A, F_B)	8.8	e^- transport
PsaD	PsaD	17.6	Binds ferredoxin, PSI-C
PsaE	PsaE	10.8	Binds ferredoxin and FNR, Cyclic e^- transport
PsaF	PsaF (Chl *a*)	17.5	Binds PC, LHCI-730
PsaG	PsaG (Chl *a*)	10.8	Binds LHCI-680
PsaH	PsaH (Chl *a*)	10.2	Binds LHCII (qT), Stabilizes PSI-D
PsaI	PsaI	4	Stabilizes PSI-L
PsaJ	PsaJ	5	Stabilizes PSI-F
PsaK	PsaK (Chl *a*)	9	Binds LHCI-680
PsaL	PsaL (Chl *a*)	18	Stabilizes PSI-H
PsaN	PsaN	9.8	Stabilizes PC

Table 2 - Light harvesting components of PSI (Scheller *et al.* 2001).

Gene	Subunit*	Mass (kDa)	Function
Lhca1	Lhca1	22	Light-harvesting, LHCI-730
Lhca2	Lhca2	23	Light-harvesting, LHCI-680B
Lhca3	Lhca3	25	Light-harvesting, LHCI-680A
Lhca4	Lhca4	22	Light-harvesting, LHCI-730

* Cofactors bound are ~10 Chl *a*, ~2 Chl *b* and ~3 carotenoids in each subunit.

PSI consists of 17 proteins in higher plants. Those belonging to the core complex (CCI) form one group. The other group, LHCI, is intimately related to CCI. In higher plants the LHCI, consisting of four proteins act as the peripheral antenna, similar to the phycobilisomes present in cyanobacteria, with obvious differences. A summary of the subunits that compose PSI is found in tables 1 and 2.

The PsaL, PsaI and PsaM proteins, located close to the three-fold axis of the PSI-trimer, far from lipid-exposed regions in cyanobacteria (Schmid *et al.* 2001) are the first group. Their function, structural in nature, was proposed several years ago during mutageneic studies, where trimers were unable to form in the absence of PsaL (Kuroiwa *et al.* 2000). PsaL is the primary link between the three monomers, harbouring some hydrophobic carotenoids and three chloropnylls. The PsaI subunit, located between PsaL and PsaM, is involved in trimerization as well. No chlorophyll is bound to PsaI, however it does form hydrophobic contacts with some carotenoids. The interactions between PsaL and PsaI have been conserved over evolution and are maintained in plant systems which employ PSI as a monomer coupled to an elaborate accessory light-harvesting complex. PsaM is the smallest of all PSI subunits (3.4 kDa) and is found in cyanobacteria. Other than its presence as merely an open reading frame in the chloroplast genome of liverwort, PsaM is yet to be found in any plant PSI preparation (Fromme *et al.* 2001).

The three stromal subunits, like the name suggests, do not contain transmembrane helices. PsaC, PsaD and PsaE are involved in docking ferredoxin or flavodoxin. Homologus polypeptide sequences of these proteins occur in green sulphur bacteria and heliobacteria (Baymann *et al.* 2001).

Two large protein subunits, PsaA and PsaB make up the reaction centre of PSI. In green sulphur bacteria, a homodimer of the PscA protein forms the reaction centre. Similarly, a homodimer of the PshA protein forms the reaction centre of heliobacteria. The homology between these transmembrane proteins is well documented (Baymann *et al.* 2001). Along with PsaC, these three proteins are the most essential part of CCI. In the reaction centre of PSI, P700 resides in the PsaA/PsaB heterodimer. As well as the primary electron acceptor A_0 (a Chl *a* molecule), A_1

(phylloquinone), and F_x (a 4Fe-4S cluster). Upon excitation of P700 to its lowest excited state, $P700^*$, primary charge separation occurs in 1- 3 ps as A_0 is reduced. The redox potential of $P700^*$ is highly negative (~-1.3 V) which makes it a strong reductant. Whether P700 occurred as a monomer or dimer in higher plants was the item of some debate fro several years (Ikegami and Itoh 1988) (see (Sétif 1992) for detailed review). Similar to the bacterial reaction centre, the dimerization of the P700 reaction centre was confirmed. However, surprising to most researchers, the P700 special pair does not employ a Chl *a* homodimer, but rather a Chl *a*/*a*' heterodimer. Chl *a*' is the C13' epimer of Chl *a* (Kobayashi *et al.* 1988; Webber and Lubitz 2001). These chlorophylls are separated by 6.3 Å (closer than the bacterial reaction centre special pair) and are found nearest the lumenal side of the thylakoid membrane. They are oriented parallel to each other, perpendicular to the membrane plane, with an interplanar distance of 3.6 Å. A weaker electronic coupling between the π electron systems in P700, relative to the bacterial reaction centre, is a product of only partial overlap of the heterodimeric chlorophyll ring structures (Fromme *et al.* 2001). The terminal electron acceptors F_A and F_B are bound to PsaC (Scheller *et al.* 2001).

A subgroup of polypeptides make up the extrinsic subunits of CCI. These include gene products *PsaD* - *PsaN*. Their functions are listed in table 1 . Most of the subunits of the extrinsic CCI are involved in binding and stabilization of other CCI subunits and/or subunits of the LHCI (Scheller *et al.* 2001).

The LHCI subunits are listed in table 2. The products of four nuclear genes, *Lhca1-4*, compose this peripheral antenna of PSI. Two others, Lhca5 and Lhca6, are present in some species in very low quantities. The LHCI binds about 70-110 chlorophylls with a Chl *a*/*b* ratio of 2.5. The LHCI can be divided into two subcomplexes. The LHCI-730 subcomplex (characterized by its 77K fluorescence emission peak at 730 nm) is formed from the Lhca1/Lhca4 heterodimer. The LHCI-680 sub complex can be further fractionated into LHCI-680A (Lhca3) and LHCI-680B (Lhca2) (Scheller *et al.* 2001; Thornber *et al.* 1991).

Low energy pigments, relative to the reaction centre P700, are present in LHCI, namely those which occur at 735 nm absorbance maximum. Removal of the LHCI reveals a peak 720 nm

emission, attributed to Chl *a* present in the inner antenna of CCI These chlorophylls act as a funnel for excitation energy towards P700 (Scheller *et al.* 2001).

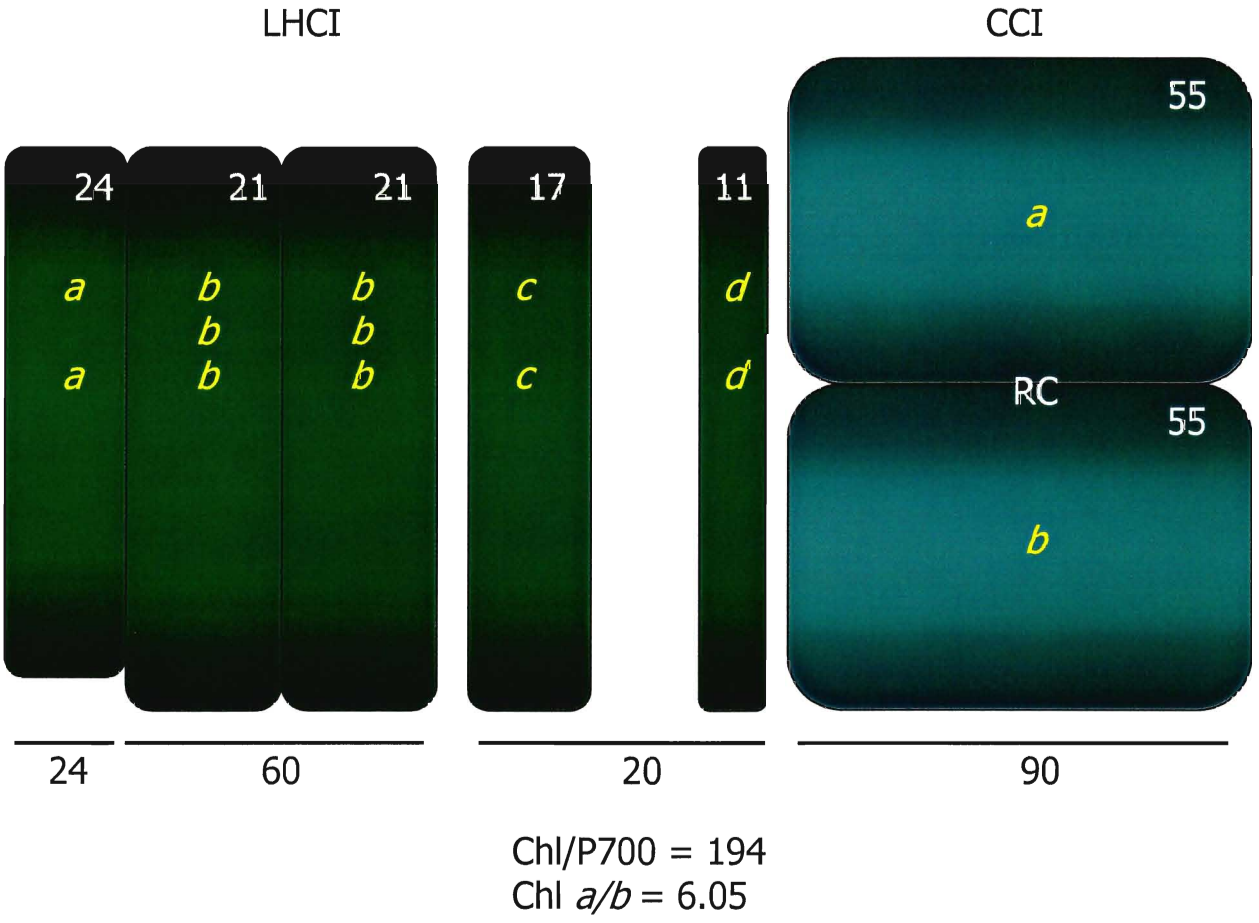

Figure 5 - Model of the pigment-protein distribution of the PSI complex including the light-harvesting complex I (LHCI)and the core complex I (CCI). Molecular weights are shown within the structures, labelled by subunit and sum of the chlorophylls they contain is described beneath (adapted from (Thornber *et al.* 1991)).

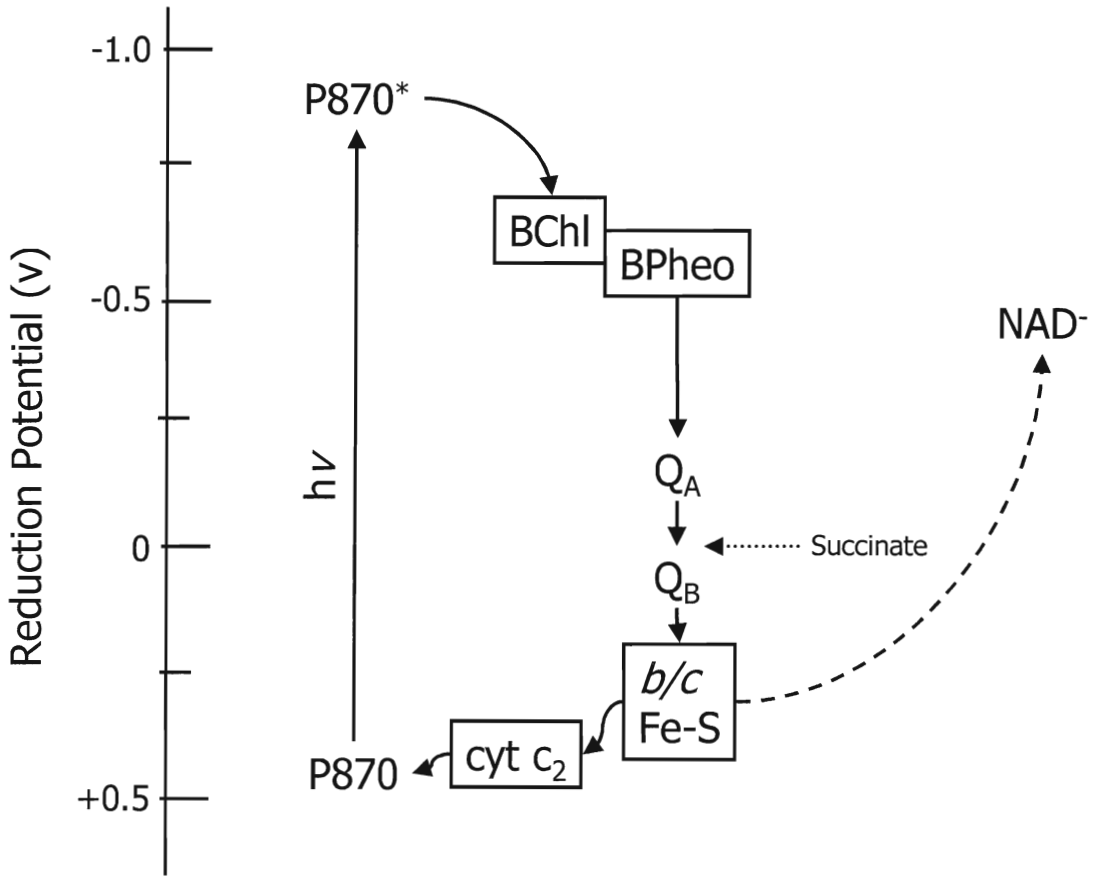

Figure 6 - Simplified schematic of purple nonsulphur bacterial photosynthesis. The oxidation of the electron source succinate precedes the reduction of NAD^+ via light driven electron transport.

2.2.2. Photosystem II - the quinone type reaction centre

Photosystem II (PSII) is an evolutionary product of anoxygenic purple photosynthetic bacteria (figure 6). PSII is, structurally, very similar to the bacterial reaction centre, but spectroscopically and functionally, remains very different (see figure 6). These differences may be correlated with its unique water-oxidizing capabilities and/or its photochemical (and non-photochemical) regulatory functions in order to minimize unwanted and damaging side reactions (Durrant *et al.* 1995). PSII performs a unique and dangerous function in nature. The generation of the strong oxidant, $P680^+$, capable of reaping electrons from energy-poor H_2O sustains all life on earth The pigment-protein complexes of PSII may be split into two related but functionally and spatially separated groups. The one group is comprised of those associated with the light-harvesting complex II and the other, those associated with the core complex II. The number of chlorophylls associated with PSII may vary, and is often species specific, however it is usually greater than 200 chlorophyll molecules make up an entire PSII complex, with a Chl *a/b* of 2.05. This Chl *b* content is relatively high, compared to the number of Chl *b* molecules associated with PSI. The vast majority of these chlorophyll molecules is associated with peripheral light-harvesting complex, the primary light capturing tool of PSII (Bassi *et al.* 1987b). The polypeptides of LHCII are immunologically distinct from those of LHCI associated with PSI (Melis 1991). Six pigment-protein complexes, Lhcb1-6, are aggregated to construct this very large antenna. LHCIIb, the most abundant, harbours 40-45% of the total chlorophyll. 10-15% of the remaining chlorophyll is bound by the other three. Lhcb4 (LHCIIa), encoded by the *Lhcb4* gene, is located relatively close to the core complex and is comprised of at most, only 5% of the chlorophyll. This may include six chl *a*, two chl *b* (Pascal *et al.* 2000). It is present in all species of higher plants and some green algae with small variations in its size, usually ranging from 29 to 31 kDa. Its molecular weight gives it its alternative name, CP29, for chlorophyll-binding protein of 29 kDa. The absorbance spectra (at room temperature) of Lhcb4 has a maximum at 675 nm and a second peak at 645 nm. Xanthophylls, leutin and violoxanthin occur in nearly equal proportions but together, with some small amounts of neoxanthin, are enriched relative to other LHCII subunits (Thornber *et al.* 1991).

Lhcb4 has also been suggested to be the site of energy-dependent quenching (qE) at the E166 residue (Pesaresi *et al.* 1997).

Lhcb5 (LHCIIc), is also called CP26 (a chlorophyll-binding protein of 26-29 kDa, depending on the species). The absorption maximum occurs at 671 nm at room temperature and a 77K fluorescence maximum at 680 nm. Pigment composition assays on LHCIIc reveal that Chl *a* occurs twice as much as Chl *b* (Bassi *et al.* 1987a) and it is relatively enriched in xanthophyll lutein, neoxanthin with smaller amounts of violoxanthin (Thornber *et al.* 1991).

Lhcb6 (CP24) has been suggested to be a linker between the abundant LHCIIb and CCII. Its absorption maximum occurs at 668 nm or 674 nm and has (Bassi *et al.* 1987a). Of the total chlorophyll present in chloroplasts, only 3% is bound to Lhcb6. The xanthophyll lutein is the most prevalent carotenoid with smaller amounts of neoxanthin (lowest of all LHCII subunits) and violoxanthin (Thornber *et al.* 1991).

The most abundant chlorophyll-binding protein of PSII is LHCIIb, which accounts for approximately one-third of the total protein of the chloroplast and about 45% of the chlorophyll. LHCIIb has received much attention since it not only serves as a large chlorophyll-binding protein, but also as a thylakoid membrane adhesion protein and as a mediator of energy transfer between PSII and PSI. LHCIIb is nuclearly encoded by 3 to 16 gene families (species specific) (Thornber *et al.* 1991).

The involvement of LHCIIb in cation-mediated grana stack formation is well documented (Armond *et al.* 1976). Not surprisingly, the appearance of grana in developing thylakoid membranes at various stages parallels the accumulation of LHCIIb. The addition of cations (divalent more so than monovalent) to thylakoid membrane suspensions causes LHCIIb in membrane vesicles to cluster within areas of membrane contact (Horton 1999; McDonnel and Staehelin 1980; Mullet and Arnzten 1980; Ryrie *et al.* 1980).

LHCIIb mediated energy transfer between PSII and PSI is accomplished through phosphorylation/dephosphorylation of this complex. State 1-state 2 transitions (qT), are a photoprotective component of non-photochemical quenching (qN). Under light conditions favouring

PSII absorption, LHCIIb is found in the grana stacks, tightly coupled to the rest of LHCII and PSII, increasing its effective absorbance cross section (Yakovlev *et al.*, 2002) (i.e. state 1). LHCIIb in this form is nonphosphorylated and promotes membrane adhesion. Upon preferential excitation of PSII, LHCIIb becomes phosphorylated by a membrane-bound kinase, consequently, the net negative surface charge on the protein increases. Higher coulombic repulsion causes a slight unstacking of the grana appressed membranes and the phospho-LHCIIb complexes (p-LHCIIb) migrate to nonappressed membrane regions, the stroma lamellae. Upon reversal of these conditions, the dephosphorylation of p-LHCIIb is performed by a membrane-bound phosphatase prior to return to appressed grana membranes and association with PSII. This well-orchestrated redistribution of absorbed excitation energy is reported to be regulated by the redox state of the plastoquinone pool (Allen *et al.* 1981) (see figure z-scheme) and by the cyt b_6/f complex (Bennett *et al.* 1988).

Recently, the *cab80* gene from pea coding for Lhcb was inserted in the cyanobacteria, *Synechocystis* sp. PCC 6803, via the *psb3* promoter on the novel pA31lhcb plasmid. Since cyanobacteria do not employ the large extrinsic light-harvesting complexes similar to higher plants, the protein was very unstable in cyanobacterial thylakoid membranes and has a very short lifetime. Only fragments of the gene product can be see following the addition of xanthophylls (He *et al.* 1999).

Table 3 - Polypeptides of the inner and outer light-harvesting complex of PSII. All are nuclear-encoded (Erickson 1998).

Gene	Subunit	Apparent MW (kDa)	Function
*psb*R	R	10	Donor and acceptor side function
Outer Antenna			
*Lhcb*1	LHCII	30	Light-harvesting+
*Lhcb*2	LHCII	31	Light-harvesting+
*Lhcb*3	LHCIIa	25	Light-harvesting+
Inner Antenna			
*Lhcb*4	CP29	35	Excitation energy transfer and dissipation+
*Lhcb*5	CP26	36	Excitation energy transfer and dissipation+
*Lhcb*6	CP24	18	Excitation energy transfer and dissipation+

+ All light absorptive protein in the LHCII employ chl *a*, chl *b*, lutein, neoxanthin, violaxanthin.

Table 4 - Polypeptides of the oxygen-evolving complex of PSII. All are nuclear-encoded (Erickson 1998).

Gene	Subunit	Apparent MW (kDa)	Function
*psb*O	OEE1	30 (33)	Stabilizes Mn, binds Ca^{2+} and Cl^-
*psb*P	OEE2	20 (23)	Binds Ca^{2+} and Cl^-
*psb*Q	OEE3	18 (16)	Binds Cl^-

The core-complex II (CCII) is comprised of four pigment-proteins which can be equally subdivided into two groups. The first subgroup consists of two pigment-proteins known as CCIIa and CCIIb, the *psbB* and *psbC* gene products respectively. The CCIIa subunit binds ~15 Chl *a* molecules and has an apparent molecular mass of 47 kDa (CP47), however the calculated mass of 56 kDa has been reported for spinach (Barber *et al.* 2000). Two to three β-carotenes are also associated with CP47. Of the 508 amino acid residues that make up the ultimate structure, 200 are present in lumenally exposed loops. An even larger portion of the polypeptide spans the thylakoid membrane six times, where the large hydrophilic loop joins at helices 5-6. The remaining portions occur as two small hydrophilic loops in the stroma that join to helices 2-3 and 4-5 and the stroma exposed N- and C-terminal ends. Evidence that suggests that the large extrinsic protein region binds chlorophyll is poor. Its function is more likely to involve water-splitting processes.

The second subgroup of CCII pigment-proteins make up the PSII reaction centre. The *psb*A and *psb*D gene products, better known as D1 (32 kDa) and D2 (30 kDa). Along with the 9 kDa and 4 kDa polypeptides that assemble to form the cytochrome b_{559} (cyt b_{559}) (Stewart and Brudvig 1998) the reaction centre is complete and houses the 'special pair' chlorophylls, P680.

A third Chl *a* binding subunit of CCII is the *psb*S gene product. This 22 kDa protein (CP22) absorbs well at 674 nm and twice in the blue, at 440 and 468 nm. Some reports indicate that in may also bind Chl *b* with a chl *a*/*b* of 1.6 - 4.3 (Funk *et al.* 1994). 77K fluorescence emission spectra of CP22 reveals a peak at 675 nm. Its role as a PSII subunit may be one of minor light-harvesting. Or, it may bind chlorophylls scavenged from other degraded components of the PSII-supercomplex. Recently, CP22 has been reported to be intimately involved in energy dependent quenching, qE, a component of nonphotochemical quenching, qN (Li *et al.* 2000). Most interestingly, this protein can be immunologically detected in the cyanobacteia, *Synechocystis* sp. PCC 6803 and *Phormidium laminosum*. Some differences among the number of transmembrane helicies, and the presence/absence of chl *b* with respect to species raise some interesting evolutionary questions (Funk *et al.* 1994).

Products of the *psbE* and *psbF* genes are the α and β subunits of the cyt b_{559} complex

respectively. The ultimate function of this complex remains obscure, however it is well known that absence of one or both the subunits inhibits the assembly of PSII. Likely proposals suggest that cyclic electron transfer around PSII may be orchestrated by cyt b_{559} in some way, protecting PSII from photoinhibition (Arnon and Tang 1988; Aro *et al.* 1993; Thompson and Brudvig 1988). Some authors suggest that cyt b_{559} may also be able to donate an electron to Y_Z^+ in the dark, to reduce this dangerous oxidant (Canaani and Havaux 1990). Cross-linking studies have demonstrated the close association of cyt b_{559} to the D1 subunit of the PSII reaction centre (Barbato *et al.* 1992; Stewart and Brudvig 1998). More recently however, high resolution x ray crystal structure suggest that the location of this subunit may be on the opposite side of the reaction centre, nearer the D2 protein (Zouni *et al.* 2001).

The similarities that exists between the P680 (due to a characteristic bleaching observed at 680 nm upon oxidation of this species) reaction centre, the primary electron donor, of higher plants (and cyanobacteria) and the bacterial reaction centre have been well documented (Rochaix *et al.* 1984; Youvan *et al.* 1984). Unlike the reaction centre of purple bacteria, the PSII reaction centre, P680, the chlorin rings of the two special pair Chl *a* molecules ligated to HIS198 on the D1 and D2 proteins may not be parallel to each other. Less overlap between the chlorin rings, at an angle of 30°, causes exciton coupling to be relatively weak, however, charge separation is twice as efficient. The consequence of weak exciton coupling is actually two-fold. First, P680 is a relatively shallow trap, since the free energy of the charge separated state is very near that of the of excited state. Compared to the bacterial primary electron donor, P870/P960, where coupling of the excited state is severely red-shifted (V = 550 cm^{-1} for P870 and 950 cm^{-1} for P960) relative to other reaction centre pigments, P680 possesses a very small red shift relative to other reaction centre pigments, hence, the shallow trap. Secondly, charge separation, although efficient, is reversible. The exciton-radical pair equilibrium (Leibl *et al.* 1989; Schatz *et al.* 1988) illustrated in equation 8, demonstrates how a charge recombination between $P680^+$ and $Pheo^-$ may follow primary charge separation and render an exciton in the antenna rather than pushing on towards charge stabilization (Karukstis *et al.* 1990).

$$(PSII\ antenna)^* \rightleftarrows (P680Pheo)^* \rightleftarrows P680^+Pheo^- \rightleftarrows P680^+PheoQ_A^- \quad (8)$$

One can see that a photon may visit the P680 reaction centre many times until it is ultimately trapped and used for photochemistry or dissipated from the antenna (see figure 7). An alternative would be a diffusion limited system, whereby the orientations of pigments and their ability to funnel absorbed excitation energy towards the reaction centre complex is the limiting factor towards primary charge separation (Vasil'ev *et al.* 2001).

The excitonic coupling of pigments depends largely on their relative distances and mutual orientations. Recently, the crystal structure of the PSII reaction centre from the cyanobacteria, *Synechococcus elongatus*, had been resolved to 8 Å (Rhee *et al.* 1997; Rhee *et al.* 1998) and then to 3.8 Å (Zouni *et al.* 2001). These structures are useful in determining the relative distances and mutual orientations of the Chl *a* present in the core complex (Vasil'ev *et al.* 2001). Until these precise structures had been released, researchers often found themselves making bold predictions regarding these parameters based on models derived from electron microscopy of 2D crystals (Barber and Kühlbrandt 2000; Lyon 1998; Marr *et al.* 1996; Mayanagi *et al.* 1998; Nakazato *et al.* 1996)

$P680^+$ has an enormous redox potential of about 1.17 V compared to a value of only 0.4 - 0.6 V for $P700^+$, the oxidized form of the primary donor of PSI. $P680^+$ is thought to be the most oxidizing species found in living organisms. Such a high oxidizing potential affords $P680^+$ the ability to liberate electrons from water, a very stable compound. As a by-product, breathable oxygen is released into the atmosphere (Barber and Kühlbrandt 2000; Karukstis *et al.* 1990). This oxidation of water is achieved by four consecutive univalent oxidation steps at the Mn-cluster where the intermediary electron transfer component is a redox active tyrosine (see (Debus 1992; Renger 1993) for review).

In order to withstand such a harsh environment, nature has afforded the PSII reaction centre with the means to prevent and deal with the oxidation of neighbouring proteins and pigments (Anderson 2001).

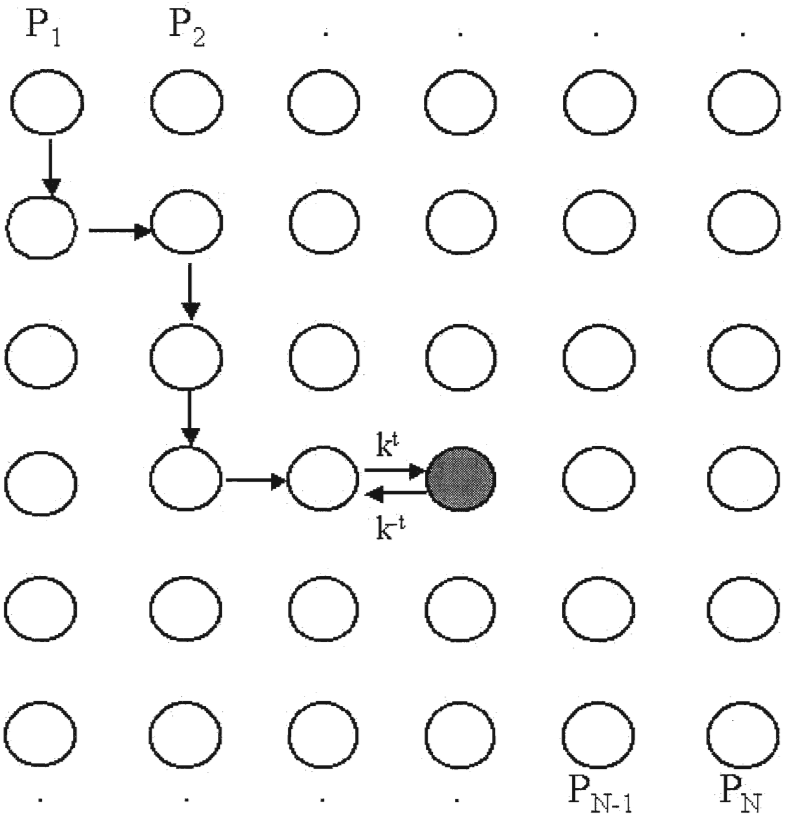

Figure 7 - The energy of light absorbed by pigment molecules (P_1-P_N) in the antenna system hops rapidly from molecule to molecule by resonance energy transfer until it is trapped (k^t) in an electron-transfer reaction in a reaction centre (shaded molecule) or released back (k^{-t}) to the antenna pigment bed where it may be dissipated as either heat or fluorescence (Renger 1992; Zubay 1993).

Table 5 - Polypeptides of the PSII core complex including the inner antenna and the reaction center (RC). All are encoded by the chloroplast genome except *Psb*W (Erickson 1998).

Gene	Subunit	Apparent MW (kDa)	Function	Associated Pigments
PSII RC				
*psb*A	D1	32	Y_z and binds Q_B, Pheo, P680, Mn	chl *a*, β-carotene
*psb*D	D2	34	Y_D and binds Q_A, Pheo, P680	chl *a*, β-carotene
*psb*E	cyt b_{559}-α	6	Binds heme, photoprotection	chl *a*, β-carotene
*psb*F	cyt b_{559}-β	4	Binds heme, photoprotection	chl *a*, β-carotene
*psb*I	I	4	PSII stability	chl *a*, β-carotene
Inner Antenna				
*psb*B	CP47	50	Excitation energy transfer, binds OEE1	chl *a*, lutein, β-carotene
*psb*C	CP43	47	Excitation energy transfer, binds OEE1	chl *a*, lutein, β-carotene
Core Complex				
*psb*H	H	9	Photoprotection	
*psb*J	J	5	PSII assembly?	
*psb*K	K	4	PSII stability, assembly	
*psb*L	L	5	Q_A function	
*psb*M	M	5	?	
*psb*N	N	4	PSII stability	
*psb*S	S	22	chl chaperonin, antenna, qE	chl *a*
*psb*T	T	3	PSII stability	
*Psb*W	W	6	?	
*psb*X	X	4	Q_A function	

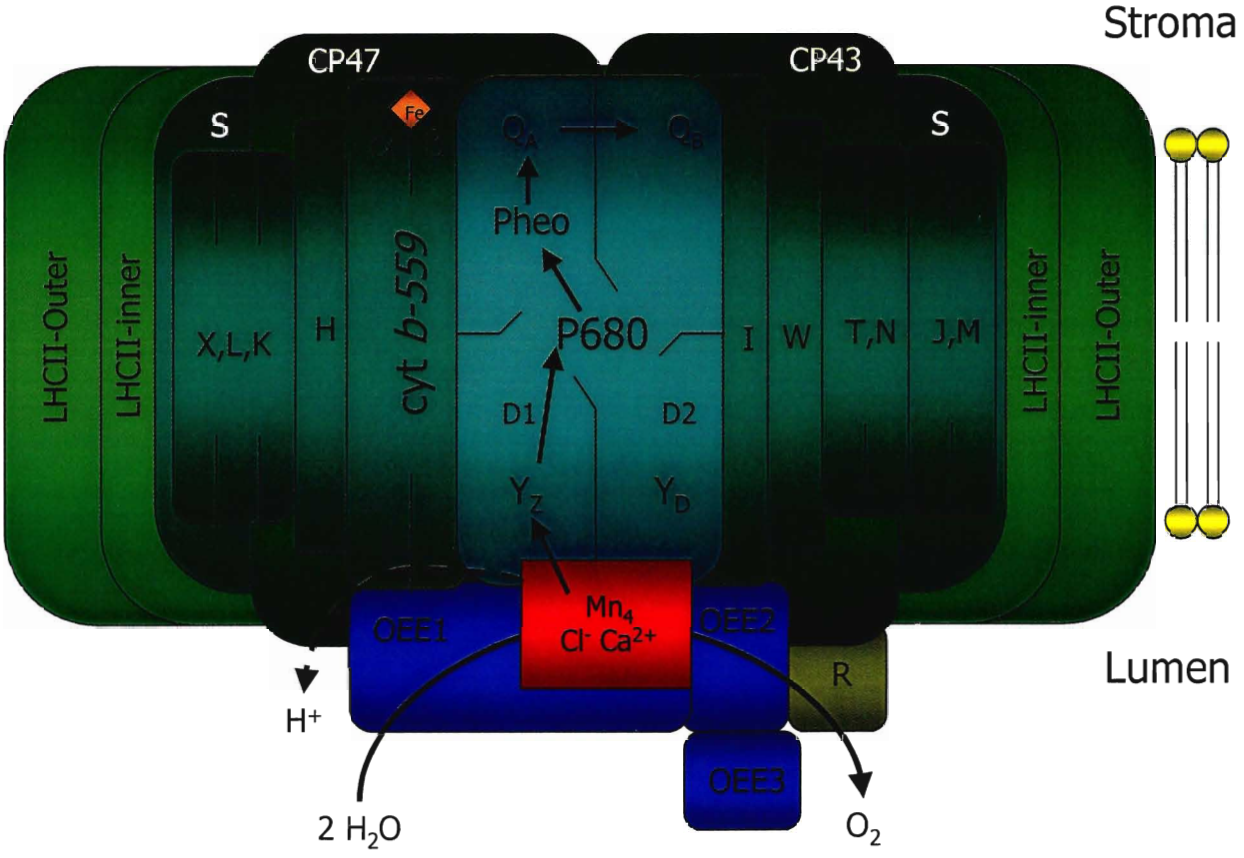

Figure 8 - Schematic diagram of PSII in the thylakoid membrane (Erickson 1998).

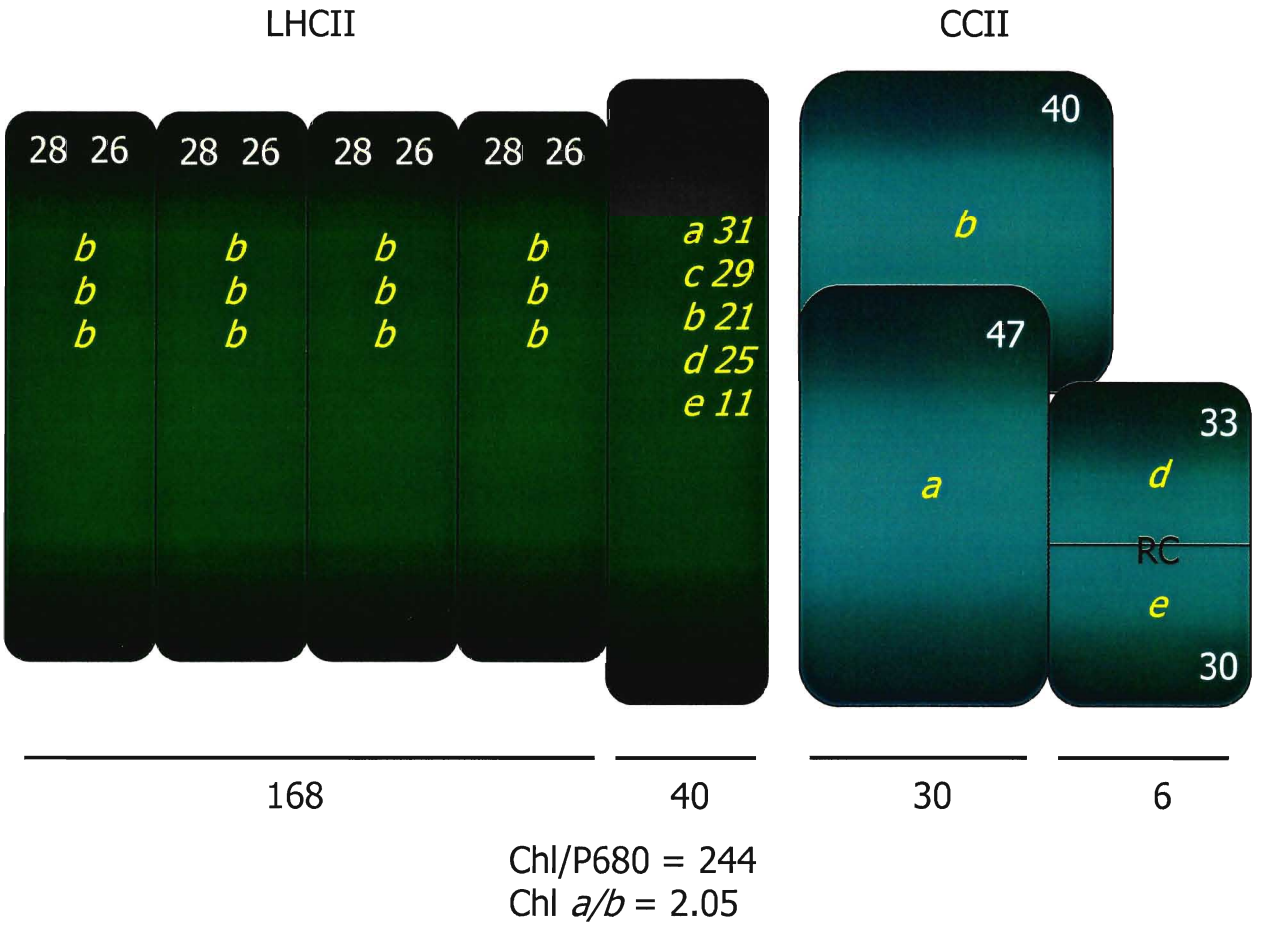

Figure 9 - Model of the pigment-protein distribution of the PSII complex including the light-harvesting complex II (LHCII) and the core complex (CCII). Molecular weights are shown within the structures, labelled by subunit and sum of the chlorophylls they contain is described beneath (adapted from (Thornber *et al.* 1991)).

One other group of very important proteins occur in the lumen of the thylakoid membrane. The oxygen evolving complex is composed primarily of 3 extrinsic polypeptides with molecular weights of 33, 23 and 16 kDa, referred to as oxygen-evolution enhancer 1 (OEE1) OEE2 and OEE3 respectively (Erickson and Rochaix 1992). A brief summary of these components of the water oxidizing complex is listed in table 4. Their function is reviewed in (Nugent *et al.* 2001). Figure 10 illustrates the S cycle, also referred to as the Kok cycle (Kok *et al.* 1970), as water is oxidized and a four step linear mechanism operates to release molecular oxygen on the donor side of PSII.

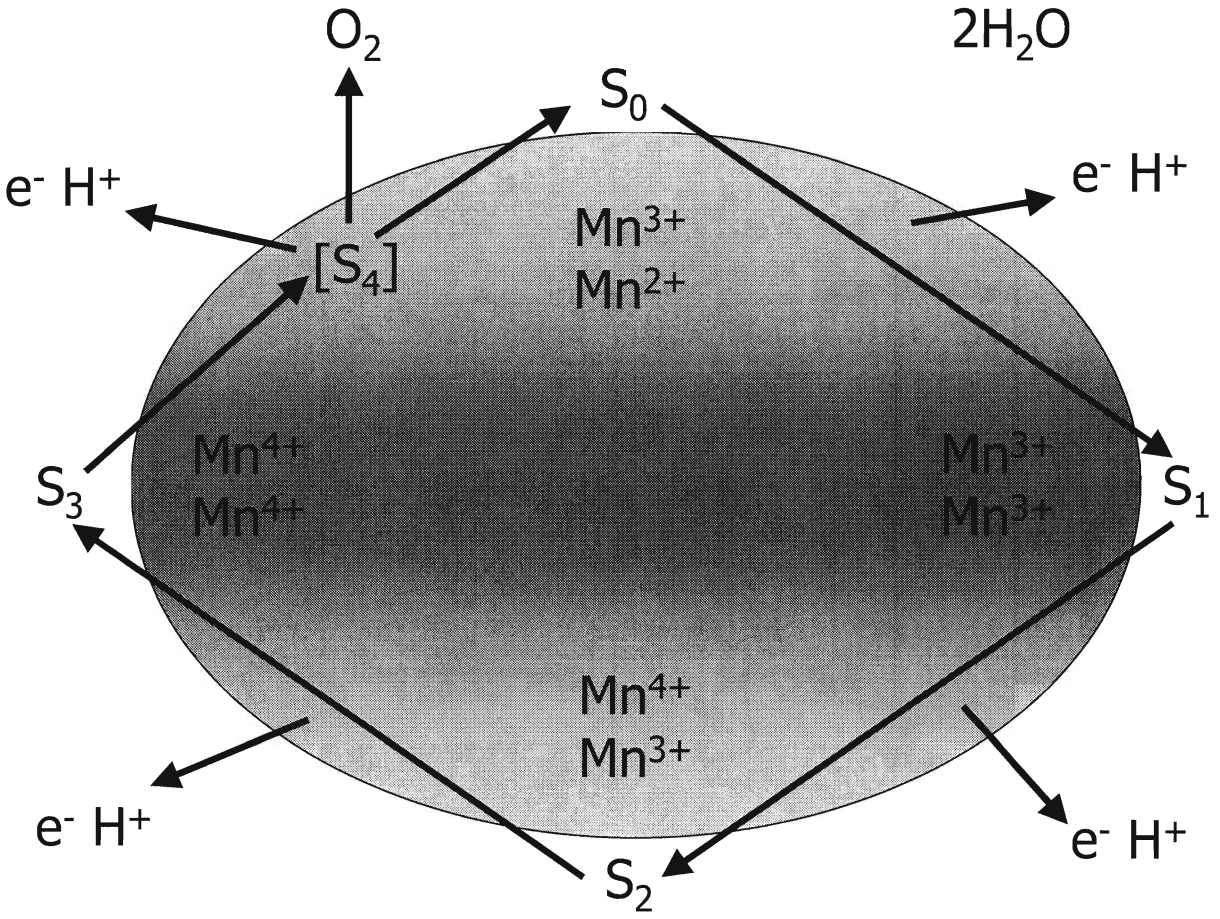

Figure 10 - The S cycle. Possible Mn oxidation state changes for two of the Mn (of four in the cluster) within the water oxidizing complex. Two others are suggested to remain in the same oxidation state. At each S state (S_n) one proton and one electron are released (Nugent *et al.* 2001).

2.2.3. Heterogeneity

Heterogeneity among photosystem II is not a new concept. More than twenty-five years ago the notion that two distinct PSII species may exist surfaced for the first time (Melis and Homann 1975). This phenomenon was expanded to further explain the biphasic nature of the kinetics of PSII activity. It may be useful to describe these early measurements with the following equation:

$$Z \cdot P680 \cdot Q \underset{k_2}{\overset{k_1}{\Leftrightarrow}} Z \cdot P680^{+} \cdot Q^{-} \underset{k_4}{\overset{k_3}{\Leftrightarrow}} Z^{+} \cdot P680 \cdot Q^{-} \qquad (9)$$

where *Z* is the secondary electron donor on the oxidizing side of the PSII reaction centre, *P680*, and Q is the primary electron acceptor. The rate constants k_1, k_2, k_3, and k_4 represent the photochemical rate constant, the thermochemical rate constants including the luminescent back reaction and the removal of primary oxidizing charges from the reaction centre, and the slow back reaction leading to the dark restoration of the fluorescence induction in DCMU poisoned chloroplasts. k_4, moderated by k_3, does not significantly alter the fluorescence kinetics (Melis and Homann 1975). Biphasic kinetic data suggested that two distinct populations of PSII were present in the chloroplast labelled PSIIα and PSIIβ (Black *et al.* 1986; Melis and Duysens 1979; Melis and Homann 1976). A slow linear phase upon examination of the kinetics of the photoreduction of Q is attributed to PSIIβ. It is described as a monophasic, first-order function of time. Its slope is described as the rate constant k_β, measured at 4.8 s^{-1}. Alternatively, the photoactivity of PSIIα reveals a fast phase described as non-first-order. The kinetics are calculated by subtracting the slow first-order phase from the global event. The rate constant, k_α, estimated from the slope of the semilogarithmic plot at the start of the kinetic, T_{init}, to be 11.2 s^{-1} is associated with PSIIα (Melis and Anderson 1983). The authors suggest that the nonlinearity of PSIIα photoreduction of Q is based on the its ability to aggregate into clusters of PSIIα centres, concomitantly, increasing its absorption cross section. As the slope (or the rate constant) of PSIIα increases progressively with time, the closure of the reaction centres becomes clear. Fewer and fewer reaction centres in the

PSIIα-aggregated clusters are open to receive absorbed excitation energy from their shared antenna. The terminal value of the slope of, k_α, T_{final}, approached 40-50 s^{-1}, four to five times higher than the value at T_{init}. The relative ratio of T_{final} to T_{init} is suggested to be useful in calculating the size the PSIIα cluster. This may suggest that up to five individual PSIIα centres aggregate to construct the cluster. Furthermore, many PSIIα clusters many occupy the appressed membrane regions of thylakoid membranes (Melis and Anderson 1983).

Different light-harvesting antenna sizes for PSIIα and PSIIβ also become apparent upon analysis of the biphasic kinetic data of photoreduction of Q by Melis and Anderson, 1983. The portion of PSII centre classified as PSIIβ is 25%. Therefore the remaining portion, 75% are PSIIα centres. The ratio of PSII to PSI is 1.9 so, the individual reaction centre ratios are; PSIIα/PSI = 1.43 and PSIIβ/PSI = 0.48. These ratios, coupled with the values of k_α and k_β, allowed the authors estimate the absolute number of chlorophylls associated with PSIIα (N_α), PSIIβ (N_β) and PSI (N_{P700}) that are involved in excitation energy transfer to their respective reaction centres. These parameters were determined this way:

$$\frac{Chl}{PSI} = \frac{PSII\alpha}{PSI} N_\alpha + \frac{PSII\beta}{PSI} N_\beta + N_{P700} \tag{10}$$

$$k_\alpha = cIN_\alpha \tag{11}$$

$$k_\beta = cIN_\beta \tag{12}$$

$$k_{P700} = cIN_{P700} \tag{13}$$

where the overall ratio of the total Chl per PSI reaction centre is represented by *Chl/PSI*, The actinic light intensity, *I*, and a proportionality constant dependent upon the quantum yield of photochemistry, *c*, couple with the rate constants associated with each of the three reaction centre types allows the calculation of the absolute number of Chl associated with each reaction centre type in equations 11, 12 and 13. In each case *c* is kept constant based on the assumption that the quantum yields for photochemistry for PSIIα, PSIIβ and PSI are similar (> 0.8). Based on these

calculations the authors report values of N_{α} = 234, N_{β} = 100 and N_{P700} = 209 (Melis and Anderson 1983). These values are in agreement with (Thielen and Van Gorkom 1981b). In summary the authors suggest that the relative amounts of chlorophyll associated with PSIIα, PSIIβ and PSI are 57%, 8% and 35% respectively. Hence, large PSIIα harbours seven times more chlorophyll than smaller PSIIβ and 1.8 times more than PSI. (Melis and Anderson 1983)

The identification of PSII heterogeneity and its characterization remains somewhat enigmatic, relative to the great deal of attention it has received. But even more mysterious is the physiological significance behind this evolutionary puzzle. Since PSII heterogeneity has been found in chloroplasts from virtually all higher plants which employ stacked and unstacked regions of thylakoid membranes, some advantage must be conferred to the organism which orchestrates this paradigm (Armond *et al.* 1976).

Melis has suggested a physiological significance for PSII heterogeneity that has rarely been debated. He reported that PSII heterogeneity exists in two modes (figure 11), both of which are dependant upon the location of PSIIα (in the grana partition regions) and PSIIβ (in stroma-exposed membranes). In the first mode, PSII antenna heterogeneity may be a product of the development of this multi-subunit pigment-protein complex (Guenther *et al.* 1988; Guenther and Melis 1990; Melis 1985; Melis 1991). PSIIβ lacks the LHCII-peripheral antenna.

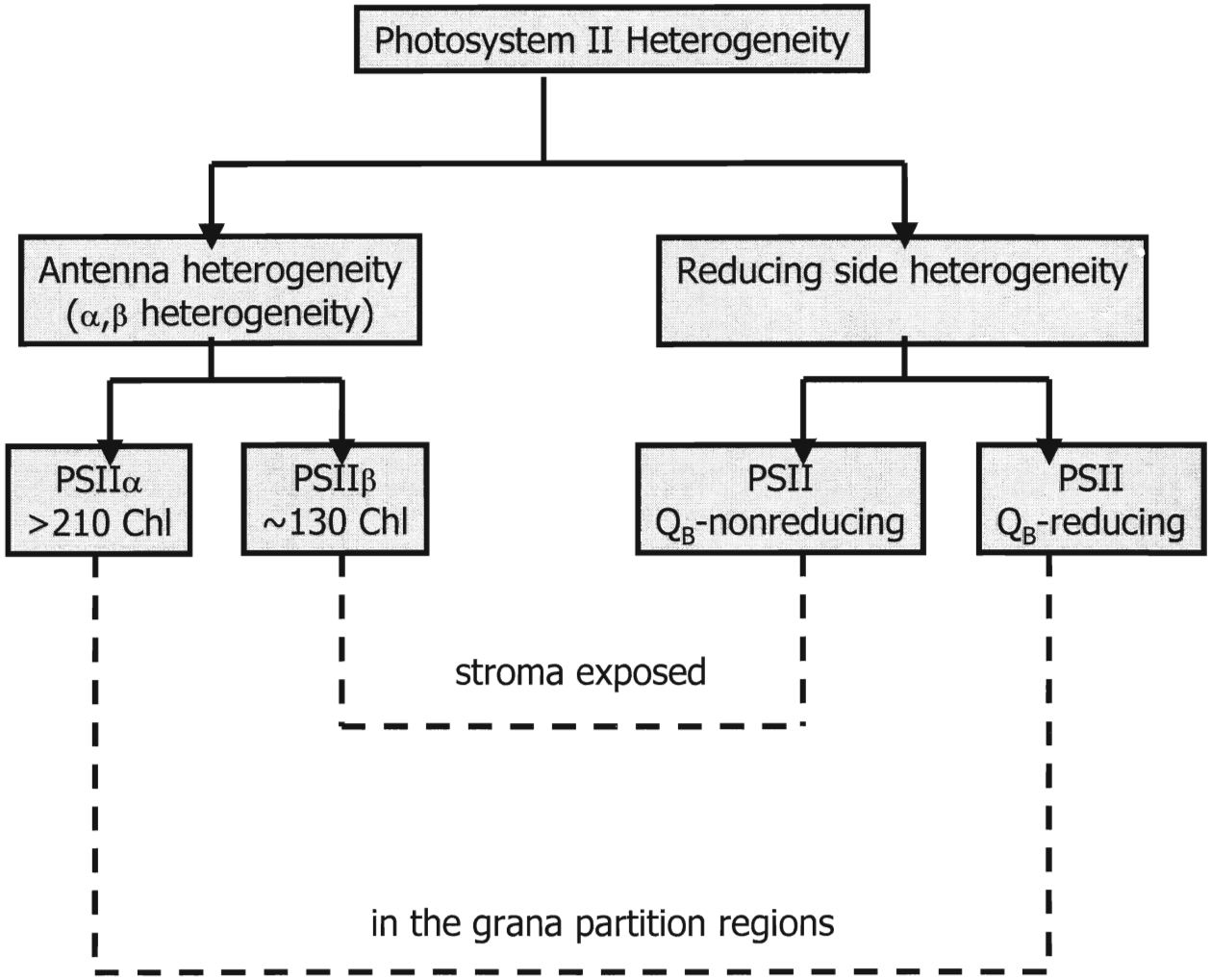

Figure 11 - The two modes of PSII heterogeneity are dependent upon the location of PSII in either grana or stroma lamellae regions of the thylakoid membrane.(Melis 1985; Melis 1991).

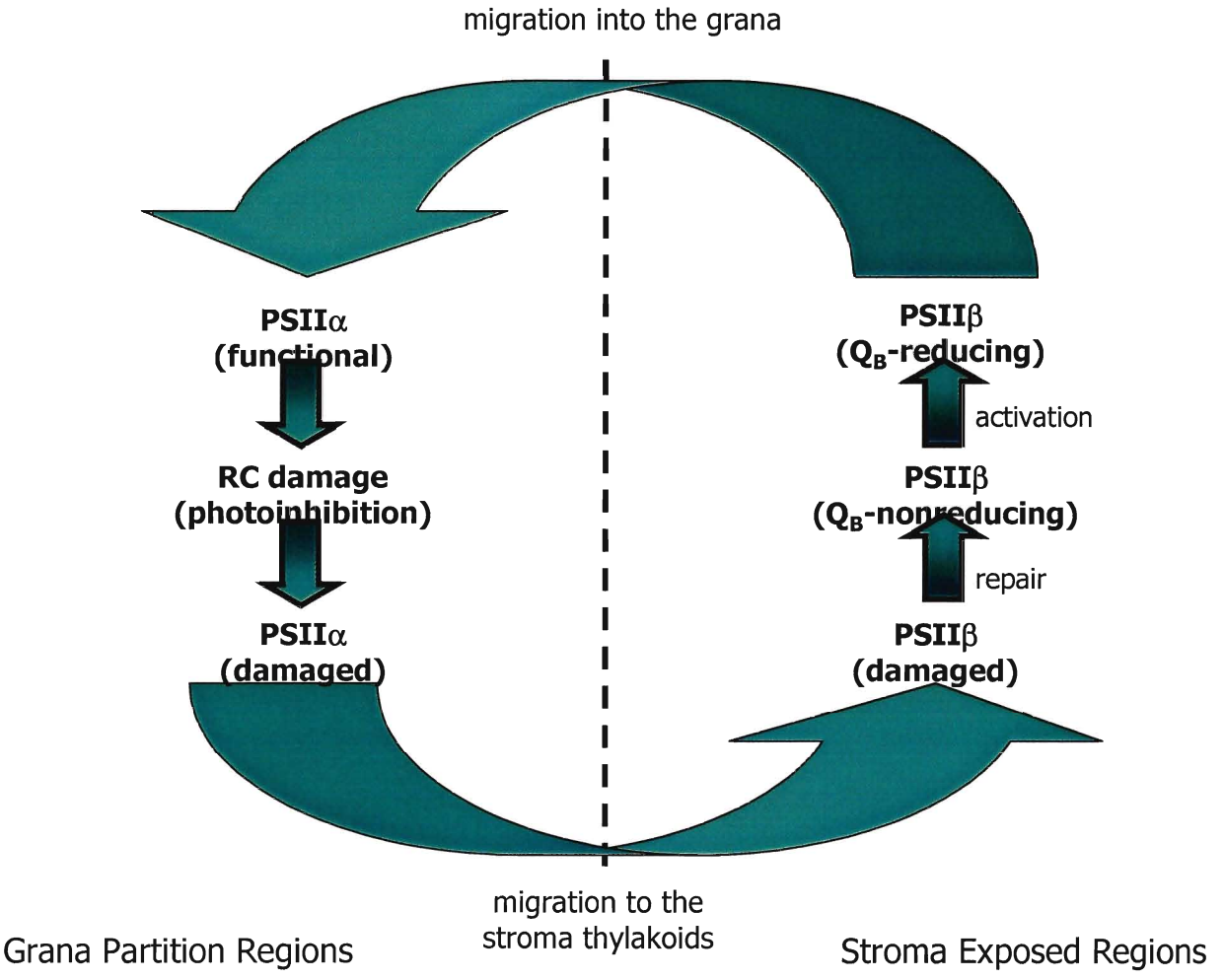

Figure 12 - The PSII repair cycle (Guenther and Melis 1990; Melis 1991).

The second mode, reducing side heterogeneity, is best described by the PSII repair cycle (figure 12). Photoinhibition is a regulatory response that plants may undergo under high light intensities. Photodamage may originate from an over-reduced PQ pool or from the oxidizing side of PSII. Both theories may be true and operate under certain conditions. Some researchers suggest that there is a threshold photon flux density for photodamage whereas others suggest that there is a constant, albeit low, probability for photodamage to occur with every absorbed photon (Anderson *et al.* 1998; Melis 1999) . Irreversible photodamage to the reaction centre proteins brings the onset of photoinactivation of electron transport (Aro *et al.* 1993; Melis 1991). PSII-Q_B-nonreducing units establish a repair state of the photochemical donor side of PSII. Here, the damaged 32 kDa reaction centre named D1 (Q_B-binding) protein is replaced. PSII repair is initiated by an uncoupling of the LHCII peripheral antenna from the damaged unit within stacked grana. The new PSIIβ-like centre migrates towards the stroma-exposed region where the damaged D1 protein is replaced, rendering it a photochemically competent centre, still incapable of Q_A-oxidation via Q_B. PSIIβ is then activated upon its conversion to the Q_B-reducing form prior to its ultimate migration back to stacked grana regions and reassociation with the LHCII-peripheral antenna. At this stage the newly functional PSIIα unit has been formed (Guenther and Melis 1990). The distinctive lipid composition of thylakoid membranes easily permits the migration of these large complexes. Only 10% of the lipid content is derived from phospholipids. The remaining 90% is made up of four-fifths mono- and digalactosyl diacylglycerols and one-tenth sulfoquinivisyl diacyglycerols. A high degree of unsaturation within the acyl chains of these lipids give the thylakoid membrane its high fluidity (Barber 1990; Voet and Voet 1995). An observed correlation with growth conditions may also support this hypothesis. However the proportion of PSIIβ centres occurring in non-photoinhibited material has been reported to be as high as one-third, a unduly large share (Hemelrijk and Van Gorkom 1996).

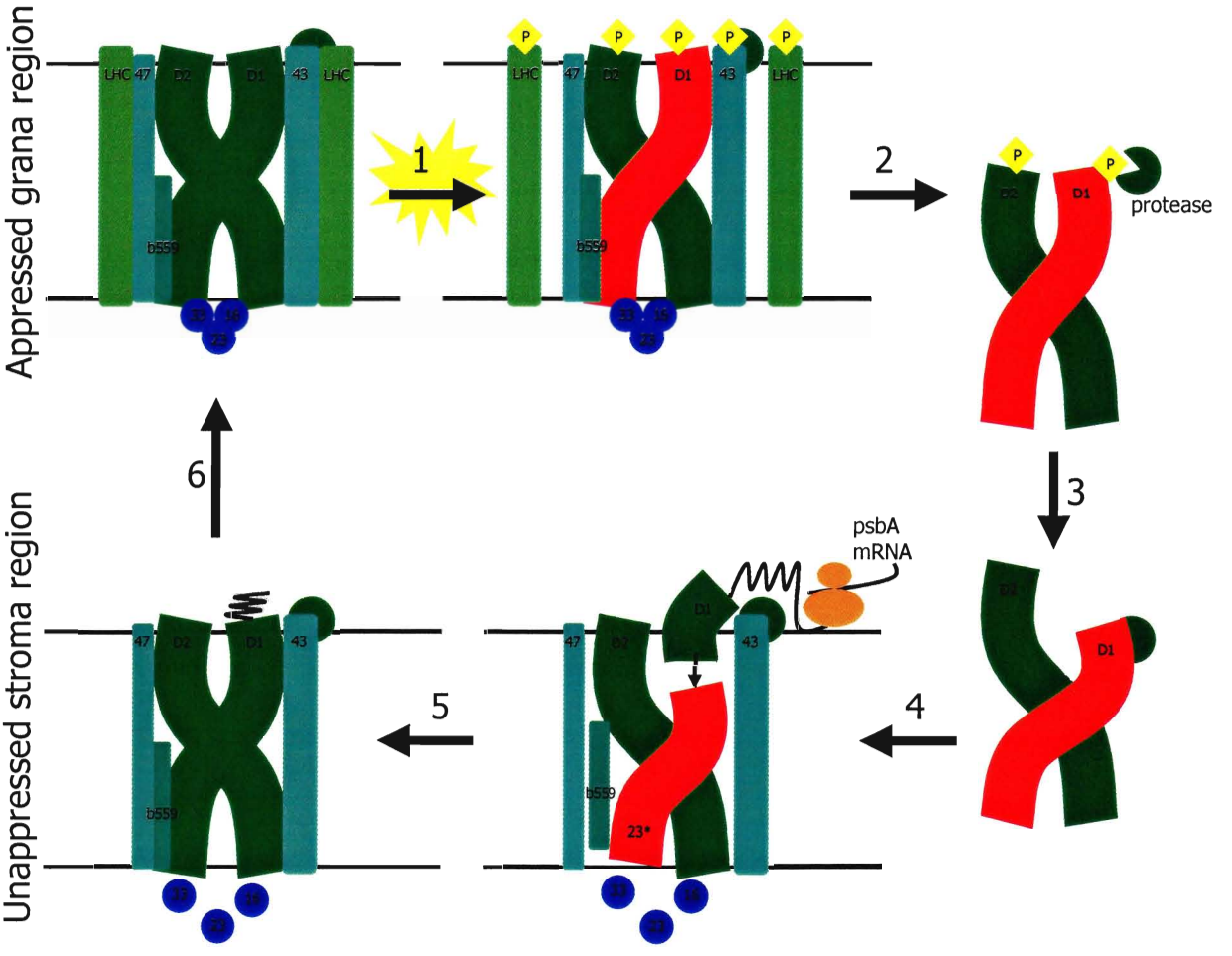

Figure 13 - A hypothetical schematic representation of the association of different phases in the PSII repair cycle (see figure 12). High light intensities cause D1 photodamage and phosphorylation of most PSII proteins within the appressed grana regions of the thylakoid membrane (1). Cleavage is triggered by conformational changes in the damaged D1 polypeptide (2). Dephosphorylation of D1 offers a superior substrate for protease (3) and is required before proteolytic cleavage (4). The 23 kDa D1 fragment is digested further as a newly synthesized D1 is inserted into the thylakoid membrane (4). Cofactors are reassociated as the new D1 is processed and palmitoylated. The repaired PSII complex migrates back to the appressed grana regions (6) and where final assembly of the LHC and OEC occur. Phases following steps (2) and (3) occur in unknown locations. For clarity, only the heterodimeric reaction centre polypeptides are shown (Aro *et al.* 1993).

A semi-related physiological significance of PSII heterogeneity has been suggested by Weis, (Timmerhaus and Weis 1990). The state transitions component (qT) of non-photochemical quenching (qN) (see (Allen 1992) for review) is a physiological adaptation in plants where excess absorbed excitation energy by PSII is alternatively channelled towards PSI via phosphorylation of the major light-harvesting antenna (LHCII). Traditionally, many authors suggest that a portion of the LHCII, bound to PSII, becomes phosphorylated (p-LHCII) and migrates into nonappressed PSI rich regions. Weis and coworkers suggest that p-LHCII may not form a complex with PSI since P700-photooxidation is not (or barely) stimulated when assayed under this condition. The supercomplex PSIIβ·LHCII-P·PSI is formed (Timmerhaus and Weis 1990; Yakovlev *et al.*, 2002). This model is not supported by the relatively low Chl *a/b* (Chl *b* being constitutive to LHCII) ratios in stroma reported by others (Guenther *et al.* 1988).

PSII heterogeneity does not end at that relatively simple separation of α- and β-centres. Many authors suggest that some sub-heterogeneity may exist amongst PSIIα within grana regions of thylakoid membranes. It has been suggested that PSIIα is regionally divided into three separate species as they occur in concentric circles with the stacked grana core as illustrated in figure 14 (Albertsson *et al.* 1990b).

Figure 14 - Heterogeneity may also exist among PSIIα centres (Albertsson *et al.* 1990b).

The significance of PSII heterogeneity discussed previously does not adequately address the conundrum of linear electron transport in series. How can an excited electron from PSII be transported to a position where it is able to reduce $NADP^+$ if functional PSII centres are located in thylakoid domains far removed from PSI? Lateral flow of electrons throughout thylakoid membranes is thought to be coordinated by two mobile carriers, the water-soluble plastocyanin and the pool of plastoquinone (five to ten per PSII). The former, migrating within the inner thylakoid space, escorts electrons from specific sites at cyt b_6/f to PSI, and the latter, associated with the acyl lipids in the thylakoid lipid bilayer, acts as a Q_B-cyt b_6/f oxidoreductase (Kirchhoff *et al.* 2000). Shortly after the non-detergent method of thylakoid membrane fractionation was established this question was addressed. In grana core fractions (BS) it was found that the ratio or PQ/Q was 6.4. This implies that the PQ pool can accept 12-14 electrons. Surprisingly, this value is near that of whole thylakoid. Therefore, PQ present in the stroma remains unavailable to PSIIα in the grana, and is not an active participant in linear electron transport (Yu and Albertsson 1993). So, if the PQ pool of the grana minds only PSIIα, then PQ does not act as an electron shuttle within the phospholipid thylakoid bilayer between grana and stroma. It is suggested that a 1:1:1 relationship among the three electron transport complexes in higher plants: PSII, cyt b_6f and PSI may exist. Since the PQ pool may occur as high as six molecules per PSI complex, the cyt b_6f complex stores reducing equivalents at a value slightly greater than 2 molecules per P700, and, more than 2 molecules of PC occur for each PSI complex (illustrated in figure 15). This is consistent with (Albertsson *et al.* 1990b) where the authors report that the operations of the grana and stroma act independently of each other. The α-centres of each photosystem perform oxygenic non-cyclic electron transport photo-phosphorylation in the grana, while PSIβ performs cyclic electron transport photo-phosphorylation in the stroma (Albertsson *et al.* 1990b; Graan and Ort 1984).

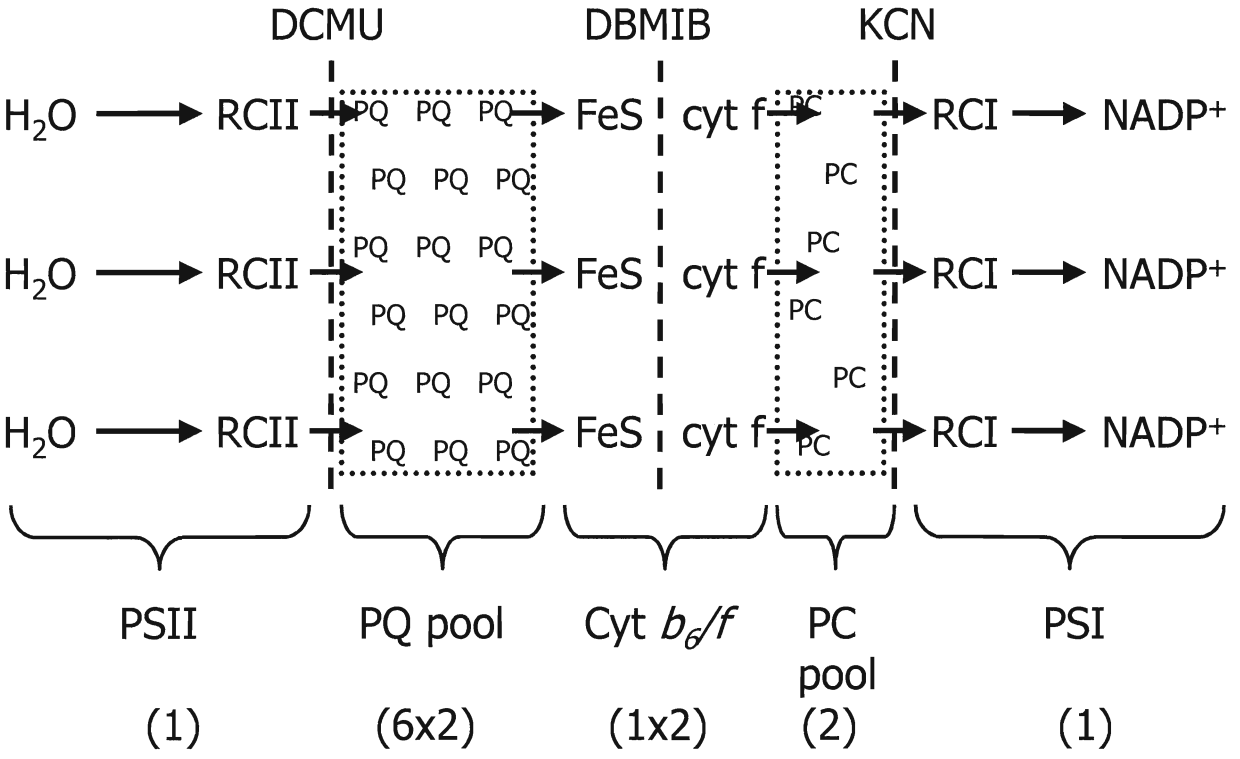

Figure 15 - The stochiometric relationship among the three large electron transport complexes (PSII, Cyt b_6/f and PSI) in thylakoid membranes and their moblie electron carriers (PQ and PC) pools from original source, H_20, to final target, $NADP^+$. Electron transport inhibitors (DCMU, DBMIB and KCN) are indicated at their specific effector sites. Electron capacity relative to PSI is shown in brackets (Graan and Ort 1984).

Table 6 - Some of the early work done to characterize PSIIα and PSIIβ centres (Hodges and Barber 1986).

Characteristic	Reference
PSIIα in grana and PSIIβ in stroma	(Anderson and Melis 1983)
PSIIα antenna > PSIIβ antenna (red shifted)	(Thielen and Van Gorkom 1981a)
PSIIβ not associated with the 2 electron gate	(Thielen and van Grokum 1981)
Different primary stable electron acceptors	(Horton 1981)
PSIIβ can be preferentially altered by high herbicide conc.	(Horváth *et al.* 1984)
PSIIα fluorescence affected by high [Mg^{2+}], not PSIIβ	(Melis and Ow 1982)
Different fluorescence emission characteristics	(Brearley and Horton 1984)

Contrary to the characteristics of PSII heterogeneity listed in table 6, the biphasic data may be interpreted as being linked to different degrees of PSII connectivity, regardless of membrane differentiation or differential antenna sizes. Or, it may be described as differences among the degree of chloroplast integrity and its link to DCMU affinity (Dekker *et al.* 1999).

Spatial separation of protein complexes within the thylakoid membranes of higher plants offers challenges other than those considering mobile electron carriers. The diffusion of protons plays an important role in energetic coupling within chloroplasts since ATP production is directly dependent upon the translocation of protons by the ATP-synthase, far removed from the source. The non-uniform distribution of transmembrane pH differences laterally among thylakoid membranes may be a product of spatial heterogeneity (Dubinskii and Tikhonov 1997).

PSII heterogeneity is not unique. Heterogeneity has also been suggested to exist among PSI centres as well. Similar nomenclature relative to PSII heterogeneity is maintained. PSI centres with large antennae are classified as PSIα centres, whereas PSI centres associated with smaller antennae are classified as PSIβ centres consisting of 65% and 35% of all PSI centres respectively (Andreasson *et al.* 1988; Svensson *et al.* 1991). Andreasson *et al.* 1988 reported that P700 photooxidation kinetics clearly indicate two distinct populations of PSI, distinguishable by their relative antenna sizes, however, it remained difficult to quantify the difference. Some authors suggest that PSIα employs an antenna 30% larger than PSIβ (Andreasson *et al.* 1988; Svensson *et al.* 1991).

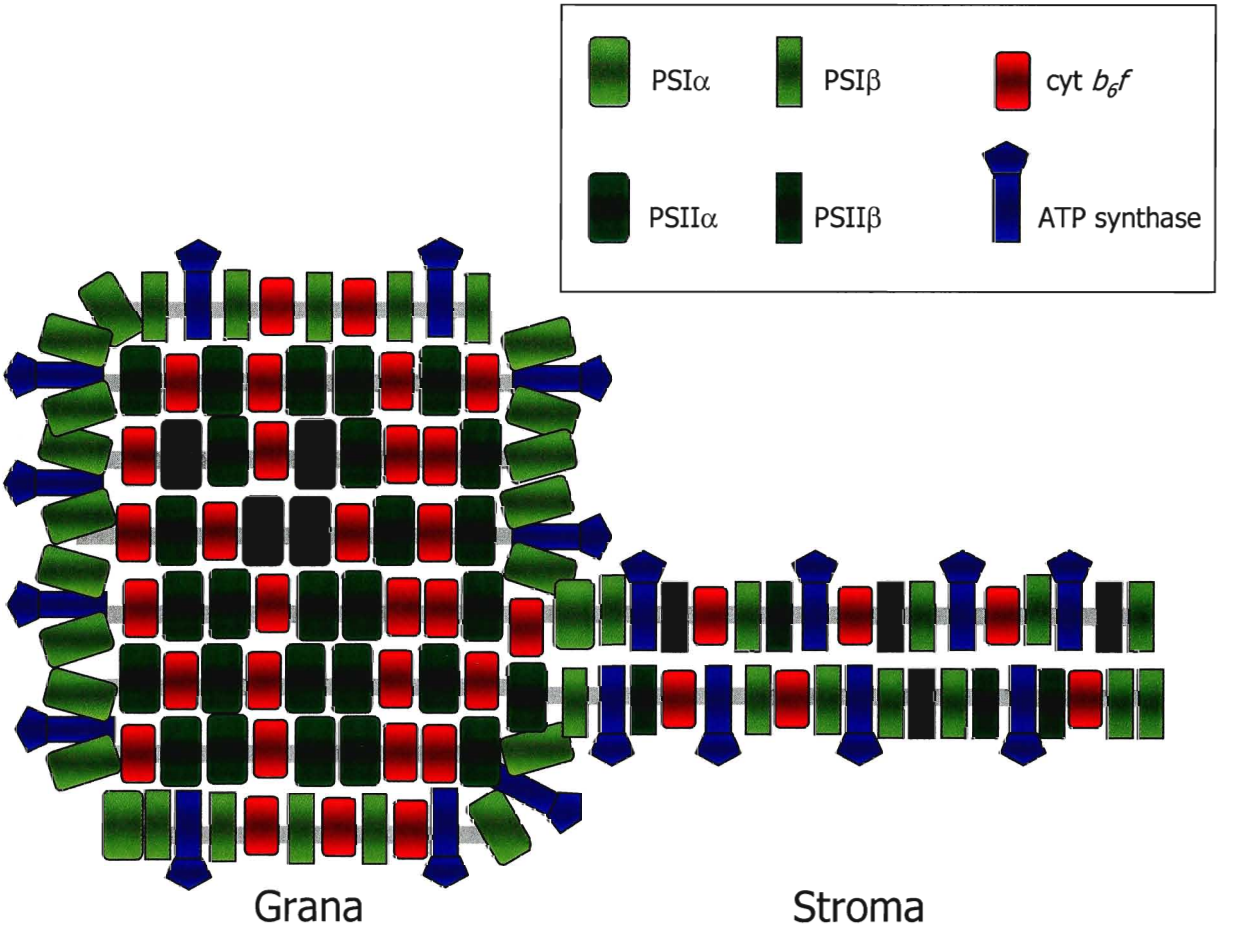

Figure 16 - The model of the thylakoid membrane system of higher plant chloroplasts. Spatial separation of α- and β-centres of PSII and PSI is clearly illustrated. PSIα is located in stroma exposed end membrane regions of the grana partition whereas PSIβ is found primarily in the stroma lamellae. PSIIα is found exclusively within the appressed regions of the grana partition, whereas PSIIβ is found primarily in the stroma lamellae. The cyt b_6-*f* and ATP synthase are ubiquitous throughout the structure (Albertsson 2001; Allen and Forsberg 2001; Svensson *et al.* 1991).

2.3. Chlorophyll Fluorescence

The key light absorbing pigments of photosynthesis are chlorophylls. In higher plants and algae this pigment is Chl *a*. In primitive photosynthetic bacteria it is bacteriochlorophyll *a* (BChl *a*) or *b*. Without one or another of these pigments, no organism is known to be able to carry out photosynthesis (Sauer 1975). The experimental portion of this study is largely based on capturing chlorophyll fluorescence. The fact that chlorophyll is green is hardly an accident. The probability that chlorophyll will absorb a green photon in its vicinity is relatively low, nearly all are transmitted through or reflect from leaves. Blue and red photons are much more readily absorbed by chlorophyll. Upon absorption, their energies are used to raise an electron from the ground state to the second excited state or first excited state respectively. Electrons in the second excited state rapidly and radiationlessly decay to the first excited state. This loss occurs so rapidly that it cannot be captured during photosynthesis. The Pauli exclusion principle states that no two electrons can be in the same detailed quantum state. In the same orbital, two electrons must maintain opposing spin orientations. In the lowest energy states, electrons fill the orbitals in pairs. The absorbance of a photon promotes an electron from the electronic ground state (HOMO, highest occupied molecular orbital) to an excited state, (LUMO, lowest unoccupied molecular orbital). An electron in an excited state with a spin opposite its former neighbour, the excited singlet state, is likely to result from excitation energy absorption since spin reversal requires a magnetic interaction between that promoted electron and its surroundings (figure 17). Triplet states (upon a spin reversal event) are more probable from an excited singlet because the energy distribution is broad, giving rise to a decrease in the magnetic couple between the electron pair, which is inversely proportional to the interactions with its surroundings. Chlorophyll in the excited triplet state, $^{3}Chl^{*}$, is dangerously reactive since its lifetime in a more widespread distribution exceeds 10^{-3} s, whereas the lifetime of an excited singlet ($^{1}Chl^{*}$) is closer to 10^{-8} s. This difference is a product of the spin reversal. A decay to the ground state would require a re-reversal of the spin polarization. It is easier to transfer the energy to O_2, which would ultimately give rise to dangerous $^{1}O_2$ following formation of the $^{3}O_2$. Interestingly, chlorophylls in photosynthesis employ singlet excited states.

This is the primary reason why energy transfer is so fast.

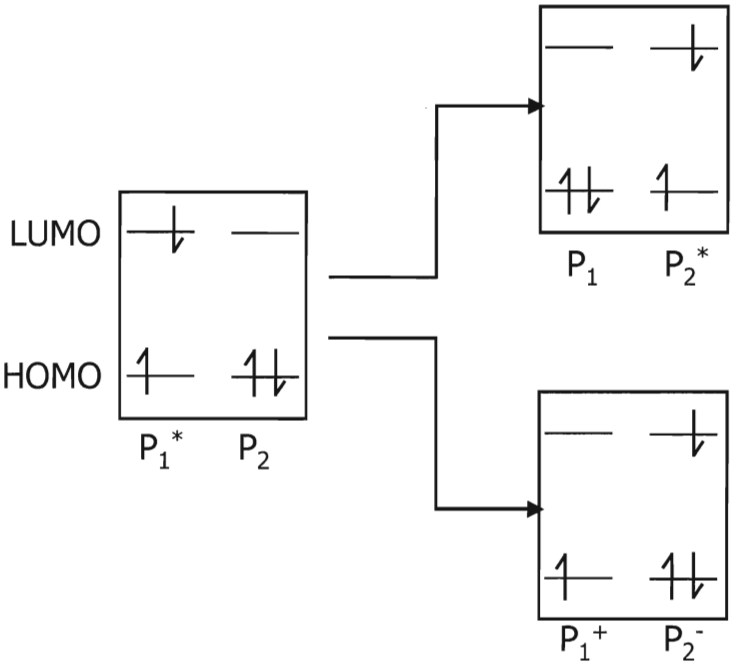

Figure 17 - Schematic representation of the electronic coupling between two identical pigment molecules, P_1 and P_2. P_1 in its lowest excited state (P_1^*) can either transfer its energy to P_2, initially in its ground state, giving rise to P_2^* (top), or, transfer the electron to P_2, reducing it, P_2^-, and itself becoming oxidized P_1^+. Exciton transfers are common in antenna complexes whereas electron transfers are common in reaction centres (Renger 1992).

Once electrons in the second excited state (or any higher excited state) rapidly and radiationlessly decay to the first excited state, bioenergetics and photochemistry begin here (see figure 18) (Seaton and Walker 1992). This is very typical of many large aromatic molecules. Also typical of these types of molecules are a) the occurrence of the Stokes's shift following the thermal relaxation of the higher excited state (figure 19), b) the short (5 ns) fluorescence lifetime in organic solvents, such as acetone, ether, and alcohols, c) a fluorescence yield of merely 30% in organic solvents due to competing processes for the deactivation of the excited state (see equations 14, 15, 16, and 17) and d) fluorescence emissions and absorption are governed by the same kind of relationships among wavefunctions. Therefore the fluorescence emission maintains essentially the same polarization as the long-wavelength absorption (Sauer 1975)

$$Chl* \xrightarrow{k_F} Chl + hv \qquad \textit{Fluorescence} \qquad (14)$$

$$Chl* \xrightarrow{k_I} Chl + heat \qquad \textit{Internal conversion, radiationless} \qquad (15)$$

$$Chl* \xrightarrow{k_T} Chl^T + heat \qquad \textit{Intersystem crossing to triplet state} \qquad (16)$$

$$Chl* + Q \xrightarrow{k_Q} Chl + Q* \qquad \textit{Quenching} \qquad (17)$$

The reactions listed in equations 14-17 are kinetically first-order in Chl^* concentration. The fluorescence lifetime of Chl^* is dependent upon the rate constants, k_{alpha}, for these equations. This is commonly referred to as the quantum yield, described by equation 18;

$$\Phi_F = \frac{k_F}{k_F + k_I + k_T + k_Q[Q] + \ldots} \qquad (18)$$

The quantum yield of fluorescence Φ_F is can be calculated by dividing the fluorescence rate by the sum of all the rates of deactivation described in equations 14-17. The rate constant k_F is an intrinsic property of the molecule, governed by both its ground and excited state quantum-mechanical properties. Its reciprocal, τ_0, the natural lifetime of the excited state, describes the

lifetime that the excited state would maintain in the absence of any competing deactivation processes. Therefore, since the denominator of equation 5 is the reciprocal of the actual (observed) lifetime, τ, equation 18 is rewritten in equation 19 (Sauer 1975)

$$\Phi_F = \tau / \tau_0 \qquad (19)$$

The fluorescence yield is dependent upon various factors, first and foremost, the redox sate of intersystem electron carriers, namely the plastoquinone pool. This is most noticeable in the presence of DCMU, an electron transport inhibitor the blocks the transfer to PQ as the electron attempts to leave PSII (see figure 15). Samples inhibited with DCMU offer the highest level of fluorescence since the reaction centres of PSII remain closed (fully reduced). Secondly, the S-state sequence (figure 10) mediates the fluorescence yield. Saturating flashes effectively reduced downstream electron acceptors. The maximum initial fluorescence follows the second flash in a series (giving rise to S_3), when steady light is applied. Furthermore, increasing electric field across the membrane, a component of the proton motive force (PMF), decreases the level of fluorescence from state P to state S witnessed in the fluorescence induction curve (Weis *et al.* 1987). And finally, LHCII, the accessory antenna of PSII, by undergoing reversible phosphorylation, and inducing qT, may alter the level of fluorescence following the state transition (Allen 1992; Allen and Holmes 1986; Gregory 1989; Wollman 2001).

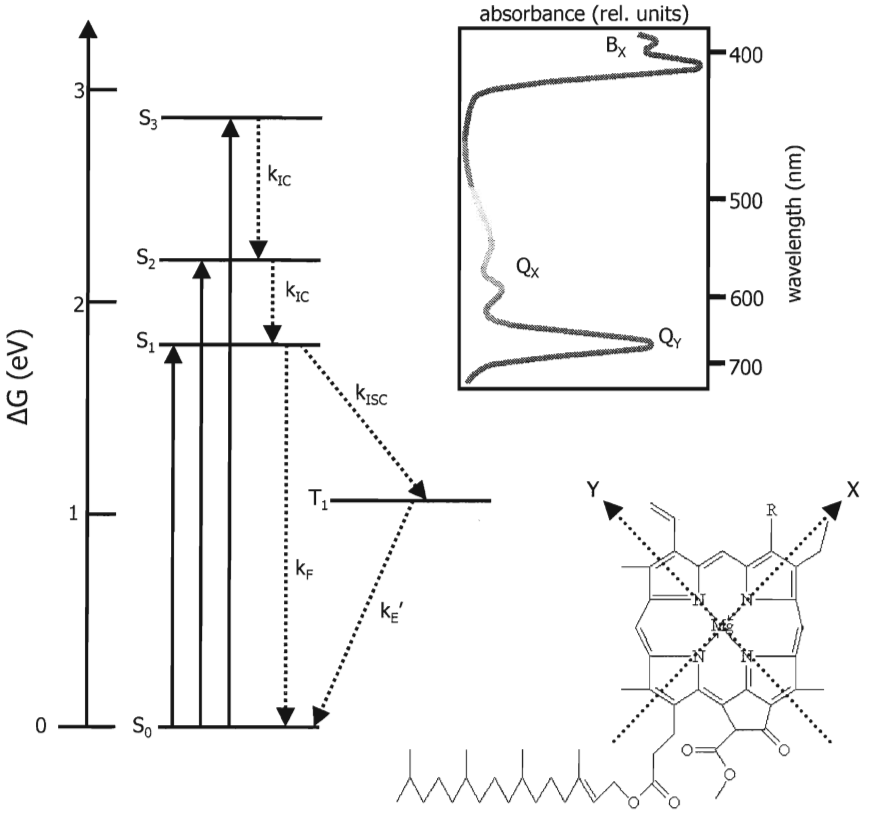

Figure 18 - Light absorbed by chlorophyll (if R = CH_3 then Chl *a*, if R = CHO then Chl *b*) in the Q_Y transition or the Q_X transition excites an electron to excited states S_1 or S_2 respectively. The absorption of shorter wavelengths (B_X) excites an electron to S_3 however the energetic difference is lost rapidly by internal conversion (IC) as heat, similar to the loss from S_2 to S_1. If in intersystem crossing (ISC) to the triplet state (T_1), followed by phosphorescence (E'), or a radiationless decay (not shown) to the ground state (S_0) does not occur, the remaining absorbed excitation energy may be given off as fluorescence (F). Each possibility is associated with its respective rate constant (k_{alpha}) (Renger 1992; Seaton and Walker 1992).

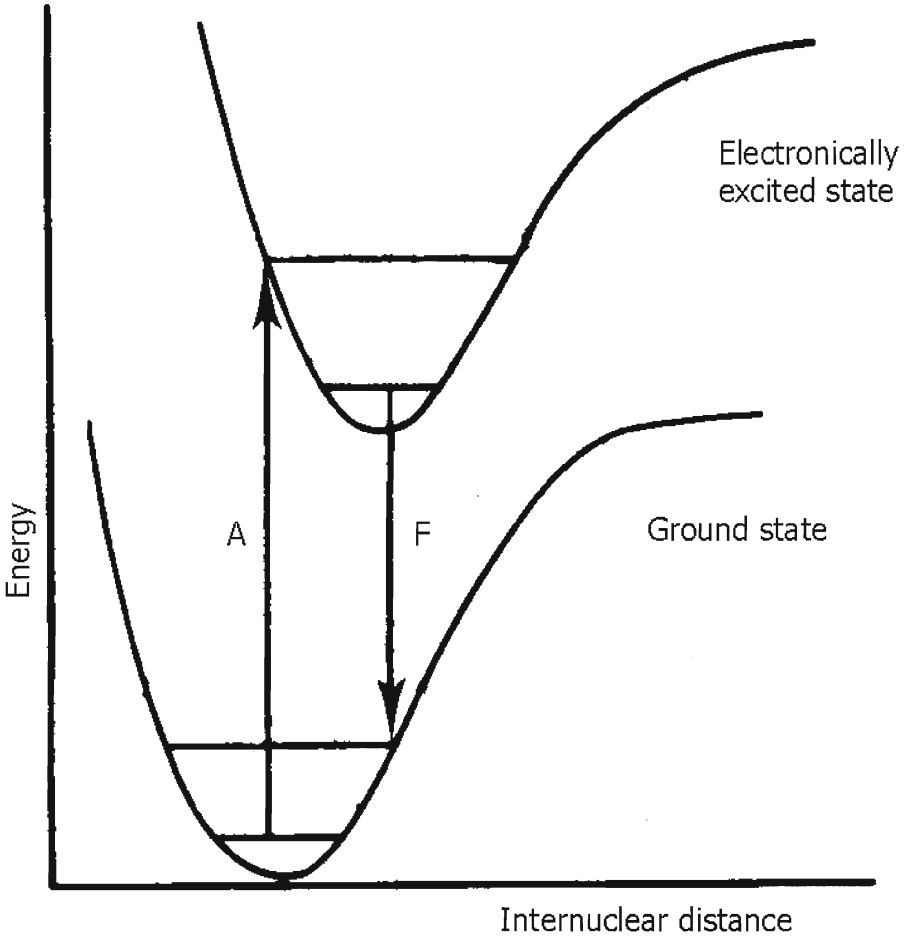

Figure 19 - Stoke's loss. The energy emitted as fluorescence (F) upon relaxation to the ground state is significantly less that the energy absorbed (A) by the molecule to promote it to the excited state (O'Connor and Phillip 1984).

2.4. Thylakoid Membrane Preparations

Evidence that PSIIα centres originate from appressed grana and PSIIβ centres originate from stroma exposed membranes is abundant. Decades ago, long before PSIIα/β heterogeneity was described, the German pioneers of chlorophyll fluorescence microscopy observed bright PSII fluorescence from grana using conventional bright-field optics (Heitz 1936), which was significantly different from the relatively non-fluorescent stroma lamellae (Metzner 1954). These results were extended by studies with confocal scanning laser microscopy which revealed brightly fluorescent grana over a non-fluorescent stroma background (van Spronsen *et al.* 1989). Isolation of thylakoid membranes enriched in particular pigment-protein complexes are of great interest in order to study their specific activities. The ability to isolate pigment-protein complexes in a state that closely resembles their native environment would be the ideal way to study them. Commonly, harsh detergents are employed to tear thylakoid membranes apart, and separate the pigment-protein complexes by centrifugation. BBY particles, named after Berthold, D.A., Babcock, G.T. and Yocum, C.F., who were the first to isolate them (Berthold *et al.* 1981), have been employed in countless studies on PSII. Triton X-100 is a nonionic detergent (octylphenol ethylene oxide condensate) which is often used in biochemical applications to solubilize proteins. It is considered a comparatively mild, non-denaturing detergent. It does absorb in the ultraviolet region of the spectrum, however, so can interfere with protein quantification. It is suggested however, that BBY particles do harbour PSIIα centres (Lam *et al.* 1983).

Another detergent method describes a procedure that involves *n*-dodecyl-α,D-maltoside (α-DM), is suggested to be relatively mild in comparison to Triton X-100. A reduced amount of chemical detergent, coupled with a minimal exposure time limits the fragmentation of the fragile macromolecular complexes to very low levels (van Roon *et al.* 2000). Various types of PSII supercomplexes, megacomplexes as well as heptameric associations of trimeric LHCII, the icosienamer, can be harvested with this relatively mild detergent (Dekker *et al.* 1999). α-DM effectively solubilizes the stroma exposed portion of the thylakoid membrane, leaving the appressed grana regions relatively intact. Appressed membrane fragments, joined in pairs,

originating from grana closely resemble PSII membranes isolated with Triton X-100, the BBY particles (Berthold *et al.* 1981), however stochiometry of PSII supercomplexes and their higher order of regularity is better preserved. The authors report that the most important advantage of the use of α-DM is the intactness of the solubilized fractions, which allow researchers to closely examine stromal proteins including native PSI and the ATP synthase complex as they occur in their intrinsic state. The authors also note that the α-DM treatment offers a relatively low yield of the PSII membranes and is not nearly as cost effective as the Triton X-100 procedure (van Roon *et al.* 2000).

The preparation of BBY particles using Triton X-100 (Berthold *et al.* 1981) and the α-DM isolation method (van Roon *et al.* 2000) differ from the isolation method developed by the Photosynthesis Group at the University of Lund, Lund, Sweden in several ways. Researchers at the University of Lund have developed a method of thylakoid membrane isolation based on native domains that is detergent free. For this study, thylakoid membranes were fractionated into five domains. The fractions were obtained via the non-detergent method illustrated in figure 20. The stacked grana were represented in three of the fractions. The grana core fraction (BS), the grana lamellae (B3) and the grana margins (Ma). The grana margin fraction is different from the other two since it is composed primarily of stroma exposed membrane. The unstacked stroma lamellae were represented in the remaining fractions, T3 and purified stroma lamellae fraction labelled Y100 (figure 21).

This novel method of isolation combines fragmentation via sonication with centrifugation in an aqueous two-phase partition system to separate different parts of the thylakoid membrane. All of the fragments are in vesicular form to maintain the highest level of photochemical activity (Albertsson *et al.* 1994). The details of the isolation are described in the appendix, section 8.1. Below, each of the different fractions are described.

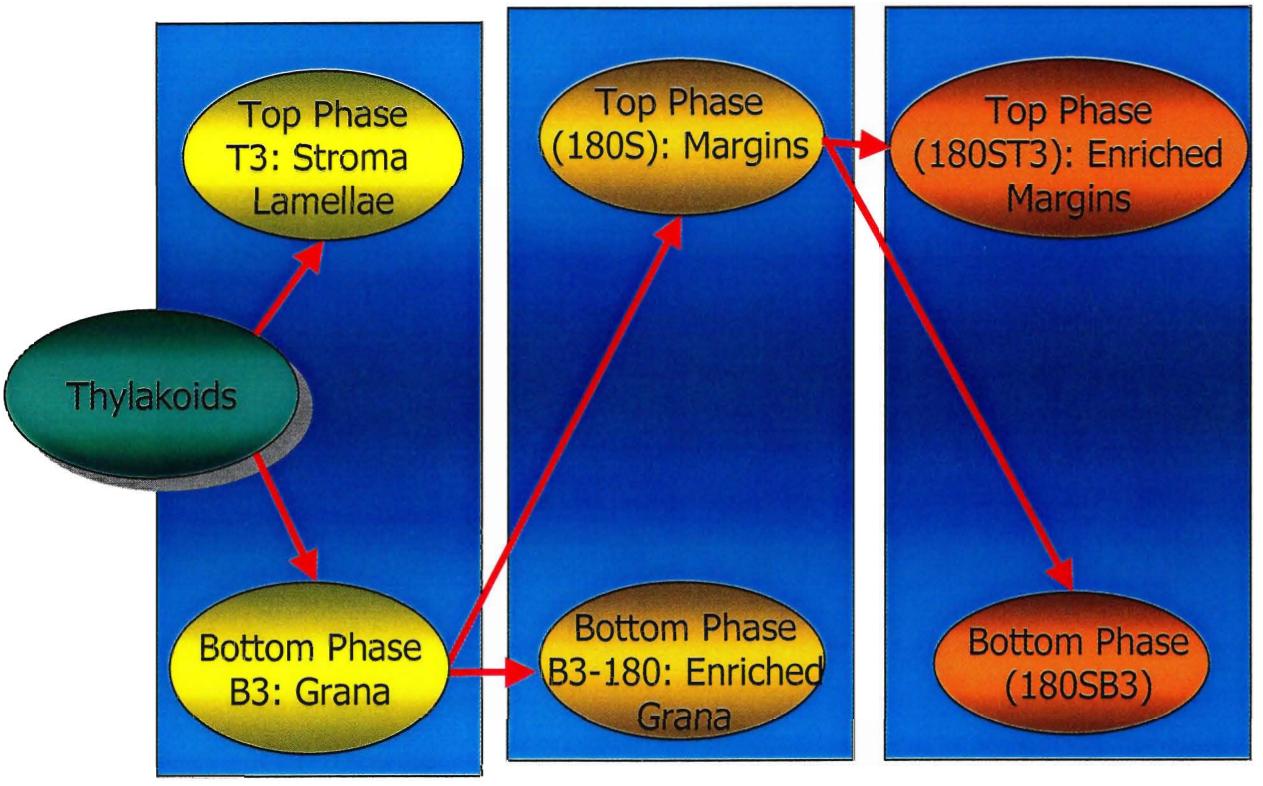

Figure 20 - Summary of the method of non-detergent domain specific thylakoid membrane isolation employed by the Photosynthesis Group, Lund Universitet, Lund Sweden, used in this study (Albertsson *et al.* 1994).

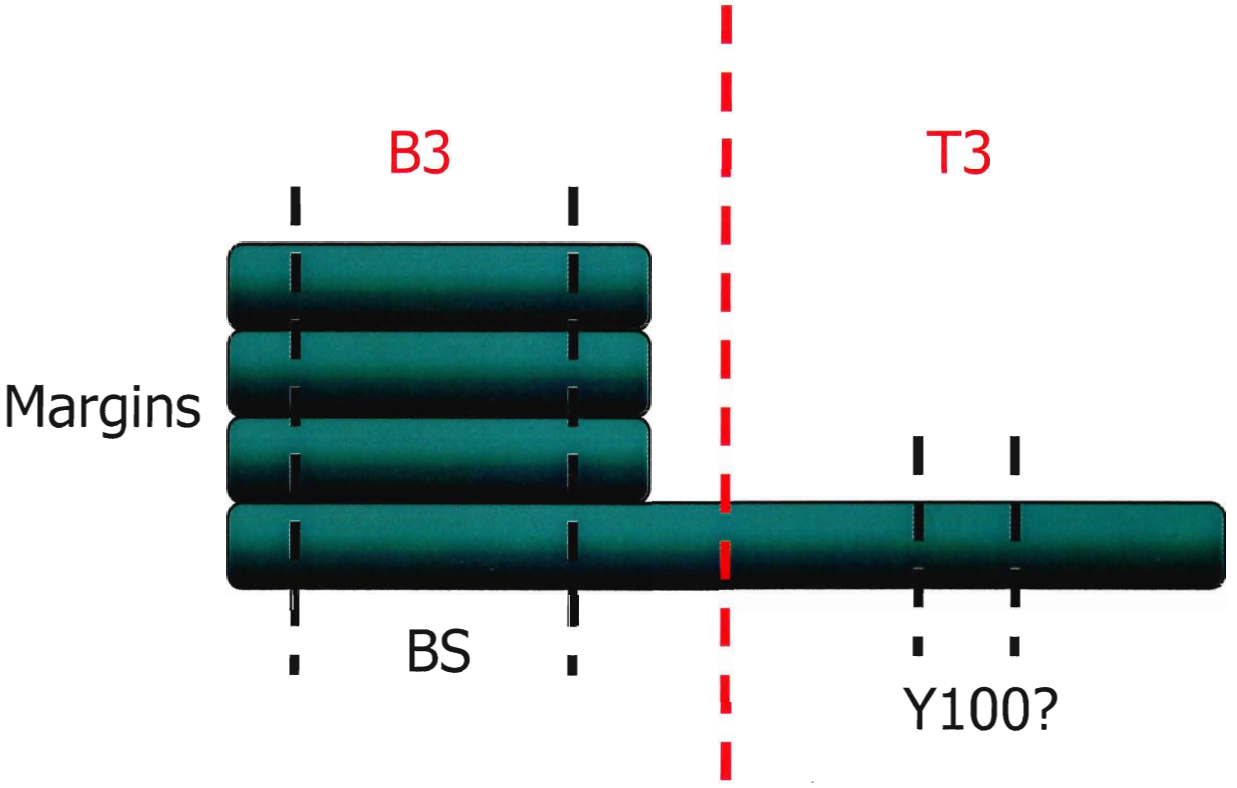

Figure 21 - Thylakoid membranes are fractionated primarily into the grana fraction (B3) and the stroma fraction (T3) along the red dashed line. The B3 fraction can then be divided into the grana core (BS) and margin fraction. The Y100 fraction is a purified stroma lamellae fraction of which its origin is not precisely known (Mamedov *et al.* 2000).

The Grana (B3)

The appressed grana regions of the thylakoid membrane are isolated in the B3 fraction during aqueous two-phase partitioning. Following the fragmentation by sonication the B3 fraction migrates to the bottom phase (Dextran T500) of the aqueous two phase partitioning system, opposite the migration of the stroma lamellae (T3) fraction towards the upper phase (PEG 4000). Evidence supporting the notion that PSIIα centres are enriched in appressed grana membranes is well founded (Anderson and Melis 1983). Of all the chlorophyll, 63% originates form the grana, whereas the remaining 37% originates from stroma lamellae. Inside-out B3 vesicles have a diameter of 0.3 µm (Albertsson *et al.* 1990d).

The Stroma (T3)

The stroma, fractionated by sonication, migrates toward the upper phase of the separation vesicle, with PEG 4000. PSII in stroma occurs as PSIIβ (Anderson and Melis 1983; Guenther and Melis 1990; Henrysson and Sundby 1990; Melis and Homann 1976). Of all the reaction centres in the T3 fraction, only 20% are PSII. Another characteristic of the stroma fraction is the occurrence of the ATPsynthase within the membrane vesicles. The large CF_1 subunit that rests on top of the CF_0 subunit simply can not fit within tightly stacked thylakoid membranes that occur in grana (Allen and Forsberg 2001; Jansson *et al.* 1997; Miller and Staehelin 1976).

The Grana Core (BS)

The procedure mentioned in section 3.1 describes how the B3 fraction can be further fractionated into two different membrane vesicles. Inside-out B3 vesicles subjected to sonication at a relatively very low ionic strength (1 mM $MgCl_2$) PSI-enriched domains are sheared off and turned right-side-out. Within an aqueous two-phase system, where inside-out vesicles prefer the lower phase and right-side-out vesicles prefer the upper phase, fragmentation and separation are achieved simultaneously (Svensson and Albertsson 1989). This second round of aqueous two-phase partitioning renders a sub-fraction of inside out vesicles containing the grana core (labelled

BS). The yield, 6% from isolated whole thylakoid membranes, is considerably low. These PSII-enriched preparations are not pure PSII. About 20-30% of all reaction centres is PSI on a per chlorophyll basis. They have a diameter of 0.2 μm and they maintain their high oxygen evolving capacity. Some promising PSII preparations obtained using detergent methods (BBY particles for example) may also maintain high oxygen evolving activity but probably do not preserve the native structure of the thylakoid membrane (Berthold *et al.* 1981; Pålsson *et al.* 1990). The BS preparation in vesicle form has not been treated with detergents, and is an interesting candidate for the study of PSII in the native form. Comparisons between these two PSII preps have illustrated the differences between them clearly. Relative light-saturation curves have revealed that the slope of the plots of BBY are much less steep that those of PSIIα. The slope of the BBY actually falls between that of PSIIα and PSIIβ. The authors have concluded that the antenna size of the BBY is smaller than that of PSIIα since the detergent treatment likely disconnected some of the LHCII. Of course this is not the case upon consideration of the slope of the light-saturation curves of BS fractions rendered by the non-detergent method. The slopes are very near those of PSIIα, therefore, no evidence of LHCII disconnection was reported (Yu and Albertsson 1993).

More evidence indicating that the BS fraction maintains antenna post-preparation is described by the absorption spectra at room temperature. A stronger absorption peak attributed to Chl *b* compliments the low Chl *a/b* reported elsewhere (Albertsson and Yu 1988; Svensson and Albertsson 1989). The BS fraction reports a lower Chl *a/b* ratio than the whole thylakoid preparations (see table 7) which is in agreement with the relatively high Chl *b* content of LHCII. At lower temperatures, resolution improves and the Chl *b* contributions are illustrate more clearly (Yu and Albertsson 1993).

The Grana Margins (Ma)

The top phase of a second round of aqueous two-phase partitioning contains right-side out vesicles which consist of the margins, or nonappressed regions of the grana (Anderson *et al.* 1999). At 1 mM $MgCl_2$, sonication shears the PSI-enriched parts from the inside-out B3 vesicles

and become right-side-out (Svensson and Albertsson 1989). Unlike the appressed membrane regions of the grana stack, these stroma exposed domains on the grana exterior harbour the ATPsnythase consisting of CF_0 and CF_1 (Allen and Forsberg 2001; Jansson *et al.* 1997; Miller and Staehelin 1976; Webber *et al.* 1987).

Purified Stroma (Y100)

The T3 fraction can be fractionated further using a mechanical press to disintegrate the right-side-out vesicles. The resultant membrane fractions from the Yeda press operating at 10 MPa of nitrogen pressure are a very pure suspension of stroma lamellae labelled the Y100 fraction. The Y100 fraction is suggested to be rich in PSIIβ. Fluorescence induction kinetics reveal that the typical biphasicity, the basis for PSII heterogeneity, is absent, and only a slow rise phase is maintained. Also noted is the tremendously low photochemical yield, F_V/F_M, relative to not only whole thylakoid, but especially other fractions derived from supposed PSIIα-rich regions of higher plant thylakoid membranes. PSIIα:PSIIβ stoichiometry, which are typically reported as approximately 3:1 in whole thylakoid, are as low as nearly 1:9 in the Y100 fraction (Henrysson and Sundby 1990).

The thylakoid membrane vesicles described above were a generous gift F. Mamedov and R. Danielsson under the direction of S. Styring from the Photosynthesis Group, Lunds Universitet, Lund, Sweden

A protein profile of these thylakoid membrane fractions is displayed in figure 22. Table 7, describes a summary of the data obtained in a recent paper which employed these fractions. Their relative activities with respect to their spatial distribution are illustrated in figure 23. Juhler *et al.* 1993 published their findings on the composition of photosynthetic pigments in the thylakoid membrane vesicles. Most interestingly, β-carotene is enriched in PSI-rich fractions. Lutein is present in a 5:2 ratio relative to Chl *b* in all fractions. Stroma fractions (T3 and Y100) contain about nearly twice as much neoxanthin per Chl b than grana fractions (B3 and BS). Violaxanthin is evenly distributed among all fractions at a ratio of approximately 5 molecules per 100 total

chlorophyll. Generally, about 1 carotenoid is present for every 4 chlorophylls throughout the thylakoid membrane (Juhler *et al.* 1993). Zeaxanthin content is less than 1% of all carotenoids in all fractions These results are best summarized in table 8. Table 9 offers a summary of the PSIIα/β stoichiometry found through out the literature to aid in the understanding of the material employed in this study.

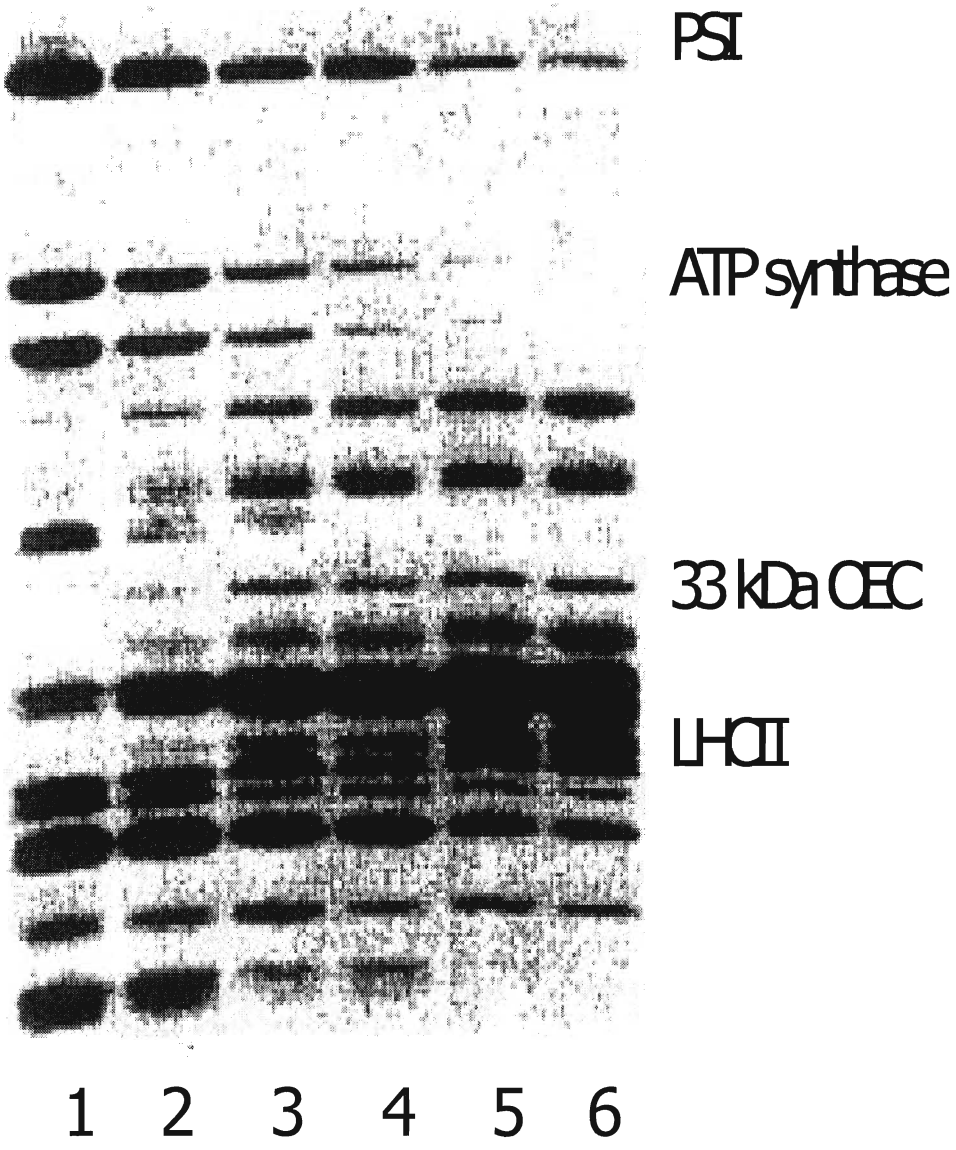

Figure 22
- SDS-PAGE in the presence of urea showing the polypeptide pattern in thylakoid membranes (lane 3) and subthylakoid membrane vesicles in lanes 1 - purified stroma, 2 - stroma lamellae, 4 - grana margins, 5 - grana, and 6 - grana core (Jansson *et al.* 1997).

Table 7 - PSII electron transfer activity in different domains of the thylakoid membranes from spinach (summarized from (Mamedov *et al.* 2000)).

Domain	O_2 evolution [μmol of O_2 (mg of Chl)$^{-1}$ h^{-1}]	O_2-centres (% of total centres, V_{H2O}/V_{DPC})	F_v/F_0	Chl *a/b*
Thy	120	80	0.7	2.9
BS	250-300	91	1.1	1.8-2.0
B3	200-250	84	0.96	2.2-2.4
Ma	102	66	0.48	3.0-3.3
T3	80	43	0.27	4.5-5.0
Y100	0	0	0.2	6.0-6.7

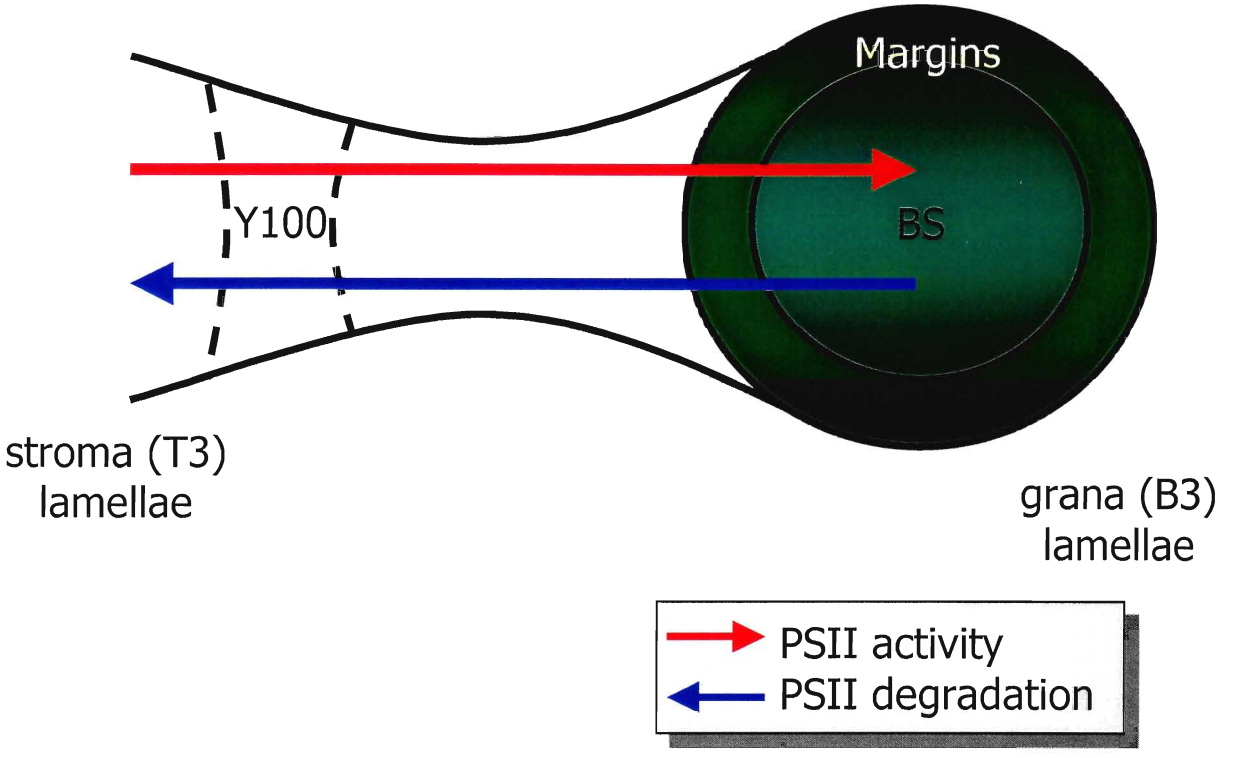

Figure 23 - PSII activity is highest in the PSIIα-rich grana core region of the thylakoid membrane, relative to PSIIβ-rich stroma lamellae regions, a phenomenon that occurs opposite its degradation (Mamedov *et al.* 2000).

Table 8 - Summary of the pigment composition of the thylakoid membrane fractions based on a % of the total molar pigment (Juhler *et al.* 1993).

Fraction	Carotenoids*				Chlorophylls	
	Neo.	Viola.	Lut.	β-car.	*a*	*b*
Thylakoid	2.5	3.7	8.1	7.1	57.5	21.2
BS	3.6	3.9	9.5	5.5	52.8	24.8
B3	3.4	3.9	9.3	5.2	55.3	22.9
Ma	2.6	4.2	7.7	7	57.6	20.9
T3	1.4	3.9	6.6	9.6	63	15.6
Y100	1	3.5	5.3	9.9	66.3	14

* Carotenoids = Neo. - neoxanthin; Viola. - violaxanthin; Lut. - lutein; β-car. - β-carotene

Table 9 - PSIIα/β stoichiometry gathered from various sources and authors.

Parameter	PSIIα	PSIIβ	Reference
% PSII	64-75	25-36	(Andreasson *et al.* 1988)
% in grana	66	33	(Albertsson *et al.* 1990b)
% in stroma	15-20	80-85	(Albertsson *et al.* 1990b)
% in BS			
% in Y100	12	88	(Henrysson and Sundby 1990)
Rel. conc.	1.43	0.48	(Melis and Anderson 1983)
Chl *a/b*	2.4*	4.6+	(Albertsson *et al.* 1990b)
% total Chl‡	38	3	(Albertsson *et al.* 1990b)
% PSII Chl	92.7	8.3	(Albertsson *et al.* 1990b)
	88	12	(Melis and Anderson 1983)
Chl *a*/core RC complex	40	40	(Melis and Anderson 1983)
Chl antenna	240	130	(Thielen and Van Gorkom 1981b)
	230	100	(Melis and Anderson 1983)
	250±40	120±20	(Melis 1991)
Chl *a/b* proteins	106 Chl *a*	45 Chl *a*	(Melis and Anderson 1983)
	84 Chl *b*	15 Chl *b*	(Melis and Anderson 1983)
Rel e^- transport	1.6	0.23	(Melis and Anderson 1983)
Q_B reduction	Yes	No	(Graan and Ort 1986; Melis 1985; Thielen and van Grokum 1981)

* 1.8-2.0 in BS
+ 6.0-6.7 in Y100
‡ PSII accounts for 41%, PSI accounts for 59% of total Chl

2.5. Gaussian Decomposition of Absorption Spectra

Proper analysis of the absorption spectra and its Gaussian decomposition of any photosynthetic apparatus can, with significant accuracy, estimate a subset of bands that may directly correspond to the relative absence and/or presence of any particular chlorophyll species in a set of samples (Ikegami and Itoh 1988; Zucchelli *et al.* 1994).

Absorption changes of pigments may be influenced by several mechanisms: (a) charge-induced energy shift, (b) pigment-pigment interaction, (c) mutual polarisability interaction and (d) distortion of the conjugated double bond system via conformation induction or nearby changes. The Q_Y transition of Chl *a* in ethanol peaks at 663 nm. The same pigment, when bound to Lhc proteins, reveals multiple absorptions in the 660 to 730 range, primarily at 677 and 670 nm with relative dipole strengths of 1:2 (Croce *et al.* 2000). Primary Q_Y transitions of chl *b* occur at 652 and 644 nm with relative dipole strengths of 2:1 (Hemelrijk *et al.* 1992). More specifically five Gaussian bands can be resolved from isolated PSII antenna. Unlike the Q_Y absorption spectra of bacterial reaction centres which consist of four bacteriochlorophylls (Bchl) over a range of as much as 3000 cm^{-1}, the PSII reaction centre employs six Chl *a* over a range of merely 500 cm^{-1} (Gall *et al.* 1998). The absorption maxima (Q_Y transitions) are present at 660, 670, 678, 684, and 695 nm. Chl *b* usually renders a single spectral band and usually absorbs maximally near 648 nm (Jennings *et al.* 1993). It is clear that the absorption spectrum of an light-harvesting complex is the product of individual chromophore absorption at different protein sites, mediated also by coupling between pigments. Attempts have been made to modify the native chlorophylls within the PSII reaction centre, but to no great achievement. Ideally, chromophore substitution would expand the Q_Y absorption range to one similar to that of the bacterial reaction centre, thereby, expediting spectroscopic discrimination of individual chromophore contributions. Nevertheless, regardless of the method of chromophore exchange, it remains unclear exactly which of the six reaction centre chlorophylls was exchanged (Gall *et al.* 1998). Longer wavelength absorption bands are typically associated with PSI (Andreeva and Velitchkova 1998; Cramer and Butler 1968; Kochubey and Samokhval 2000)

Linear dichroism studies have shown that Q_Y transition dipoles of Chl *b* within the PSII antenna are oriented greater than 35° out of the membrane plane. Similarly shorter wavelength Chl *a* molecule Q_Y transitions are oriented right about that same angle. Long wavelength forms of Chl *a* ($\lambda > 676$ nm) employ Q_Y transition dipoles very near to the plane of the membrane (Breton and Vermeglio 1982; Zucchelli *et al.* 1994).

2.6. PSII Absorbsance Cross-section

Energy transfer among Chl within the antenna of PSII is governed by the distance between them. It can occur in two ways. Resonance energy transfer (intermolecular transfer, also known as Förster transfer) depend on the degree of overlap between the fluorescence emission spectrum of the donor and the absorption band of the acceptor. This excitation transfer is not a series of fluorescence emissions followed by rapid reabsorptions, but rather a intimate coupling among the closely spaced chlorophyll molecules in the antenna. The relative orientations of the donor and the acceptor within the pigment-protein matrix affects the efficiency of the transfer. This transfer is inversely proportional to the sixth power of the distance between donor and acceptor. A distance of 2 nm between pigments takes approximately 1 ps. Förster R_0 values (critical distance) have been known for some time. Typically, a Chl *a*-Chl *a* transfers requires an R_0 of 100 Å, whereas a Chl *b*-Chl *a* transfer requires only 80-90 Å (van Grondelle 1985). The beauty of the Lhc proteins that make up the bulk of the PSII antenna is their ability to hold chlorophylls at precise orientations and proper distances for optimal energy transfers. This distance is typically less than 5 nm, however chlorophylls held too close to one another may quench each other. Ultimately, resonance excitation energy transfer is a means to funnel exciton towards and into the reaction centre, P680.

The second method, delocalized exciton coupling (intramolecular transfers) occurs when pigment molecules are within 1.5 nm of each other. Direct interaction among molecular orbitals of two molecules exists such that excitation is shared between them. Delocalized exciton coupling occurs at much faster rates than resonance energy transfers, such that they are virtually instantaneous since the distance travelled is so short. In PSII antenna, which harbour carotenoids

(Car) as well as Chl *a* and Chl *b*, intramolecular energy transfers are required to move excitation from the short lived Car^* within van der Waals distances for efficient energy transfer.

The measurement of PSII absorbance cross sections is dependent on these inter- and intramolecular interactions and quantifies the functional size of the chlorophyll network employed by the photosynthetic unit to drive primary photochemistry. Single turnovers of PSII to generate Q_A^- are accomplished by pump flashes of varying intensities. The pump flash is short enough (6 ns in this study) to close PSII centres shortly before a weak probe flash used to assay the fluorescence yield. A typical pump-probe experiment measures the fluorescence yield at various pump flash intensities from zero, F_0, to saturating, F_{SAT}, the maximal level of fluorescence achieved with a single turnover saturating flash. F_{SAT} is not to be confused with F_M, since the fluorescence yield following a short high light single turnover flash can not reach the maximal level of fluorescence, severely underestimating F_V/F_M. Not until the flash lasts for longer than 200 ms can F_M be accurately measured (Lazár 1999).

2.7. Fluorescence Induction Kinetics

Chl *a* fluorescence induction is a widely used technique to probe primary photochemistry non-invasively, but with high sensitivity. The data collected with this technique, employed for more than six decades, is often difficult to interpret. About ten years ago researchers began questioning whether or not to continue pursuing its elusive benefits (Holzwarth 1993; Lazár 1999). More recently however, these intriguing measurements are proving to be useful in determining biophysical parameters such as antenna size with respect to PSII heterogeneity in addition to rates of quinone reduction (Lazár *et al.* 2001).

The purpose of structural heterogeneity of PSII has been assayed by fluorescence induction. The area over the fluorescence induction curve is a measure of the number of photons (quanta) not released as fluorescence while open PSII centres are reduced and converted to their closed states. Conceivably, this yield may be used to perform photochemistry. Time resolution offers insight into the progress of said photochemistry. Furthermore, the size of the acceptor pool

may be estimated by measuring the size of the area if the light-induced charge separation is maintained in these pools (Melis and Homann 1975). Semilogarithmic plots have illustrated two kinetically different phases, one fast and nonexponential, and the other slow and exponential. These two phases have been attributed to the two distinct forms of PSII discussed previously, PSIIα and PSIIβ respectively (Hodges and Barber 1986).

2.8. Picosecond Fluorescence Decay Kinetics

Light energy absorbed by a chlorophyll molecule establishes an exciton with some finite equilibration time in the antenna chlorophyll. Both thermal equilibration within protein matrices and spatial equilibration among the entire chlorophyll antennae are considered here. Rapid equilibration times, relative to the fluorescence lifetimes, are indicative of a trap-limited system, since the fluorescence emission spectra are maintained constant, regardless of the excitation wavelength. If this were not so, in a diffusion-limited system, the equilibration time is comparable to the overall fluorescence lifetime, therefore, the excitation at far-red wavelengths would shorten substantially the fluorescence lifetimes since molecules neighbouring the reaction centre would be preferentially excited.

The origins of the various variable fluorescence parameters are resolved by picosecond fluorescence decay kinetics at any given fluorescence yield, be it F_0, F_M or F_{SAT}. Fluorescence decay offers much more information than other "slower" fluorescence measurements by revealing more intricate interpretations of fluorescence yield changes. Coupled with a suitable kinetic model of the origins of chlorophyll fluorescence decay components, fluorescence decay measurements are useful in the development of simulations of experimental results. Unfortunately, the time-resolved spectroscopic techniques that attempt to measure these kinetics remain problematic since excited state transfer processes that precede electron transfer obstruct their detection. The rate constants derived from this measurement, however, remain useful in illustrating the primary photochemical events in photosynthesis and add to the accurate description of a comprehensive kinetic model of the energy transfer processes in PSII (Vasil'ev *et al.* 2001).

Since the primary events in photosynthetic energy transfer are multicomponent in nature, the observed kinetics depends upon not only λ_{exc}, but also the detection wavelength, λ_i. In a series of λ_i, within a certain range, at a particular λ_{exc}, the contribution of each component is very likely to change as one scans the data set. These kinetic components, or fluorescence lifetimes, can be analysed in a couple of different ways. Traditionally, these types of data were analysed separately using single-decay analysis. A biexponential decay:

$$I(t,\lambda_{exc},\lambda_i) = \sum_{j=1}^{n} (\lambda_{exc},\lambda_i)\cdot \exp(-t/\tau_j) \qquad (20)$$

with n=2 would render four unique parameters with two amplitudes, A_j, coupled to two fluorescence lifetimes. This analysis offers only these two lifetimes with the same amplitude at all λ_{exc} and λ_i. Single-decay analysis does not account for the fact that certain fluorescence lifetimes are connected, or even constant, across all individual decay data collections. Therefore, more fitting parameters are determined from the data set than required (Holzwarth 1996).

The alternative to single-decay analysis is global analysis. A single parameter set for all experiments from a combined analysis performed in a single analysis run may be generated by taking explicit account of connected parameters within a systems across an entire experiment. In the example illustrated above with a biexponential decay where n=2, a relationship exists among the fluorescence lifetimes across the experiments that can be describe by the simple identity;

$$\tau_1(\lambda_1) = \tau_1(\lambda_2) = \ldots \tau_1(\lambda_i) \qquad (21)$$

and;

$$\tau_2(\lambda_1) = \tau_2(\lambda_2) = \ldots \tau_2(\lambda_i) \qquad (22)$$

This simple relationship, where one of two fluorescence lifetimes, τ_1 and τ_2, is associated with each detection wavelength, λi, in a series, illustrates how these lifetimes may be commonly connected across experiments. With global analysis of this simplified example the total number of parameters, P generated from a complete data set is with M experiments,

$$P_{global} = 2 * M + 2 \quad (23)$$

whereas, with single-decay analysis, P is;

$$P_{\sin gle} = 4 * M \quad (24)$$

P_{single} is larger than P_{global} in all cases where $M > 1$. Therefore, from identical data sets, a global analysis provides the same information with less parameters. Global analysis allows increased accuracy in the values of the extracted parameters so, more complex systems, with fluorescence lifetimes very close to one another can ultimately be achieved (Holzwarth 1996).

Global analysis was first applied by Knorr and Harris, 1981. Within the realm of photosynthesis research, global analysis was first applied by Holzwarth *et al.,* 1987, Wendler *et al.,* 1986 and, Wendler and Holzwarth 1987. Global target fitting, and its employment within PSII heterogeneity is a decade old exercise (Roelofs *et al.* 1992). The authors have suggested from, this pioneer paper, that PSIIα and PSIIβ exhibit different molecular functioning with respect to the primary processes. These differences may emerge from a different molecular structure of the reaction centres and/or a different local environment of these centres. Spatial heterogeneity was suggested as well.

Several studies have suggested that separate lifetime components can be observed from PSIIα and PSIIβ. Lifetimes of 250 ps and 500 ps have been observed for PSIIα centres at F_0. Meanwhile lifetimes of 100 ps and 500 ps have been reported for PSIIβ (Beauregard *et al.* 1991; McCauley *et al.* 1990; Schatz *et al.* 1988). At F_0 it is reported that one lifetime is expected to reflect the Pheo re-oxidation kinetics of several hundred picoseconds. The other, much shorter lifetime, is believed to be proportional to the number of pigment molecules in the antenna. Accordingly, a PSIIβ centre, with 100 chlorophyll molecules associated with its antenna should have a fluorescence lifetime slightly longer than that which is observed for reaction centres isolated from *Synechococcus* PCC 7942 (80 ps) which contain 80 chlorophyll molecules per antenna. Furthermore, one may also predict that the 250 chlorophyll antenna of PSIIα centres should emit a fluorescence lifetime three times longer than that of the cyanobacteria. Common to both α- and

β- centres, is a third component of about 500 ps, originating from reaction centre primary photochemistry (McCauley *et al.* 1990).

The current study is a comprehensive effort with one goal. To characterize PSIIα and PSIIβ comparatively and quantitatively. Comparisons to some of the top photosynthesis research within the realm of PSII heterogeneity will aid in this endeavour. The five biophysical techniques employed in this study to describe the significance of these differences are:

- Low temperature absorption spectroscopy
- PSII absorbance cross section
- Fluorescence induction kinetics analysis
- 77K fluorescence emission spectroscopy
- Time-correlated single photon counting (TC-SPC) of chlorophyll fluorescence decay kinetics

These techniques, some of which based on tested models of the primary events in photosynthesis, have been chosen for this study for three reasons. First, three of the five have never been performed on the domain specific thylakoid membrane fractions, only on the whole thylakoids of higher plants. Secondly, they offer superior resolution to probe deeply into the structure and function of photosynthetic complexes. Lastly, together, these techniques are best suited to analyse the two modes of PSII heterogeneity discussed earlier. Antenna heterogeneity with respect to pigment composition and size will be probed by the low temperature absorption spectra and the PSII absorbance cross sections, respectively. PSII antenna size will also be described with respect to the fluorescence induction kinetics. The heterogeneity of PSIIα (Albertsson *et al.* 1990c; Albertsson *et al.* 1990d) will also be addressed. TC-SPC of chlorophyll fluorescence decay kinetics will illustrate the reducing side heterogeneity. The data presented here, representative of PSII in different domains of the thylakoid membrane, may be compared to proposed properties and distributions of PSIIα and PSIIβ centres.

3. Materials and Methods

3.1. Preparation of Thylakoid Membrane Fractions

All thylakoid membrane fractions were prepared by the photosynthesis group at the University of Lund, Lund, Sweden, under the direction of S. Styring. The nondetergent method (Albertsson *et al.* 1994) of isolation is described in detail in appendix 8.1.

3.2. Gaussian Decomposition of Absorption Spectra

Measurements were obtained at 10K using a cryostat (Advanced Research Systems, Inc., model DE-202, Allentown, PA) coupled with a helium compressor (APD Cryogenics, Inc., model HC-2D-1, Allentown, PA) controlled by a microprocessor-based digital temperature indicator/controller (Scientific Instruments, Inc. Series 9600, West Palm Beach, CA). Thylakoid fractions were resuspended in resuspension buffer (see appendix 1) with 60% glycerol as a cryoprotectant and sealed between two, 2.5 cm polycarbonate lexan discs, separated by a 2 mm thick PVC ring and sealed in the cryostat chamber. A beam of white light was cast through a pinhole towards the chamber. Transmitted light was then sent through frosted glass towards an intensified diode array detector interface (model 1461 EG&G Princeton Applied Research, Princeton, NJ). The resultant signal was plotted as the log of transmittance (minus the background) against wavelength.

Nonlinear curve fitting was done with the commercial software package Origin 4.1. Ten Gaussian sub-bands where strategically placed according to major negative peaks present in the second-order derivative of the absorption spectra similar to (Schmid *et al.* 2001). The shape of each sub-band was determined by the equation;

$$y = y_0 + \frac{A}{w\sqrt{\pi/2}} e^{-2\frac{(x-x_c)}{w^2}} \qquad (25)$$

where A is the area contained beneath the curve, w is its half-width in nanometres and x_c is the centre wavelength of its peak. All thylakoid membrane fractions were fitted globally by sharing nine

of the ten peak centres (all but *xc7* at ~676 nm) and letting their half-maximum widths and contained areas free using the Levenberg-Marquardt non-linear curve fitting algorithm to a reduced Chi-square of 6.68×10^{-6}.

3.3. PSII Absorbance Cross-section

The pump-probe method of fluorimetry was used to determine the absorption cross-section of PSII. A pulsed Neodynium:Yttrium-Aluminum-Garnet laser, Nd:YAG (Spectron Laser Systems, Rugby, U.K. model SL456G-10) coupled with an Beta-Barium Borate Optical Parametric Oscillator (GWU-Lasertechnik VirIR 2, Erftstadt, Germany) was used to fire a 6 ns pump flash at 435 nm via a fibre optic cable to a 250 µL flow through cuvette (~1 mL/sec) containing a thylakoid preparation (5 µg·Chl·ml^{-1}) to obtain F_{SAT}, the saturating level of fluorescence induced by a single-turnover pulse of light. Non-actinic 60 µs probe pulses of light were supplied by four low intensity light-emitting diodes, at 450 nm excitation, focussed at 90° to the direction of the pump flash 100 µs after the pump flash. Chlorophyll fluorescence was measured at 90° to the direction of the probe flash from the cuvette through a fibre optic light guide towards a photomultiplier tube (Hamamatsu RG967) behind the monochromator. In the absence of the pump flash, the level of chlorophyll fluorescence obtained from probe flashes alone represented F_0.

A motorized light polarizer was used to adjust the flash energy before the beam was cast on the flow through cuvette. Relative intensities of each pump flash were gathered from reflected actinic light from a glass slide positioned between the light polarizer and the fibre optic, to a photodiode connected to a 9-volt biassing battery. The pump-probe triggers, photodiode and the photomultiplier tube are connected to channels 1, 2 and 3, respectively of a digital storage oscilloscope (Tektronics, model TDS 540) and uploaded to a computer data collection program. Each data point was the average of 20 signals at a pulse frequency of 2.5 Hz. Flash saturation curves were acquired using a set program of positions on the motorized light polarizer in the path of the pump pulse (Figure 24).

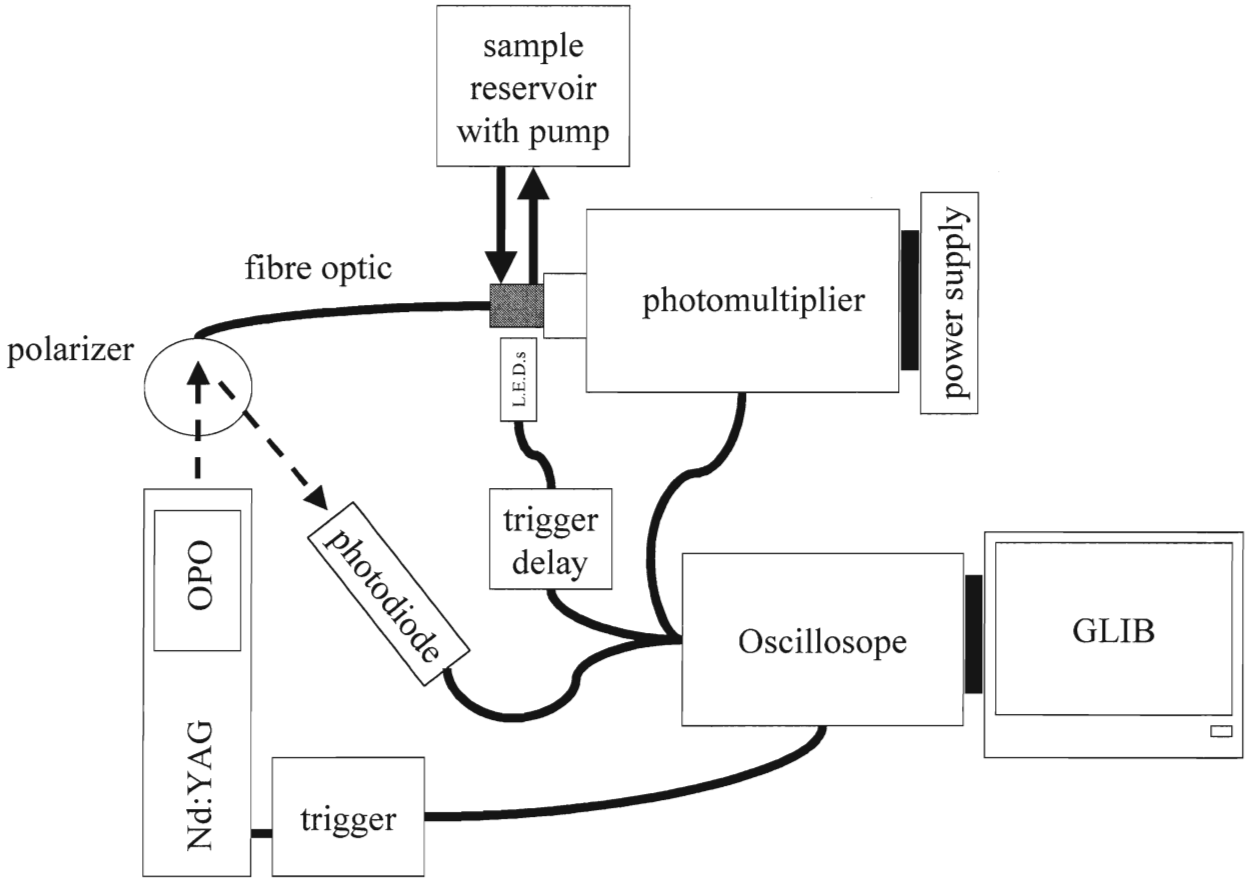

Figure 24 - PSII absorbance cross-sections were collected using this experimental setup. Increasing relative fluorescence was measured as flash intensity increased and managed by the DOS-based software program GLIB.

Curve-fitting was performed with Origin 4.01. The cumulative Poisson single-hit probability distribution (Mauzerall and Greenbaum 1989) was used to fit the data:

$$\Phi(I) = \Phi_{MAX}(1 - e^{-I \times \sigma}) \quad (26)$$

For variable fluorescence fro F_0 to F_M equation 26 is written as:.

$$F(I) = F_0 + F_M(1 - e^{-I \times \sigma}) \quad (27)$$

where *I* is the flash intensity, $\Phi(I)$ is the yield of photoproduct measured (fluorescence), Φ_{MAX} is the maximum yield (F_M) and σ is the effective absorption cross-section, representing a homogeneous population of photosystems.

3.4. Fluorescence Induction Kinetics

The photochemical events mediated by PSII can be measured with room temperature fluorescence induction kinetics as an intrinsic probe. At room temperature fluorescence is emitted primarily from PSII. The contribution from PSI is merely 20% of the fluorescence signal in whole thylakoid. The first fluorescence induction experiments where conducted by Kautsky and Hirsh in 1931, hence it is often referred to as the Kautsky effect. Basically, fluorescence induction represents a plot of the measured fluorescence intensity as a function of time of continuous illumination (Lazár 1999).

The theoretical model of chl *a* fluorescence induction with consideration of a heterogenous population of PSII is described in Strasser and Stirbet, 1998. This model is based solely on the acceptor side of PSII (referred to as the complex model (Stirbet and Strasser 1996)). The portion of electron transport chain which involves Pheo, Q_A and the PQ pool are included in their simulations (Strasser and Stirbet 1998).

The theoretical relative variable fluorescence, *V(t)*, of PSII centres of type *i* can be calculated by equation 31, reported in (Strasser and Stirbet 1998; Strasser and Stirbet 2001);

$$V_i(t) = \frac{B_i(t)}{1 + C_i[1 - B_i(t)]} \tag{28}$$

where $B_i(t)$ is the fraction of the closed reaction centres (reduced QA) of the unit type *i* with:

$$C = \frac{p(F_M - F_0)}{F_0} \tag{29}$$

where *C* is the parameter for the curvature of the hyperbola, and *p* is the overall probability of connectivity between the PSII units.

According to Strasser's model, PSIIβ centres are considered isolated units (therefore $C_\beta = 0$). So, if *C*=1 for a mature plant, on average, then a heterogenous system with 60% of the total PSII centres being α-centres, C_α is predicted to be equal to 1.67. Subsequently, the total relative variable fluorescence, $V_{sum}(t)$ can be calculated as:

$$V_{sum}(t) = \sum_i f_i V_i(t) \tag{30}$$

where f_i is the fraction of PSII centres of type *i* relative to the total number of PSII centres in the sample (Strasser and Stirbet 1998).

Limited sample quantities allowed for the collection of fluorescence induction kinetics from the whole thylakoid membrane vesicles , B3, grana partition vesicles and T3, stroma lamellae vesicles only. For each sample a small volume (3 mL in a quartz cuvette) of membrane vesicles at a chlorophyll concentration of 10 µg/mL was dark adapted for 5 min. A 650 nm beam triggered by a pulse generator (Hewlett Packard 8011A), pulse width 200 ms at 500 $\mu mol \cdot m^{-2} \cdot s^{-1}$, was focussed on a randomizing fibre optic cast on the cuvette 90° to the photomultiplier (Hamamatsu

RG967) screened by a monochromator with a 680 nm longpass filter. The data were visualized on a digital storage oscilloscope (Tektronics, model TDS 540) and uploaded to a computer data collection program (GLIB). The averages of four kinetic traces was plotted semi-logarithmically as relative fluorescence (a.u.) versus time (s). During the fitting procedure, performed with a user-defined fit function in Microcal Origin 4.1, a model for homogeneous populations was employed. The more complex heterogenous model was unnecessary since fractionated thylakoid membranes offer nearly pure PSIIα and PSIIβ from the B3 fraction and the T3 fraction respectively. Also, the connectivity constant in equation 31 was left free during the fit to solve for B(t). Values of B(t) were calculated at the slow initial rise of fluorescence, B(O), the inflection point of the exponential rise, B(M), and the final plateau, B(P).

3.5. 77K Fluorescence Emission Spectra

A small volume (30-40 µL) of thylakoid membrane fractions at a chlorophyll concentration of 10 µg/ml in resuspension media were frozen at 77K in a heat-sealed Pasture pipette. At this temperature, the resolution of the multiple pigment-protein complexes is greatly enhanced. A monochromatic beam (435 nm) from a arc lamp screened with a monochromator (ScienceTech, model 9055) struck the sample 90° to the angle of emission detection by an intensified diode array detector interface (model 1461 EG&G Princeton Applied Research, Princeton, NJ). The resultant signal was plotted as relative fluorescence (a.u.) versus wavelength.

3.6. Picosecond Fluorescence Decay Kinetics

Measurement of time dependent fluorescence intensity may offer tremendous insight into the primary events in photosynthesis. More explicitly, this measurement allows researchers to predict, with significant accuracy, the relative fates of $P680^*$. Time-resolution is obtained when the excitation beam is pulsed (or modulated), rather than continuous in intensity. The signal intercepted is commonly the response to an optical excitation this brief (within the picosecond range in this study) excitation pulse at a particular wavelength λ_{exc} and is time-resolved by the

detector (Sauer and Debreczeny 1996). The arrival of a photon released by fluorescence at the detector is compared to the time of the excitation pulse. These photons arriving at particular time delays relative to the excitation pulse are gated into channels of a predetermined temporal width. A multichannel analyzer collects the fluorescence decay kinetic over a time scale determined by the time per channel, multiplied by the number of channels. In this study the time resolution is approximately 0.012 ns per channel on about 1000 channels. High signal-to-noise data in a relatively short time is permitted since fluorescence photons at multiple time delays are collected simultaneously. Time resolution is limited only by the pulse width of the excitation beam and the time response of the emission detector (Sauer and Debreczeny 1996).

A single photon timing apparatus driven by a picosecond pulsed diode laser was used to determine the kinetics of chlorophyll fluorescence decay on a sub-nanosecond time scale. (Bruce and Miners 1993). Excitation pulses were delivered at 406 nm from a pulsed diode laser (PicoQuant GmbH, Berlin, Germany, PDL 800-B, model LDH-C-2-042) with a pulse width of 54 ps (figure 25). Chlorophyll fluorescence was measured from the sample (5 $\mu g \cdot Chl \cdot ml^{-1}$) by a Hamamatsu R-3809 microchannel plate photomultiplier behind a double monochromator (model DH-10, Instruments SA, Inc., Metuchen, NJ), 90° to the angle of incident light yielding and instrument response function (IRF) of approximately ~58 ps. This IRF was collected as a background decay at 406 nm under experimental conditions. Data are collected as voltage when a photon emitted as chlorophyll fluorescence. Upon its capture, the time difference from excitation is used to plot its amplitude with respect to decay time. It is done this way since the entire fluorescence yield is produce by only about 10% of the photons from the pulsed diode laser. If the data collection started upon trigger of the excitation beam, the chlorophyll fluorescence signal would almost never be detectable. The electronic design of SPC apparati discussed in (Ainbund *et al.* 1992) in great detail. A diagram of the experimental set up is displayed in figure 26.

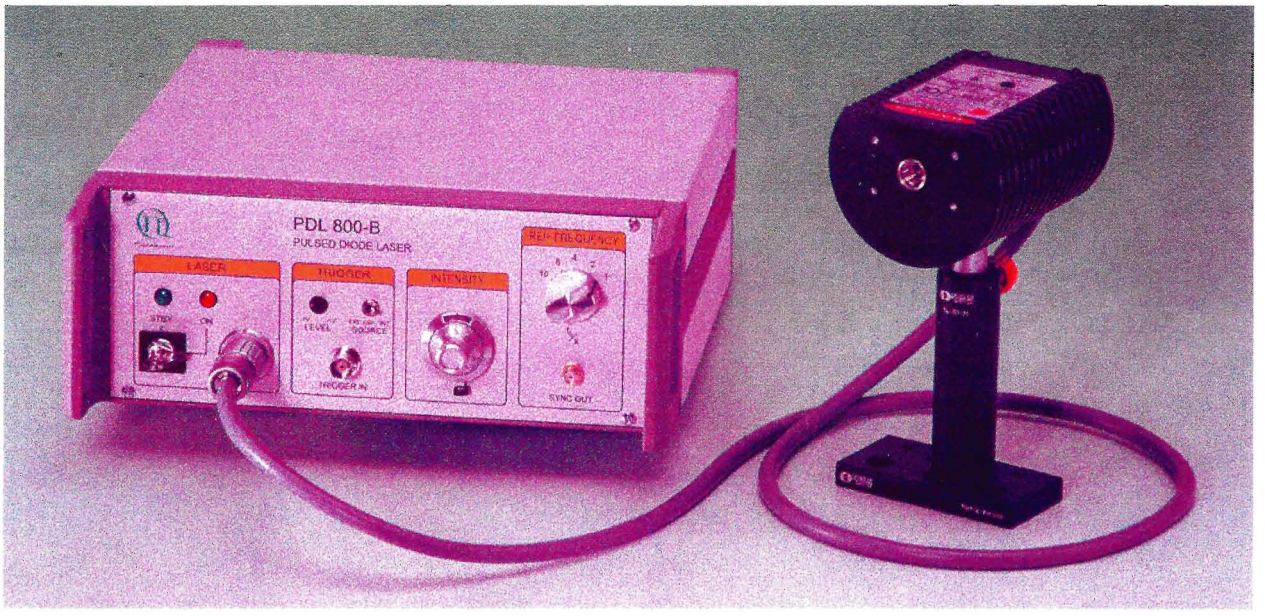

Figure 25 - The PicoQuant, PDL 800-B with the LDH-C 400 laser head.

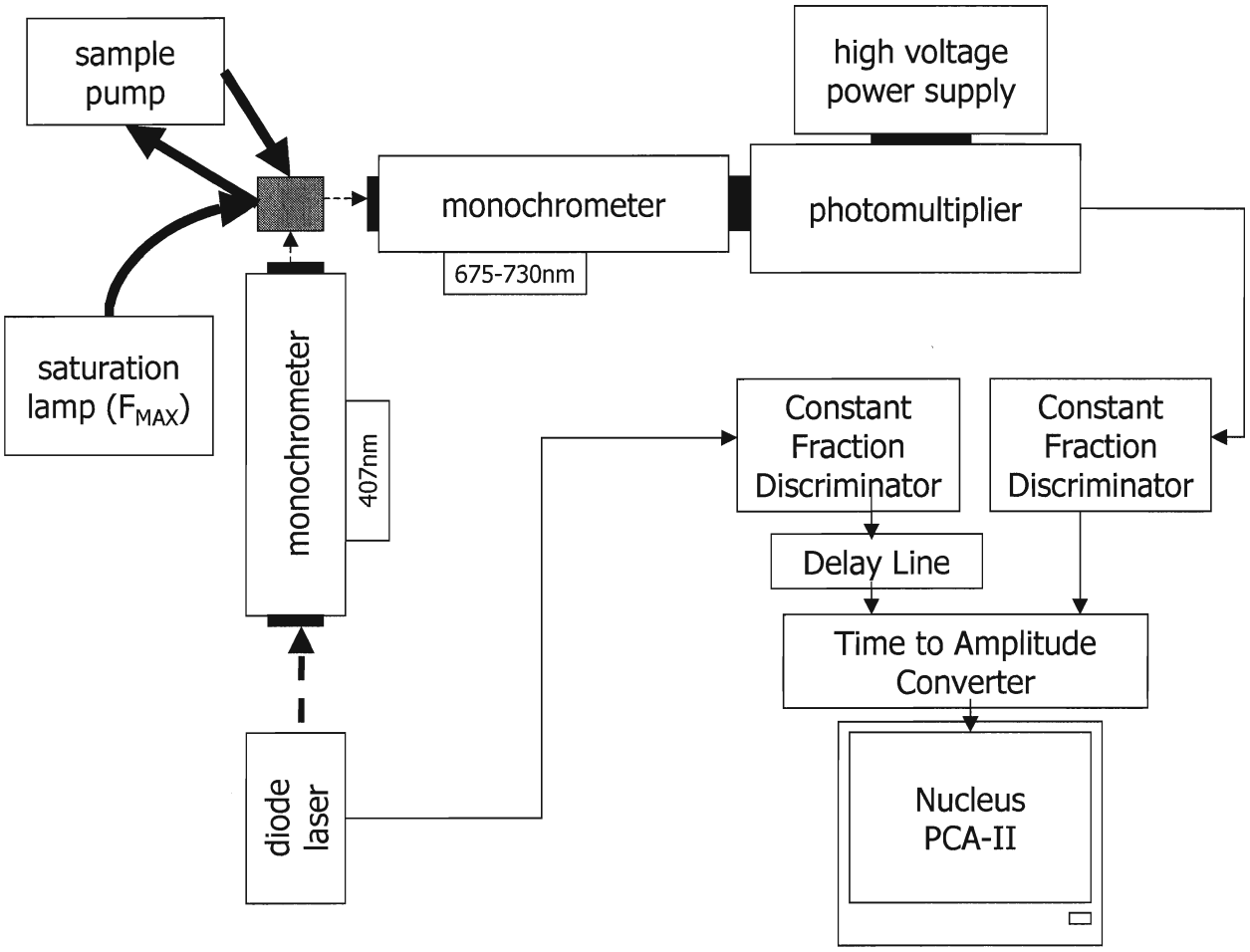

Figure 26 - Single-photon counting apparatus employed in picosecond chlorophyll fluorescence decay kinetics studies.

Measurements when PSII centres are open (F_0) and when PSII centres are closed (F_M) were performed at an excitation frequency of 5 MHz and 10 MHz and cold flow rates of ~1 mL/s and ~4 mL/s respectively.

Fluorescence decay data were collected for nine detection wavelengths between 675 nm and 730 nm at F_M, with 20,000 counts in the peak channel, each of which representing approximately 0.012 ns.

Data analyses were performed using a global target analysis and fitting package on a Linux-based system written by S. Vasil'ev similar to (Vasil'ev *et al.* 1998). Global analysis is a procedure in which all decays from the various emission wavelengths collected are analysed simultaneously in order to minimize the number of free parameters to fit. The fluorescence emission decay kinetic traces collected at each of the nine wavelengths where compared to the room temperature fluorescence emission spectra and fit, simultaneously for the desired number of components. As a general rule, more components are easier to fit to the data than fewer components. The resultant plot is a decay associated spectra (DAS). The DAS illustrate the relative contributions of each of the components in the fitting parameters to the spectra of emission wavelengths collected. Each decay component is measured with respect to the fluorescence lifetime and may be assigned to an early event in photosynthesis.

In each DAS fit with five unique exponentials a 120 ps to 260 ps component at F_M and a 100 ps to 140 ps component at F_0 can be subsequently deconvoluted in to two separate components. A PSII-type component with an amplitude most dominant in the short wavelength region of the DAS and a PSI-type component, most dominant in the long wavelength region of the DAS are easily resolved from the mixed component by calculating the sum of a known PSII decay (multiplied by a factor) and a known PSI decay. Therefore, the result is two distinct components with identical lifetimes representative of PSII and PSI from a single mixed component with that lifetime.

4. Results

4.1. Gaussian Decomposition of Absorption Spectra

It is reasonable to suspect that each specialized thylakoid membrane fraction may offer its own unique pigment-protein profile. Low temperature absorption spectroscopy, and its very fine resolution, offers the best opportunity to probe this uniqueness. Each absorption spectrum (figures 27-32) is plotted as absorption (a.u.) versus wavelength (nm). Ten Gaussian bands have been resolved in each spectrum. The analyses of these spectra is described in table 10. Table 22 (see appendix 8.2) offers insight in to their relative assignments.

The ratio of Chl *a/b* was calculated by the sum of the Chl *a* absorption bands (multiplied by the molar extinction coefficient) divided by the Chl *b* band (multiplied by the molar extinction coefficient). Appendix 8.3 shows a plot of these molar extinction coefficients in cm^{-1}/M versus wavelength (Du *et al.* 1998).

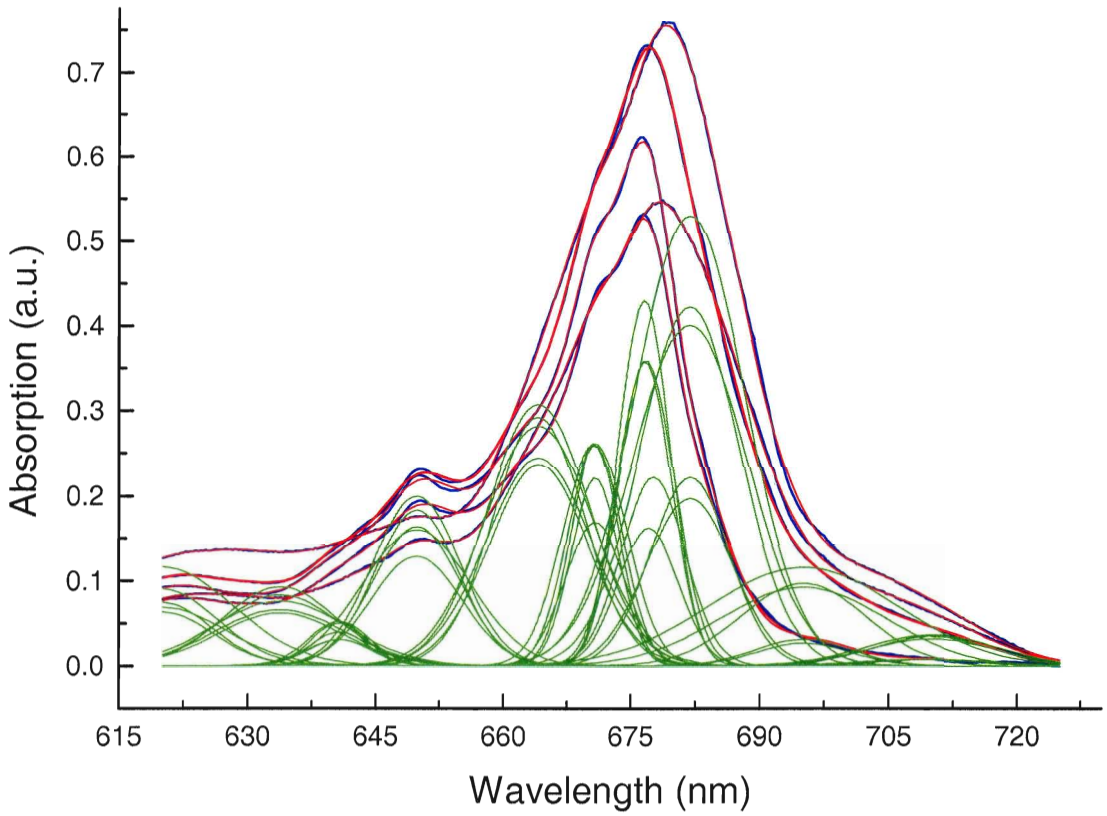

Figure 27 - Ten Gaussian sub-bands were fit globally to al five thylakoid membrane fractions simultaneously. Each plot represents the sub-bands (green), the data (blue) and the fit (red).

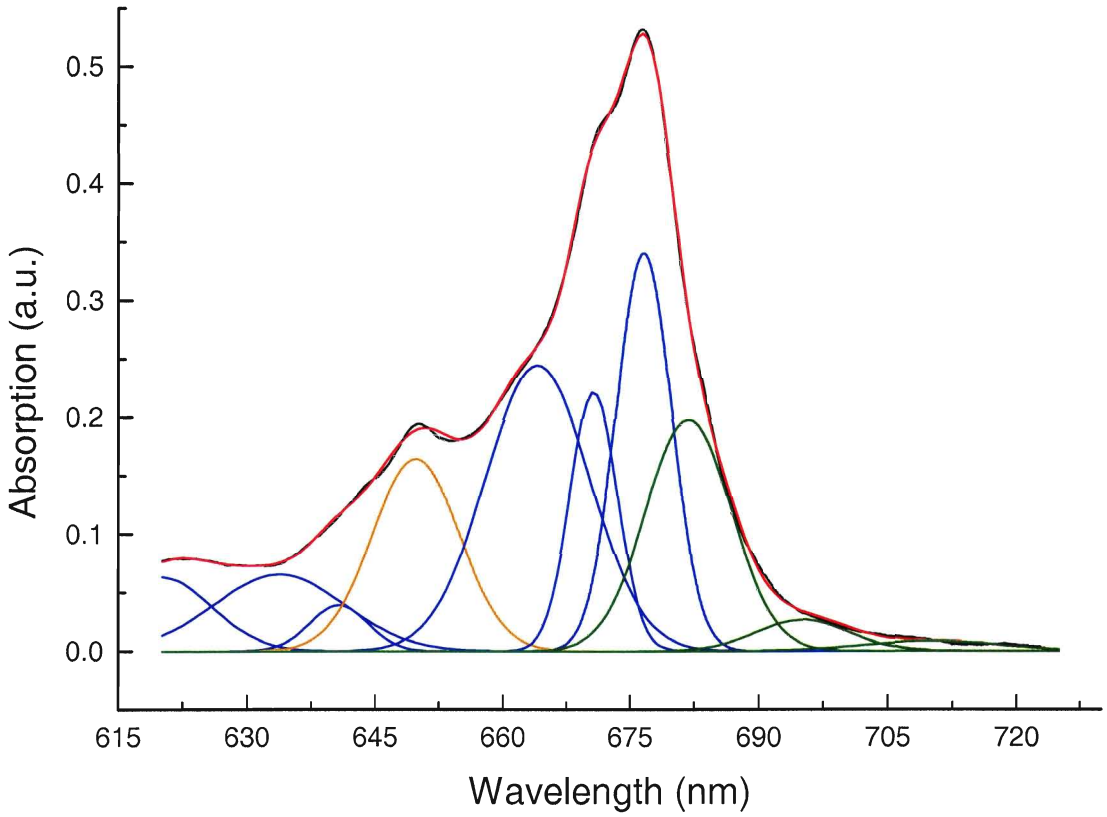

Figure 28 - Global Gaussian decomposition of the 10K absorption spectrum (black) of the grana fraction (B3) and its fit (red). Green bands (centred at nm, nm and nm) represent red shifted PSI components, whereas the orange band represent chl *b* Q_Y transition (centred at nm), primarily associated with PSII.

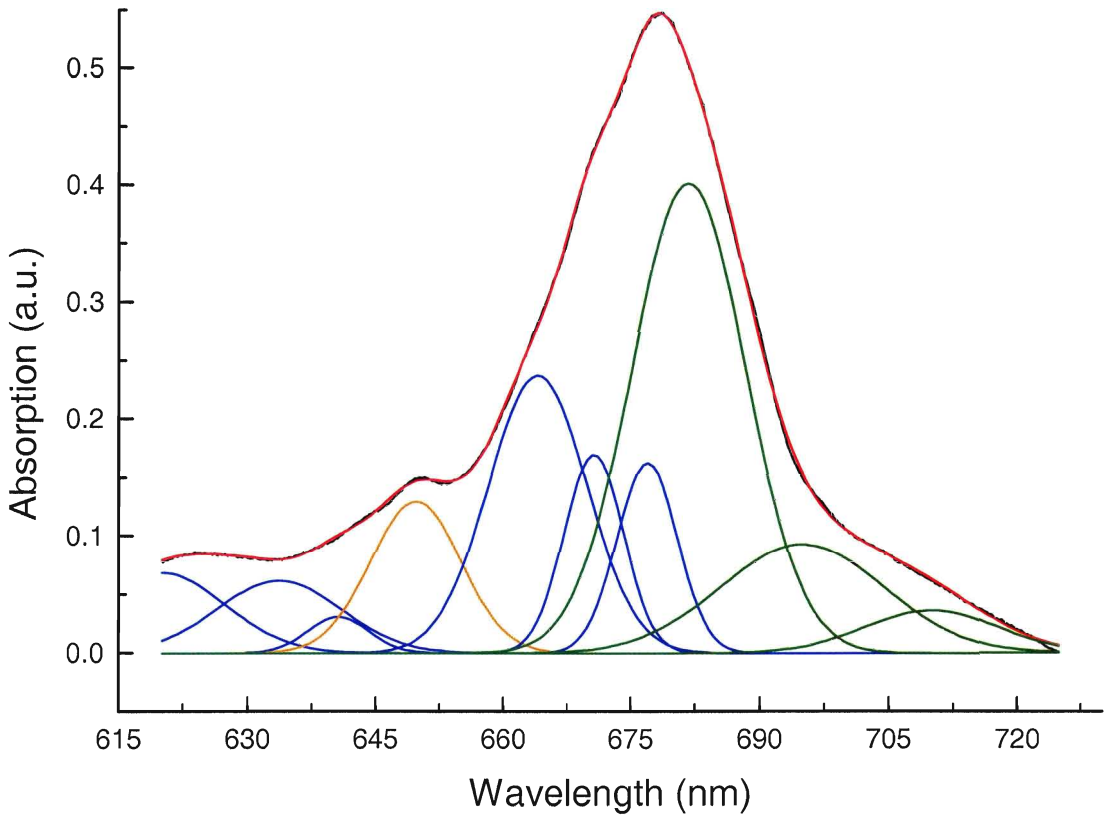

Figure 29 - Global Gaussian decomposition of the 10K absorption spectrum (black) of the stroma fraction (T3) and its fit (red). Green bands (centred at nm, nm and nm) represent red shifted PSI components, whereas the orange band represent chl *b* Q_Y transition (centred at nm), primarily associated with PSII.

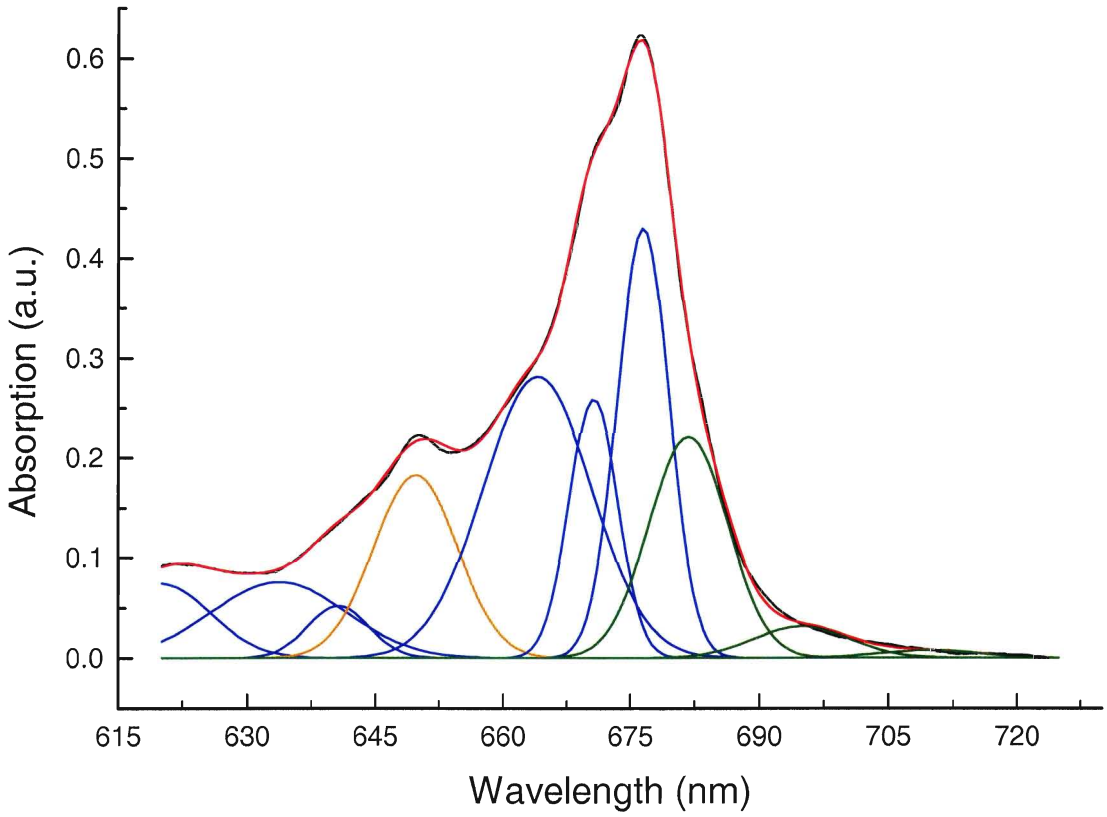

Figure 30 - Global Gaussian decomposition of the 10K absorption spectrum (black) of the grana core fraction (BS) and its fit (red). Green bands (centred at nm, nm and nm) represent red shifted PSI components, whereas the orange band represent chl *b* Q_Y transition (centred at nm), primarily associated with PSII.

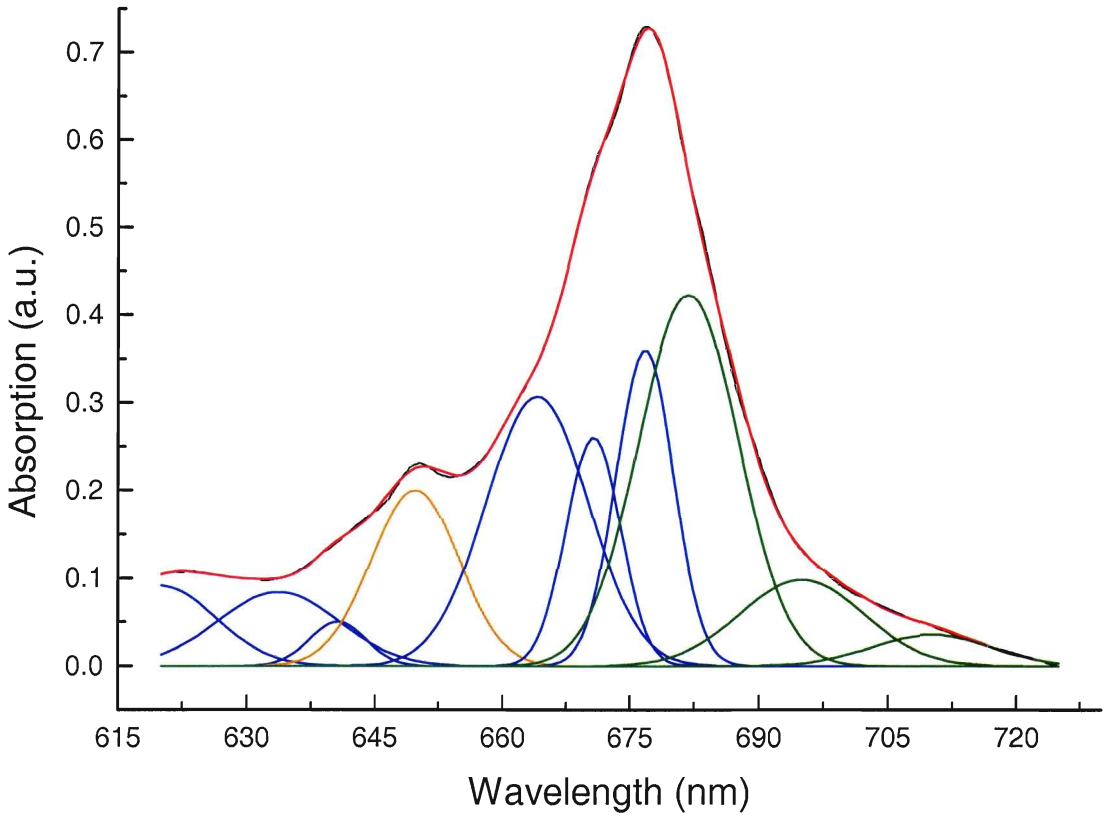

Figure 31 - Global Gaussian decomposition of the 10K absorption spectrum (black) of the grana margins fraction (Ma) and its fit (red). Green bands (centred at nm, nm and nm) represent red shifted PSI components, whereas the orange band represent chl *b* Q_Y transition (centred at nm), primarily associated with PSII.

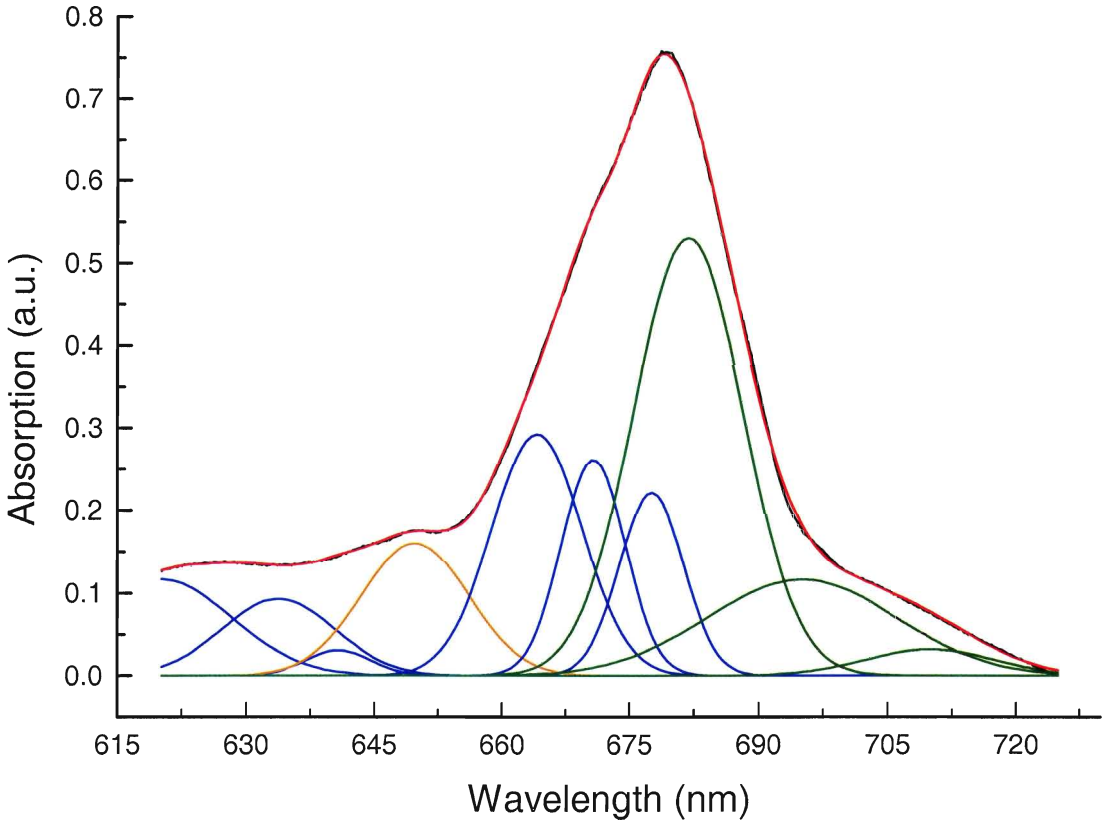

Figure 32 - Global Gaussian decomposition of the 10K absorption spectrum (black) of the purified stroma fraction (Y100) and its fit (red). Green bands (centred at nm, nm and nm) represent red shifted PSI components, whereas the orange band represent chl *b* Q_Y transition (centred at nm), primarily associated with PSII.

Table 10 -Ratio of the Chl *a*/*b* (Q_Y-transition) for thylakoid membrane fractions from Gaussian bands in figures 27 - 32.

Fraction	Chl *a*/*b* (Q_Y)
BS	3.2
B3	3.0
Ma	4.0
T3	5.3
Y100	4.6

4.2. PSII Absorbance Cross-section

Antenna side heterogeneity is illustrated further upon examination of the absorption cross-sections of PSII as it occurs in different thylakoid membrane fractions. Each flash saturation curve is plotted as relative fluorescence (a.u.) versus the log of light intensity, each step was kept constant among all membrane fractions. PSII absorbance cross-sections are easily interpreted by the coordinates of the inflection point of the sigmoidal curve. Relatively large PSII centres (with respect to their antennae) will demonstrate curves that are shifted to the left, or towards lower photon densities. This is very apparent upon examination of the PSII absorbance cross-section of the grana core (figure 34).

The opposite is true for smaller PSII centres. The probability of striking a small PSII antenna at lower photon densities is quite low. Therefore, the PSII absorbance cross-section of thylakoid fractions with small chlorophyll antennae will be shifted to the right, or towards higher photon densities. The purified stroma fraction illustrates this phenomenon very well (figure 34).

PSII absorbance cross-sections of the grana, stroma lamellae, and grana margins are presented in figures 33 and 34 respectively. Table 11 offers a summary of the data demonstrated by these measurements. The δ-value is numerical measure of the effective absorbance cross section. They have been normalized to a grana core relative absorbance cross section of 1. The grana core employs the largest relative absorbance cross section, $\delta = 1$, whereas the purified stroma employs the smallest, $\delta = 0.20$.

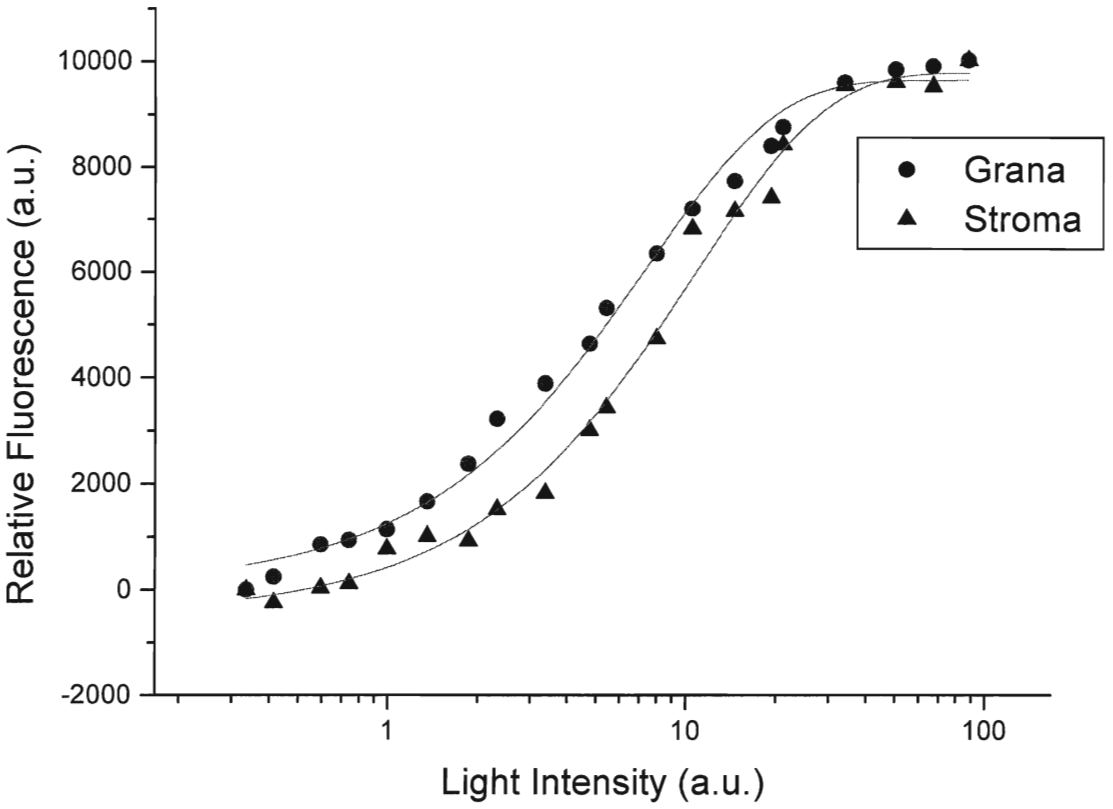

Figure 33 - Flash saturation curves of the grana fraction (B3) and the stroma lamellae fraction (T3). Each point represents the average of twenty individual single-turnover flashes. Lines are best fits to Poisson distribution with a computer-generated error of ~3%.

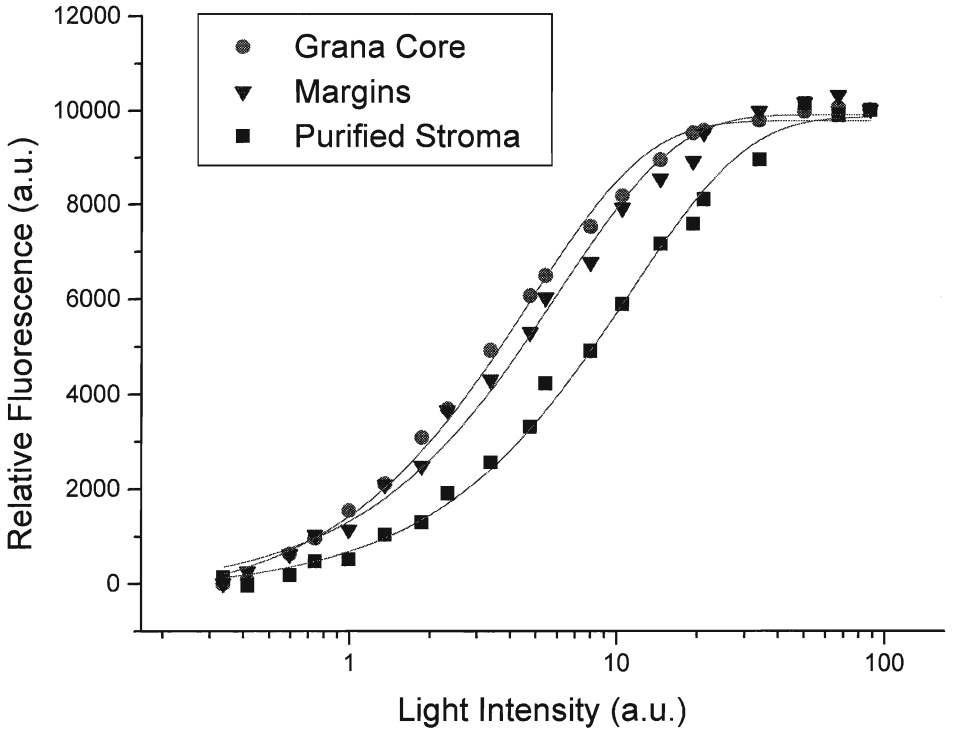

Figure 34 - Flash saturation curves of the grana core fraction (BS) and the purified stroma lamellae fraction (Y100). Each point represents the average of twenty individual single-turnover flashes. Lines are best fits to Poisson distribution with a computer-generated error of ~3%.

Table 11 - PSII absorbance cross section (δ) obtained from flash saturation curves, figures 33 and 34. The fit error is no more than ± 5%

Fraction (χ^2)	δ (Relative Cross section*)
BS	1
B3	0.90
Ma	0.31
T3	0.27
Y100	0.20

* Relative to the grana core fraction with a fixed cross section of 1.

4.3. Fluorescence Induction Kinetics

The rise of chlorophyll fluorescence has been an intrinsic probe of both antenna heterogeneity and reducing-side heterogeneity. Here the rate of PSII closure may be measured by applying model fitting functions to experimentally obtained data. Figures 35, 36 and 37 are semilogarithmic plot of the fluorescence rise curves for whole thylakoid membrane vesicles, stacked grana membrane vesicles and unstacked stroma lamellae vesicles respectively. With each curve its fit, generated by Strasser's model for homogenous populations of PSII, is plotted as well (Strasser and Stirbet 1998; Strasser and Stirbet 2001).

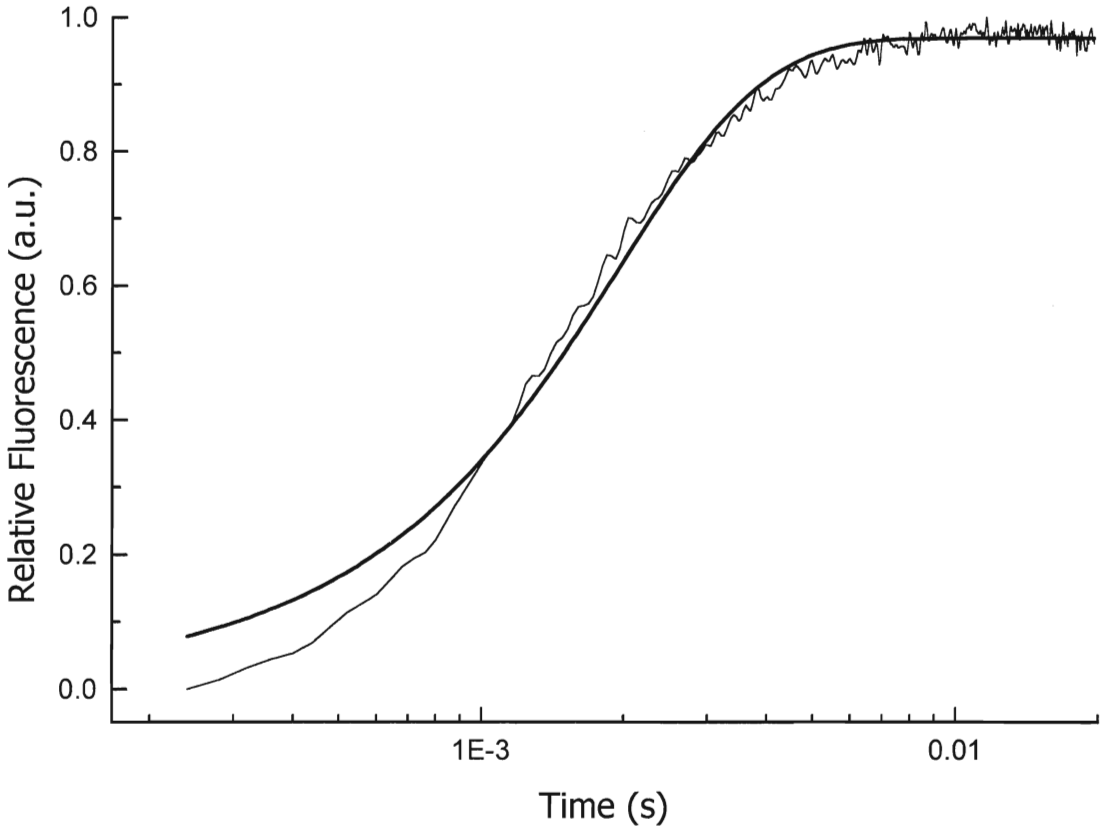

Figure 35 - Fluorescence induction kinetic from whole thylakoid and its fit (bold) using Strasser's model for connectivity within homogeneous PSII populations (Strasser and Stirbet 1998; Strasser and Stirbet 2001).

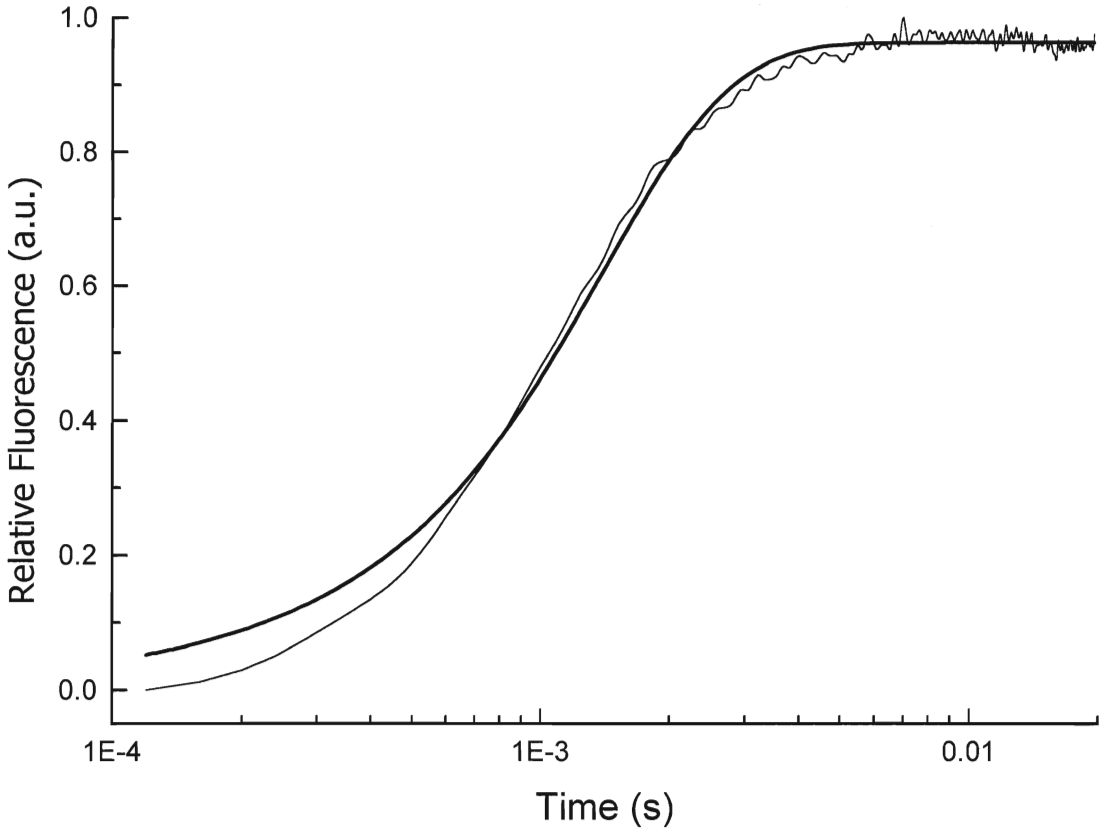

Figure 36 - Fluorescence induction kinetic from B3, grana partition, and its fit (bold) using Strasser's model for connectivity within homogeneous PSII populations (Strasser and Stirbet 1998; Strasser and Stirbet 2001).

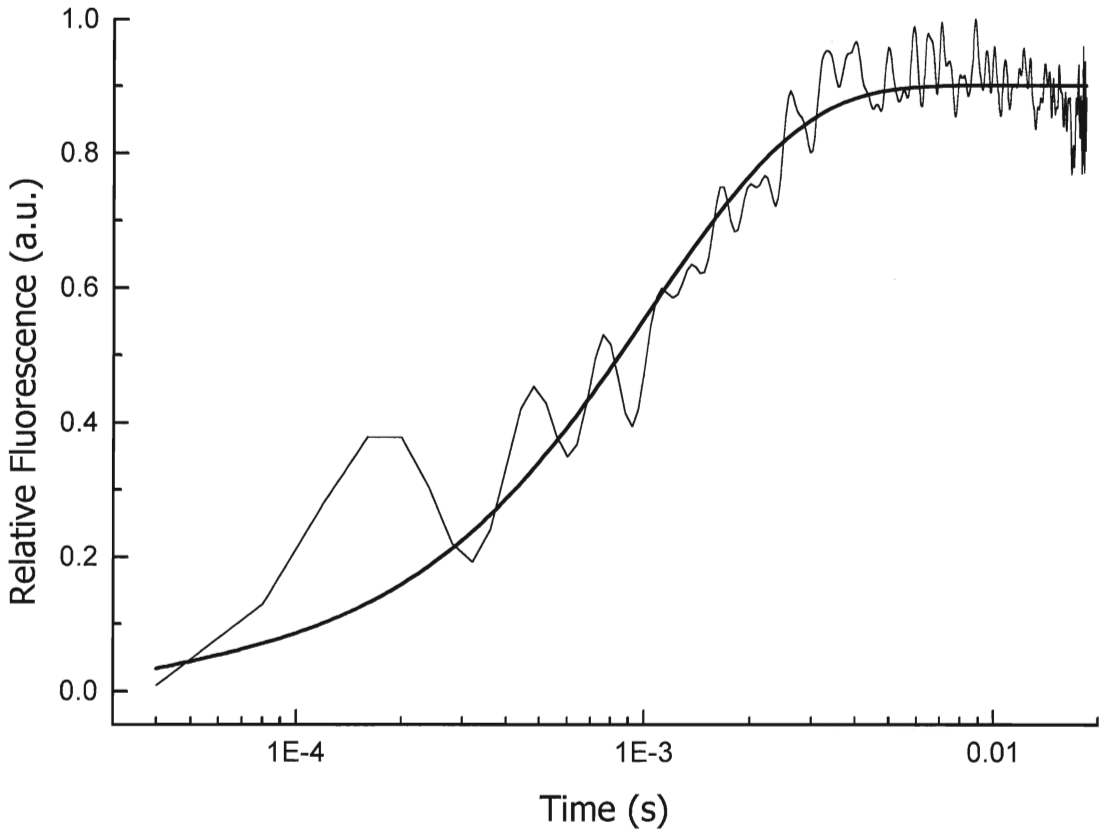

Figure 37 - Fluorescence induction kinetic from the T3, stroma lamellae, fraction thylakoid membranes and its fit (bold) using Strasser's model for connectivity within homogeneous PSII populations (Strasser and Stirbet 1998; Strasser and Stirbet 2001).

Table 12- Connectivity and rate constants obtained from the fitting fluorescence induction kinetic traces with Strasser's model for homogenous populations (Strasser and Stirbet 1998; Strasser and Stirbet 2001)*.

Fraction (χ^2)	Connectivity	Rate constant
Thylakoids (3.6×10^{-4})	1.89	941.48
Grana (2.2×10^{-4})	2.08	1350.19
Stroma Lamellae (2.45×10^{-3})	0.00	956.68

4.4. 77K Fluorescence Emission Spectra

The 77K fluorescence emission spectra in figure 38 have been clearly divided into PSII-rich thylakoid membrane fractions and PSI-rich thylakoid membrane fractions. These high resolution spectra were assayed for their relative ratios of typical PSII emissions (F_{695}) to typical PSI emissions (F_{730}). The F_{695}/F_{730} is useful in determining PSII:PSI ratios, employed in the kinetic modelling of the primary events in PSII performed in section 4.6. Also determined from these spectra are the F_{685}/F_{695} ratios. This parameter offers insight into the degree of LHCII association among the thylakoid membrane fractions. Both of these measurements are presented in table 13.

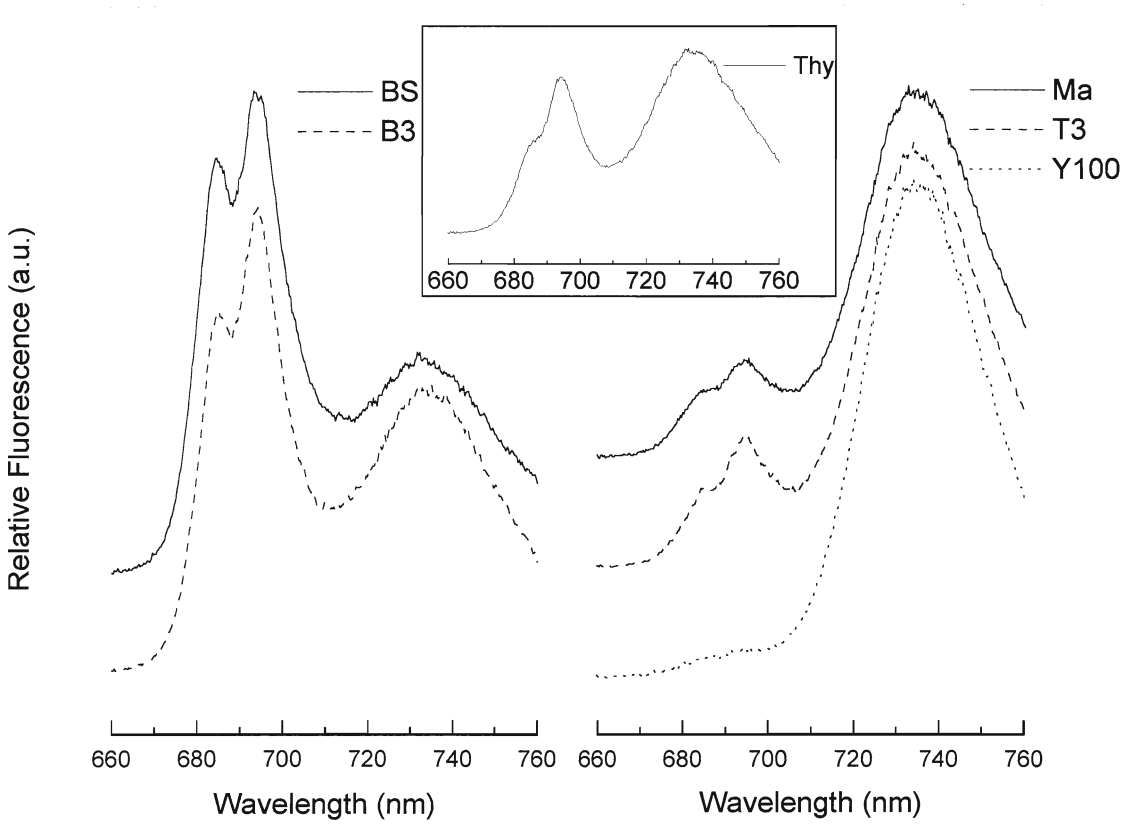

Figure 38 - 77K fluorescence emission spectra of PSII-rich thylakoid membrane fractions (left) and PSI-rich thylakoid membrane fractions (right) and whole thylakoid membranes (inset). See table 13.

Table 13 - Ratios of F_{695}/F_{730} and F_{685}/F_{695} derived from the 77K fluorescence emission spectra in figure 38. The error of these spectra is less than 3%.

Fraction	F_{695}/F_{730} (a.u.)	F_{685}/F_{695} (a.u.)
Thylakoid (Thy)	0.88	0.60
Grana Core (BS)	2.20	0.88
Grana (B3)	1.62	0.81
Margin (Ma)	0.29	0.73
Stroma Lamellae (T3)	0.34	0.65
Purified Stroma (Y100)	0.08	-.-

4.5. Picosecond Fluorescence Decay Kinetics

The primary events in photosynthetic energy transfer and electron transport towards the production of stored chemical energy are under investigation here. These analyses are useful in predicting the earliest events in photosynthesis, up to the reduction of Q_A. Picosecond chlorophyll fluorescence decay kinetics are collected in two states. The first of these is F_M. Simply by slowing the sample pump speed to the measurement cuvette to 1 mL/s, increasing the frequency of the pulsed diode laser (407 nm) to 10 MHz and applying a saturating halogen lamp upon excitation, PSII centres are essentially closed (Q_A reduced) and the chlorophyll fluorescence level is at a maximum. The herbicide DCMU is used to enhance the certainty that F_M is achieved. The addition of DCMU also permits the use of a reduced intensity saturating light intensity (relative to DCMU-absent measurements), since higher intensities damage PSII centres (Aro *et al.* 1993; Krause 1988; van Wijk *et al.* 1993).

Each emission wavelength is associated with a weighted residual demonstrating how well the decay curve fits along the ~12 ns time window (see figure 39 for example). Weighted residual plots in the appendix for whole thylakoid and each of the five membrane fractions at F_M reveal a good distribution about the median in every wavelength with the exception of some noise at the fit start.

Figures 40, 41, 42, 43, 44 and 45 are the globally fit DAS at F_M for all six thylakoid membrane preparations including whole thylakoid, the grana fraction, the stroma lamellae fraction, the grana core fraction, the grana margin fraction and the purified stroma lamellae fraction respectively. Each DAS plots the amplitude of four components of a five component fit versus the fluorescence emission wavelength.

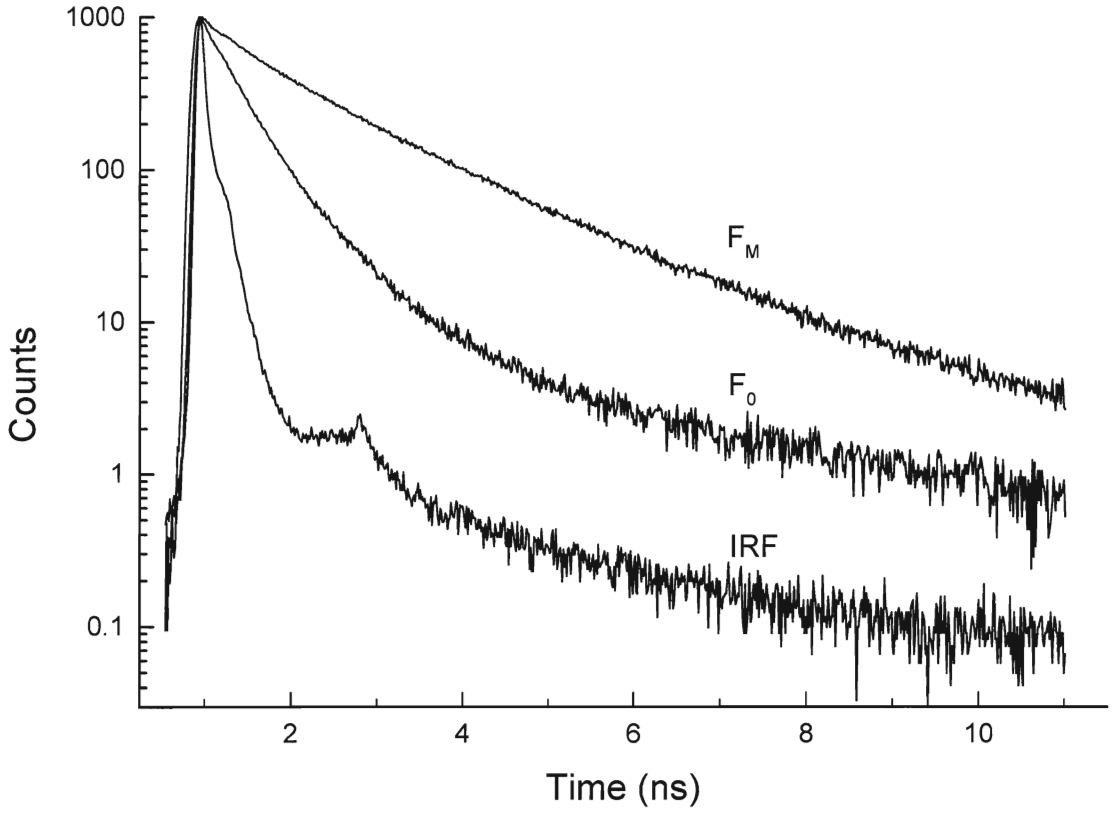

Figure 39 - Picosecond decay kinetics from dark adapted whole thylakoid membranes (685 nm fluorescence emission) representative of the difference between F_M and F_0, including the instrument response function (IRF).

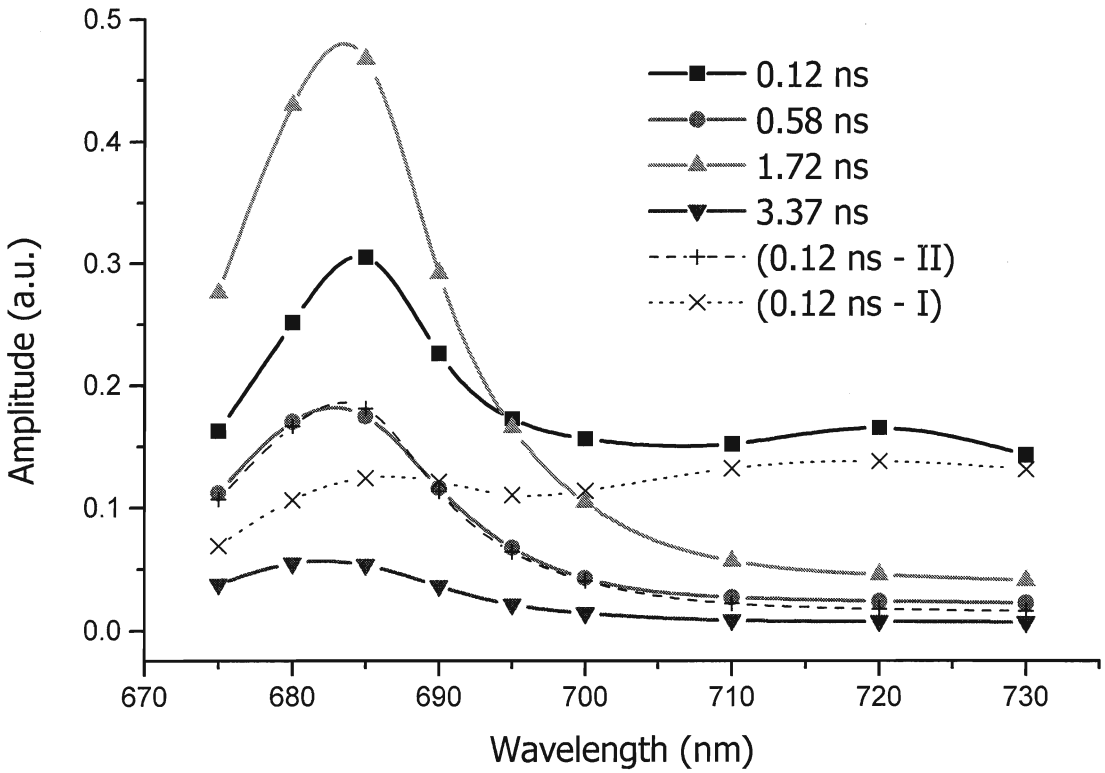

Figure 40 - Decay associated spectra of globally fitted picosecond chlorophyll fluorescence decay kinetics from whole thylakoid at F_M. Four components of a five component fit are plotted. An 11 ps component has been omitted (Durrant *et al.*, 1992).

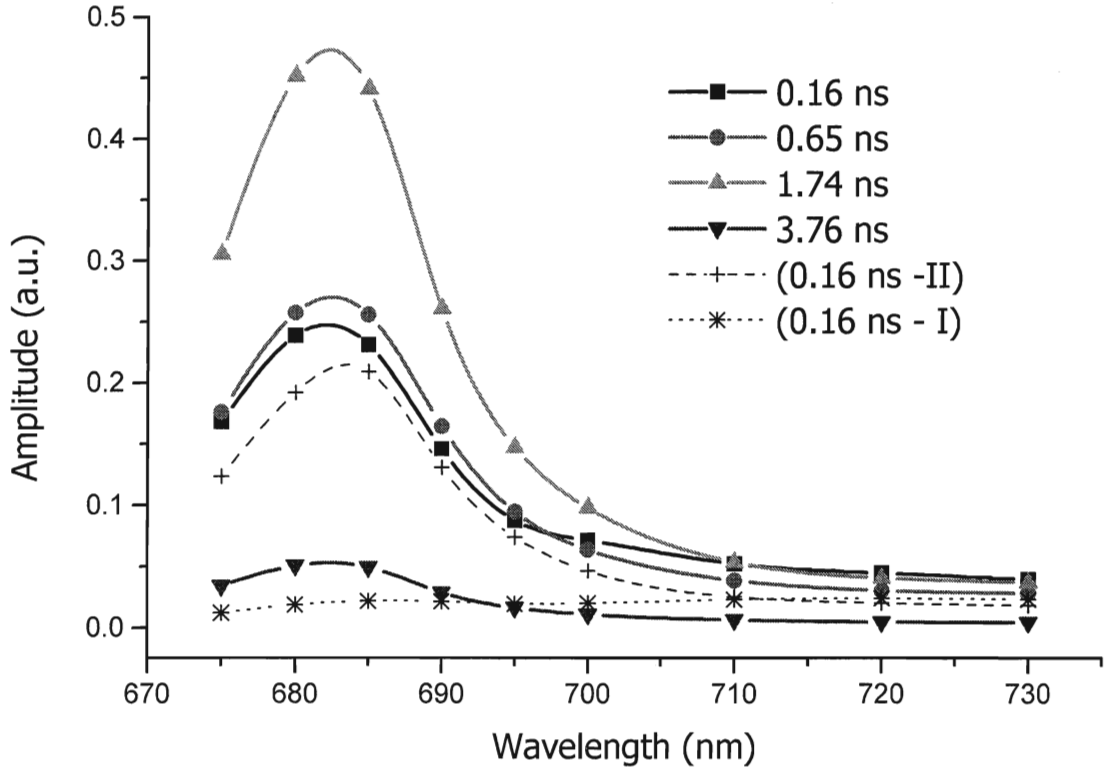

Figure 41 - Decay associated spectra of globally fitted picosecond chlorophyll fluorescence decay kinetics from grana core at F_M. Four components of a five component fit are plotted. An 11 ps component has been omitted (Durrant *et al.*, 1992).

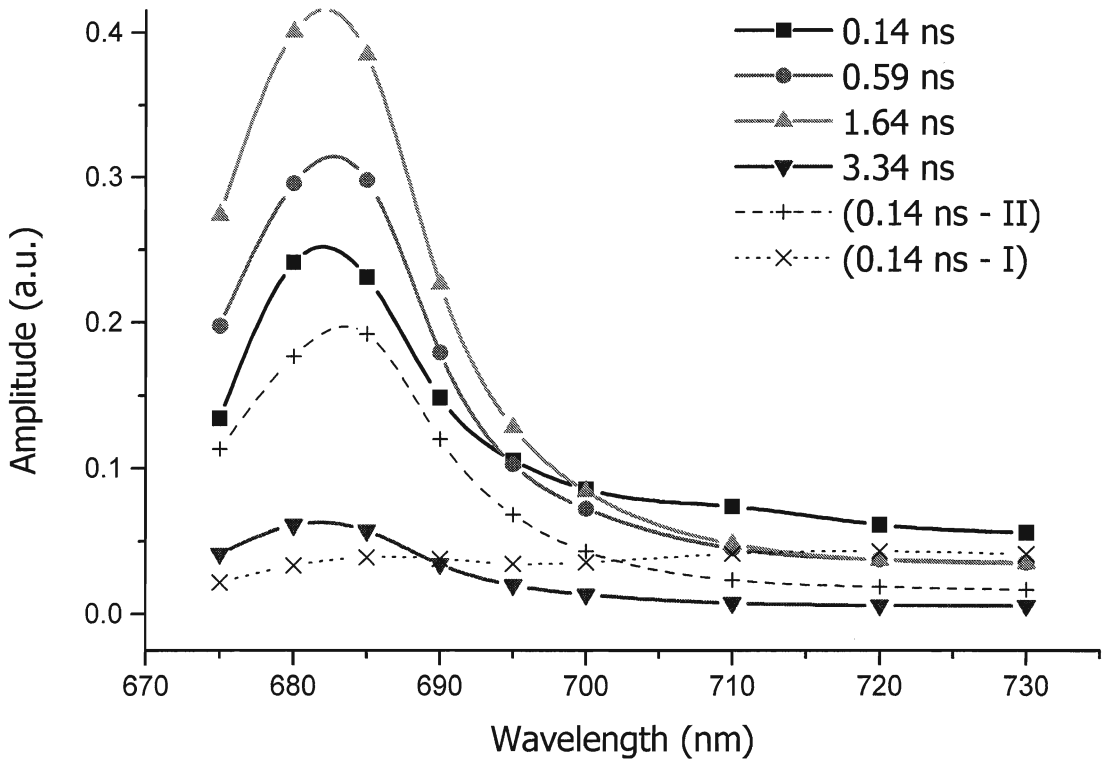

Figure 42 - Decay associated spectra of globally fitted picosecond chlorophyll fluorescence decay kinetics from whole grana at F_M. Four components of a five component fit are plotted. An 11 ps component has been omitted (Durrant *et al.*, 1992).

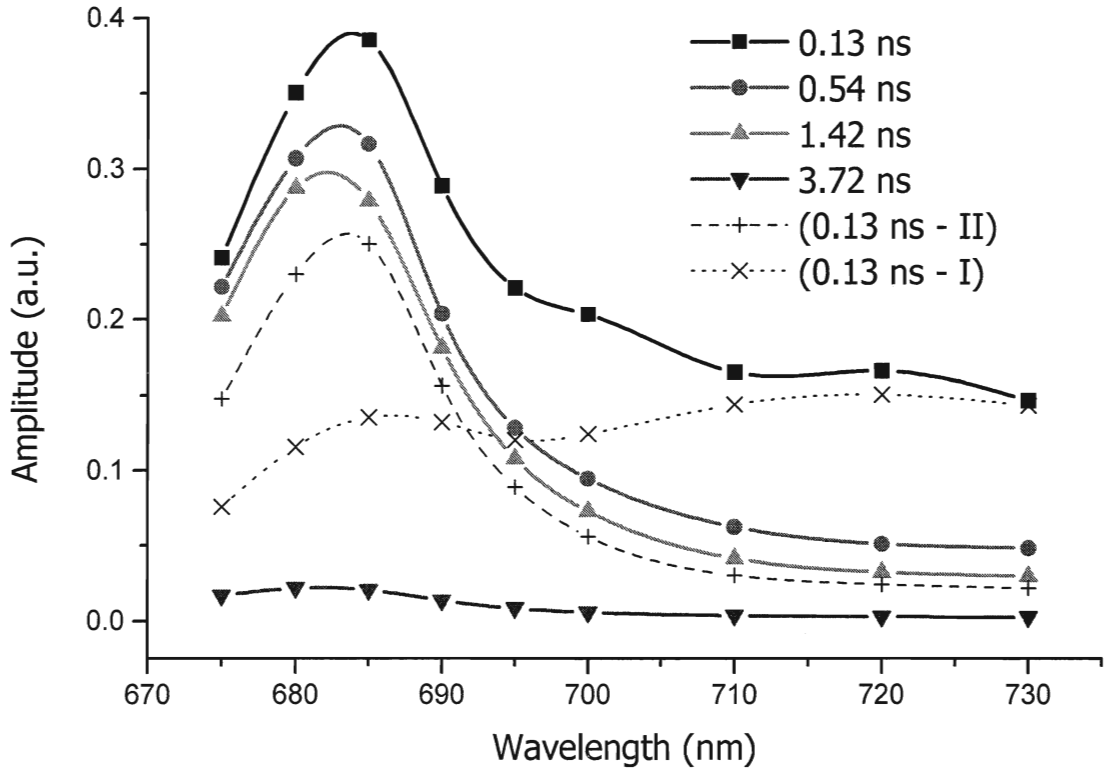

Figure 43 - DAS of globally fitted picosecond chlorophyll fluorescence decay kinetics from grana margins at F_M. Four components of a five component fit are plotted. An 11 ps component has been omitted (Durrant *et al.*, 1992).

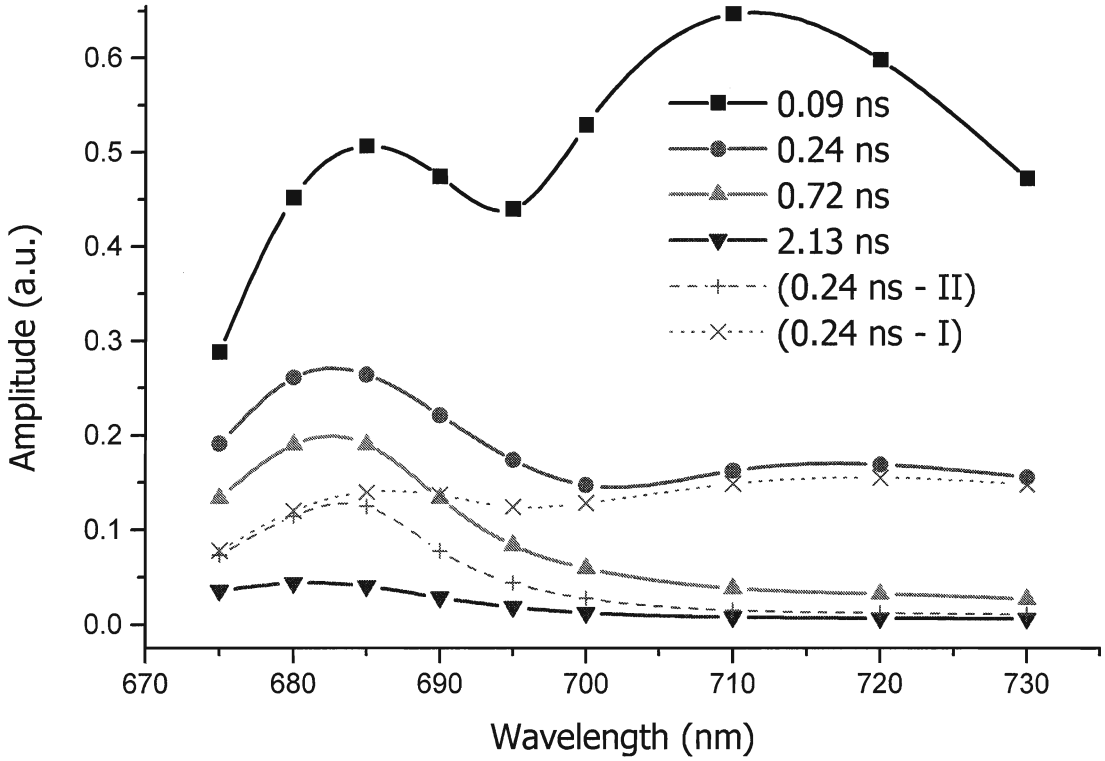

Figure 44 - DAS of globally fitted picosecond chlorophyll fluorescence decay kinetics from whole stroma lamellae at F_M. Four components of a five component fit are plotted. An 11 ps component has been omitted (Durrant *et al.*, 1992).

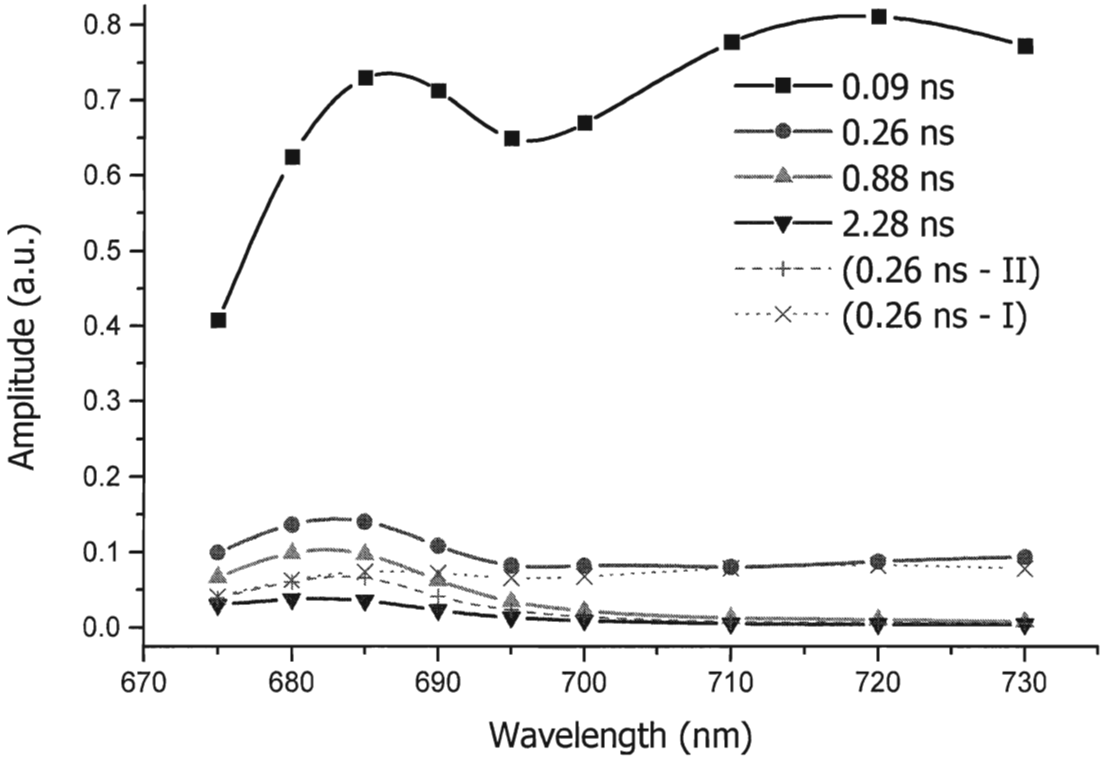

Figure 45 - DAS of globally fitted picosecond chlorophyll fluorescence decay kinetics from purified stroma lamellae at F_M. Four components of a five component fit are plotted. An 11 ps component has been omitted (Durrant *et al.*, 1992).

Table 14 - Fluorescence lifetimes, and their relative yield (%), from global fitting analysis for thylakoid fractions at F_M. T_1 of 11 ps (exciton equilibrium (Roelofs *et al.* 1992)) has been omitted. Uncertainty of lifetimes and yields is approximately 10%.

Fraction (χ^2)	Fluorescence Lifetime (ns)			
	T_2	T_3	T_4	T_5
Thy (1.216)	0.12 (15.7*, 22.5+)	0.58 (16.3)	1.72 (40.4)	3.37 (5.1)
BS (1.162)	0.16 (20.1*, 4.4+)	0.65 (26.6)	1.74 (44.0)	3.76 (4.9)
B3 (1.1)	0.14 (18.3*, 7.7+)	0.59 (29.9)	1.64 (38.3)	3.34 (5.8)
Ma (1.135)	0.13 (20.5*, 23.2+)	0.54 (29.2)	1.42 (25.1)	3.72 (1.9)
T3 (1.25)	0.09 (61.5)	0.24 (7.0*, 16.4+)	0.72 (12.3)	2.13 (2.3)
Y100 (1.191)	0.09 (80.8)	0.26 (3.5*, 8.2+)	0.88 (5.4)	2.28 (2.1)

* - deconvoluted PSII component
\+ - deconvoluted PSI component

At F_0, the measurement is very similar to that at F_M. Experimentally, these kinetics are determined with a few minor differences in the equipment set up relative to the F_M collection set up. The flow through the pump is increased to ~4 mL/s from ~1.5 mL/s, the frequency of the pulsed laser diode is decreased to 5 MHz from 10 MHz and the saturating halogen lamp is set to off. These technical alterations, coupled with the absence of the herbicide, DCMU, permit PSII centres to remain open (Q_A oxidized). At F_0, the chlorophyll fluorescence decays much faster than those occurring at F_M. This is demonstrated in figure 39. Weighted residuals, similar to those obtained at F_M are displayed in figure 56 for all six thylakoid membrane preparations. The globally fit DAS generated from chlorophyll fluorescence decay curves at F_0 are shown in figures 46, 47, 48, 49, 50 and 51 for whole thylakoid, the grana fraction, the stroma lamellae fraction, the grana core fraction, the grana margin fraction and the purified stroma lamellae fraction respectively. Each DAS plots the amplitude of four components of a five component fit versus the fluorescence emission wavelength.

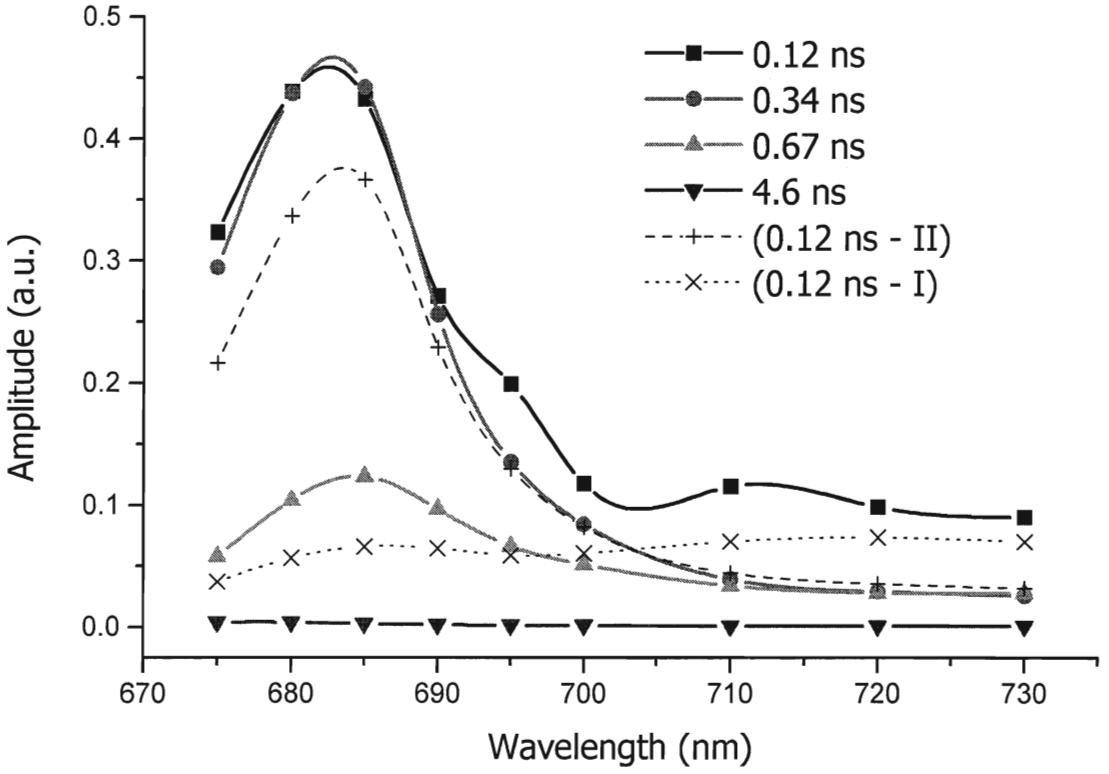

Figure 46 - Decay associated spectra of globally fitted picosecond chlorophyll fluorescence decay kinetics of whole thylakoid at F_0. Four components of a five component fit are plotted. An 11 ps component has been omitted (Durrant *et al.*, 1992).

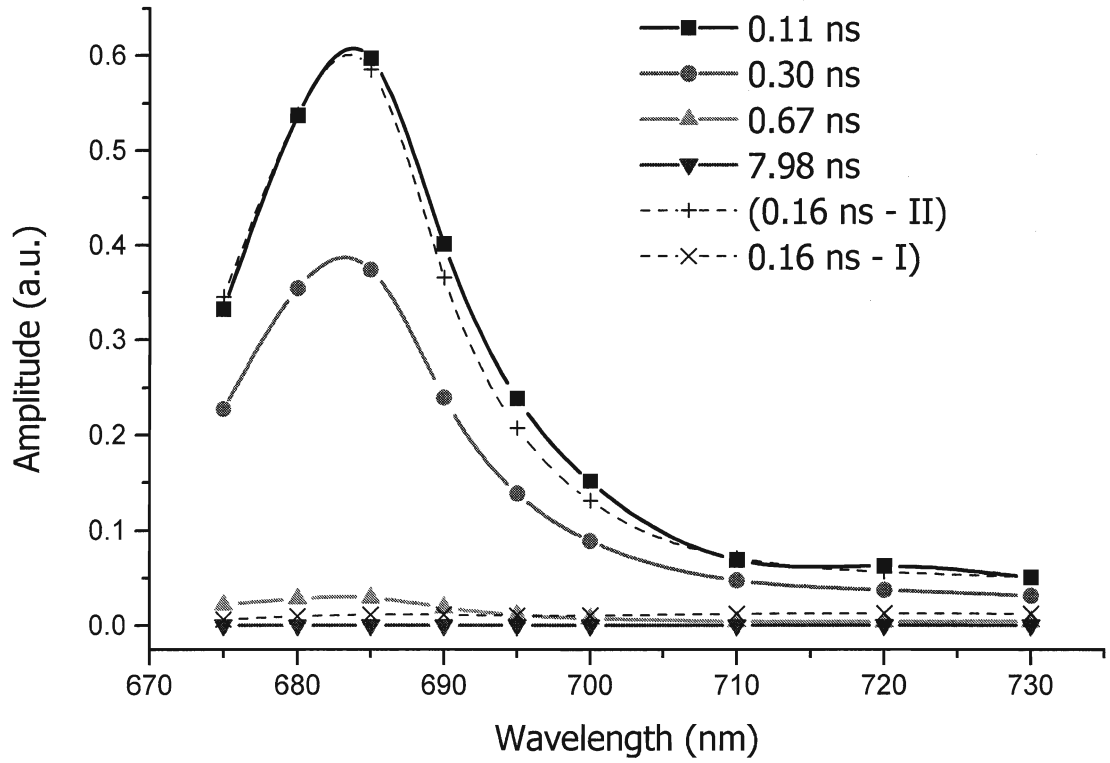

Figure 47 - Decay associated spectra of globally fitted picosecond chlorophyll fluorescence decay kinetics from the grana core at F_0. Four components of a five component fit are plotted. An 11 ps component has been omitted (Durrant *et al.*, 1992).

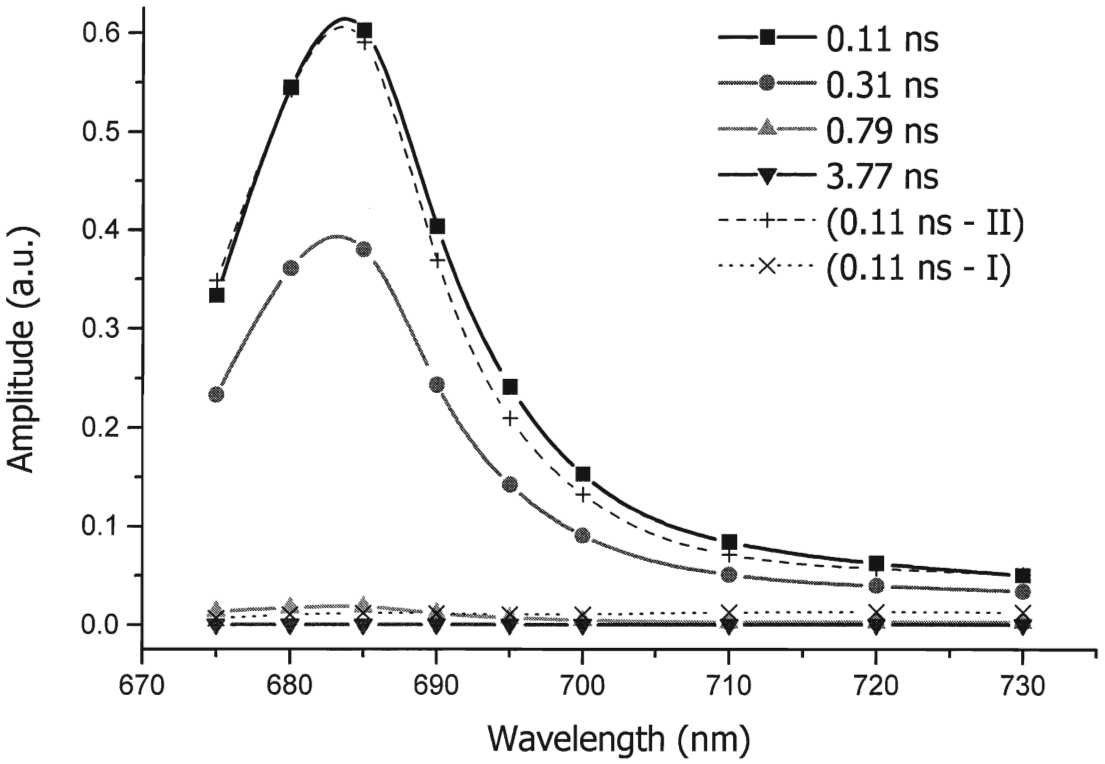

Figure 48 - Decay associated spectra of globally fitted picosecond chlorophyll fluorescence decay kinetics of whole grana at F_0. Four components of a five component fit are plotted. An 11 ps component has been omitted (Durrant *et al.*, 1992).

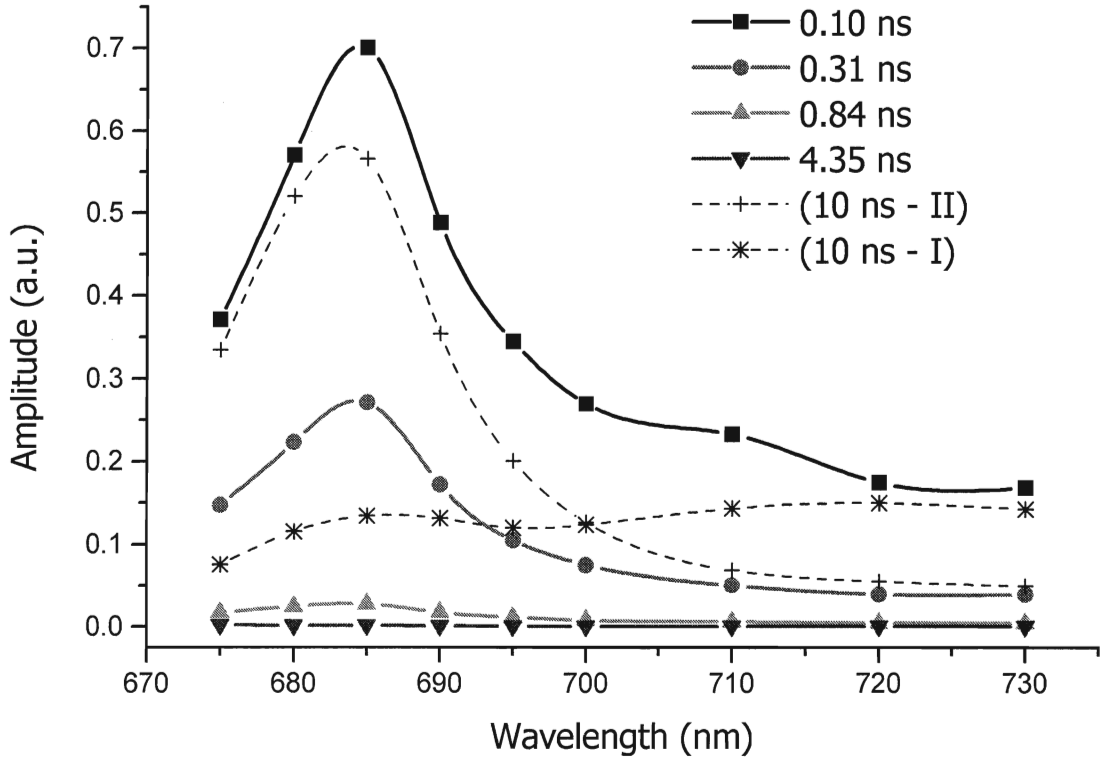

Figure 49 - Decay associated spectra of globally fitted picosecond chlorophyll fluorescence decay kinetics grana margins at F_0. Four components of a five component fit are plotted. An 11 ps component has been omitted (Durrant *et al.*, 1992).

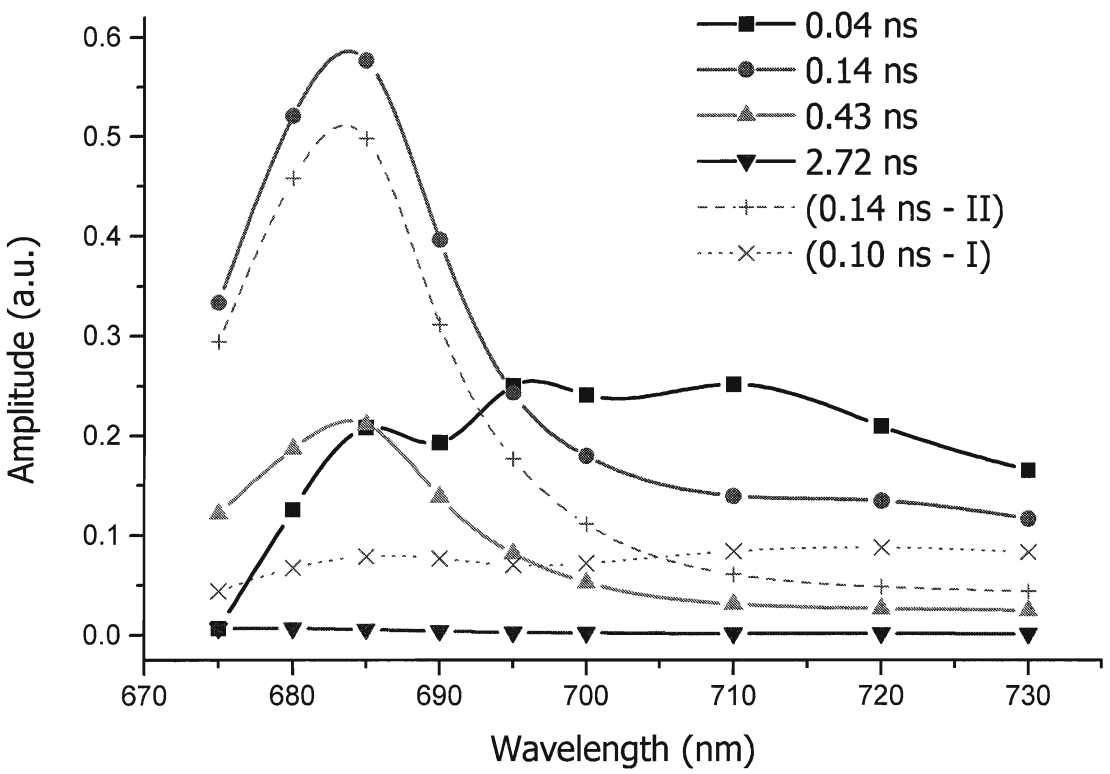

Figure 50 - Decay associated spectra of globally fitted picosecond chlorophyll fluorescence decay kinetics whole stroma lamellae at F_0. Four components of a five component fit are plotted. An 11 ps component has been omitted (Durrant *et al.*, 1992).

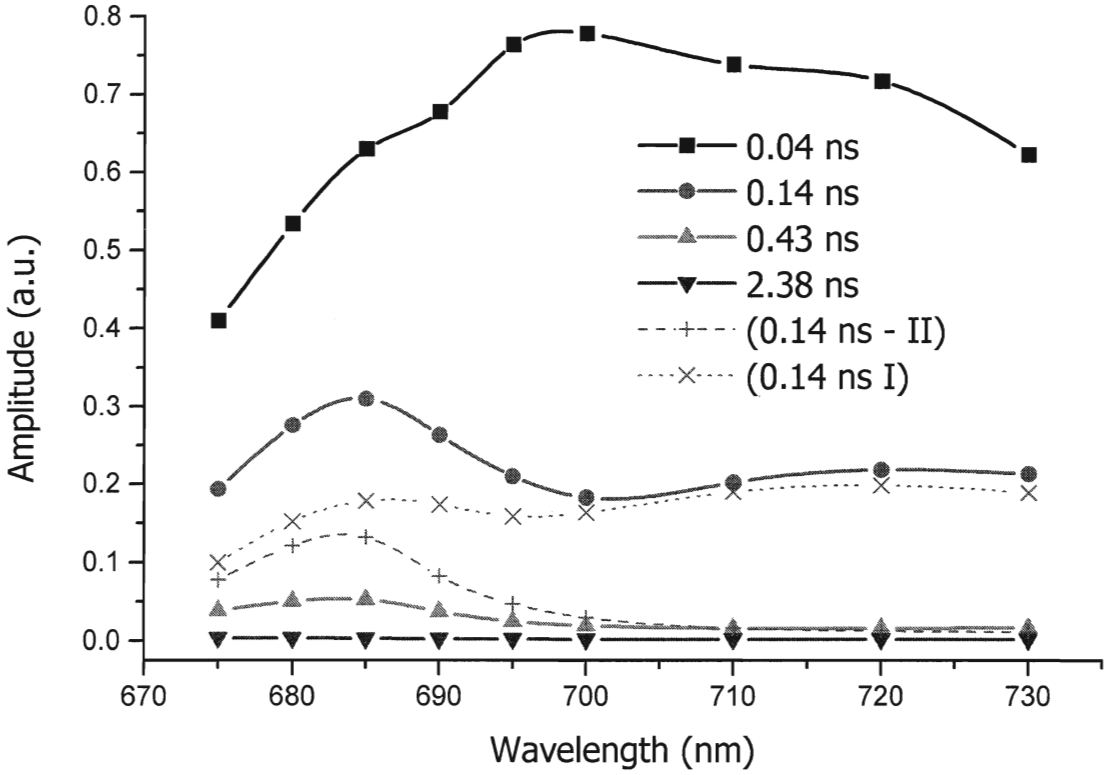

Figure 51 - Decay associated spectra of globally fitted picosecond chlorophyll fluorescence decay kinetics of purified stroma lamellae at F_0. Four components of a five component fit are plotted. An 11 ps component has been omitted (Durrant *et al.*, 1992).

Table 15 - Fluorescence lifetimes, and their relative yield (%), from global fitting analysis for thylakoid fractions at F_0. T_1 of 11 ps (exciton equilibrium (Roelofs *et al.* 1992)) has been omitted. Uncertainty of lifetimes and yields is approximately 10%.

Fraction (χ^2)	Fluorescence Lifetime (ns)			
	T_2	T_3	T_4	T_5
Thy (1.18)	0.12 (33.6*, 12.7+)	0.34 (39.8)	0.67 (13.4)	4.6 (< 1)
BS (1.331)	0.11 (57.5*, 2.4+)	0.30 (38.2)	0.67 (1.9)	7.98 (< 1)
B3 (1.293)	0.10 (48.2*, 5.8+)	0.30 (38.6)	0.54 (7.3)	5.04 (< 1)
Ma (1.281)	0.10 (48.8*, 24.4+)	0.31 (24.1)	0.84 (2.6)	4.35 (< 1)
T3 (1.25)	0.04 (37.1)	0.14 (38.4*, 12.7+)	0.43 (16.8)	2.72 (< 1)
Y100 (1.27)	0.04 (71.7)	0.14 (6.5*, 18.3+)	0.43 (3.3)	2.38 (< 1)

* - deconvoluted PSII component
\+ - deconvoluted PSI component

A visual analysis of the DAS clearly indicate the 100 to 200 ps component (T_2 in grana derived fractions, and T_3 in stroma lamellae derived fractions) consists of a mixture of PSII and PSI fluorescence decays. Representative PSII and PSI components were used to deconvolute these mixed spectra into separate PSII and PSI components maintaining their respective lifetimes. This process offered two advantages. First, it is now clear what amount of these mixed spectra is associated with PSII fluorescence decay and PSI fluorescence decays. The DAS at F_M, figures 40-45, at F_0, figures 46-51, illustrate this deconvolution. The newly calculated PSII and PSI components are represented by broken lines. They are plotted in the same colour as the original mixed component that they were deconvoluted from. The addition of these novel spectra renders a near perfect match their respective two component origins. Secondly, the normalized yield of the PSII component derived from the mixed component, coupled to the remaining original PSII components in the DAS permit a more precise calculation of F_V (calculated by $F_M - F_0$) associated with each thylakoid fraction. The parameter F_V/F_0 was utilized by Mamedov *et al.*, 2000, to describe the robustness of the same thylakoid membrane fractions as those employed in the current study. The values that they obtained are relatively low due to the method used to measure these fluorescence levels. These data are presented in tables 16, 17 and 18.

Table 16 - Ratios of the relative contributions of deconvoluted fluorescence decay components from the DAS at F_M (figures 40-45).

Fraction	PSII/PSI (T_2)	PSII/PSI (T_3)
Thylakoid	0.7	N.D.
Grana Core	4.57	N.D.
Grana	2.38	N.D.
Grana Margins	0.88	N.D.
Stroma Lamellae	N.D.	0.43
Purified Stroma Lamellae	N.D.	0.43

Table 17 - Ratios of the relative contributions of deconvoluted fluorescence decay components from the DAS at F_0 (figures 46-51).

Fraction	PSII/PSI (T_2)	PSII/PSI (T_3)
Thylakoid	2.65	N.D.
Grana Core	23.96	N.D.
Grana	8.3	N.D.
Grana Margins	2.02	N.D.
Stroma Lamellae	N.D.	3.02
Purified Stroma Lamellae	N.D.	0.36

Table 18 - Comparison of variable fluorescence between (Mamedov *et al.* 2000) employing flash-induced fluorescence measurements and the current study using novel DAS.

Fraction	Mamedov *et al.*, 2000	This study
	F_V/F_0	F_V/F_0
Thylakoid	0.7	2.94
BS	1.1	4.72
B3	0.96	4.32
Ma	0.48	3.18
T3	0.27	2.25
Y100	0.2	10.2

5. Discussion

The non-detergent method of thylakoid membrane fractionation employed in this study is clearly a superior preparation tool relative to harsh detergent methods of isolation. Oxygen evolution in the BBY particles (Berthold *et al.* 1981) is high, but, since detergent concentrations as low as 0.01-0.02 % are known to interrupt the energy transfer among LCHII and the reaction centre of PSII, they make a very unreliable candidate for studies on exciton migration in PSII-LHCII complexes (Yu and Albertsson 1993).

The collective literature describing PSII heterogeneity since Melis and Homann, 1975, has rendered a concrete and broad data set. Consistency with the wealth of research that has been undertaken since the first notion of PSII heterogeneity is crucial to the current study. First, many trends that illustrate the widespread idea of spatial separation (Albertsson *et al.* 1992; Albertsson *et al.* 1994; Anderson and Melis 1983) become apparent upon examination of the Gaussian decomposition of the absorption spectra illustrated in figures 27 - 32. The absorption band assigned to Chl *b* at ~651 nm is most dominant in the grana fraction and more so in the grana core fraction. Longer wavelength bands, typical of PSI absorptions add more weight to the spectra in stroma derived fractions. The Chl *a*/*b* ratios have been calculated based on these Gaussian bands, and are listed in table 10. A firm trend exists in these data that suggest that grana and grana core are enriched in PSII relative to the stroma derived fractions. This trend is also apparent in the 77K fluorescence emission spectra in section 4.4. A high F_{695}/F_{730} is indicative of a relatively large PSII population, and subsequently smaller PSI population in a heterogeneous sample of thylakoid membranes. The spatial distribution of PSII and PSI centres (Albertsson *et al.* 1990b; Albertsson *et al.* 1992; Anderson and Melis 1983) is well illustrated by the Gaussian decomposition of the absorption spectra and the 77K fluorescence emission spectra in this study since these data were obtained from domain specific regions of the thylakoid membrane.

These data are consistent with the proposed distribution in this way. The grana core, suggested to be PSII-rich (Svensson and Albertsson 1989; Yu and Albertsson 1993), maintains the highest F_{695}/F_{730} of all thylakoid membrane vesicles. The grana fraction, consisting of whole grana

membrane vesicles, maintains an F_{695}/F_{730} between that of the grana core and the grana margins. This is not surprising since the grana margins, unlike the grana core are suggested to be a PSI-rich region of thylakoid membrane (Anderson *et al.* 1999; Webber *et al.* 1987; Webber *et al.* 1988; Wollenberger *et al.* 1994; Wollenberger *et al.* 1995). The PSI-rich (and PSII-poor) characteristics are also true of the stroma lamellae and purified stroma lamellae fractions. These data are consistent with the Chl *a*/*b* ratios that were calculated from the Gaussian deconvolution of the absorption spectra in section 4.1, table 10.

One further line of evidence that is consistent with these notions of spatial separation of the photosystems lies in the deconvolution of the mixed component from the DAS. Tables 16 and 17 list the novel PSII/PSI ratios from within the mixed component at F_M and F_0 respectively. From these DAS, the mixed component was determined by a visual test and was apparently T_2 in grana derived fractions and whole thylakoid and T_3 in stroma derived fractions. In any case, the lifetime of the mixed component was between 120 ps and 260 ps at F_M, and between 100 ps and 140 ps at F_0. T_2 in stroma derived fractions was clearly not mixed since its lifetime was too short (below 100 ps at F_M and F_0) and its amplitude was most dominant in the low energy region of the DAS, a typical characteristic of PSI fluorescence decays. The highest novel PSII/PSI, not surprisingly was measured from the deconvolution of T_2 of the grana core. The relative yields of the novel components are 20.1% and 4.4% from the overall sum of all of the exponentials. The novel PSII/PSI ratio decreases steadily as the measured parameter moves away from the grana core, towards the stroma lamellae regions of the thylakoid, where this measurement plummets to 0.43, more than ten times less than grana core. Furthermore, the grana margin region of the thylakoid membrane renders a novel PSII/PSI below one.

Secondly, the notion of spatial separation of PSIIα and PSIIβ centres needs to be addressed with respect to these novel thylakoid membrane fractions. The first piece of evidence that suggests that this innovative distribution may exist appears in the 77K fluorescence emission spectra. Previously the measurement of the F_{695}/F_{730} parameter proved useful upon description of the spatial separation of PSII and PSI. A similar measurement may be employed to gain insight

into the relative amounts of PSIIα and PSIIβ in domain specific regions of the thylakoid membrane. The relative association of the LHCII complex with PSII increases as the F_{685}/F_{695} ratio at 77K increases. This degree of association between the accessory light-harvesting antenna and the core complex is highest in grana core (2.20) and decreases as one moves towards the stroma lamellae (0.65), as described in table 13. This parameter was not measurable in the purified stroma lamellae fraction since these peaks were present at the same level as noise in the spectrum. Visually, one notices that this region of the spectrum, figure 38, is far below measurable values relative to the other fractions. This may give an indication of its shear lack of LHCII (and PSI-richness) in the membrane vesicles. Using the model of the pigment protein distribution of the PSII complex figure 9, the F_{685}/F_{695} measurement may be used to estimate the number of chlorophylls maintained by PSII centres in these thylakoid membrane vesicles. A number of assumptions are required for this analysis. First, one must assume that equal coupling among the chromophores of each thylakoid membrane fraction exists, as well as equal rates of primary charge separation within the reaction centre. Assuming that PSII in grana core, reported to employ the largest antenna (Mamedov *et al.* 2000; Svensson and Albertsson 1989; Yu and Albertsson 1993), harbours the full 244 chlorophylls as stated in this model, it may be possible to estimate what portions of the whole complex may be retained by other PSII centre species in these isolated fractions. This analysis suggests that the smallest F_{685}/F_{695}, which is indicative of a poor association between PSII and the accessory LHCII, exists in the stroma lamellae fraction. A value of only 0.65 translates to 180 chlorophylls. The most parsimonious resolution states that only two or three, of four, LHCIIb pigment-protein complexes may be associated with PSII centres in this region of the thylakoid membrane.

Of course the LHCIIb subunit may not be the only possible target for dissociation. LHCIIa, -c, -d and -e could be likely candidates as well. A large number of combinations of associations among these proteins could suit this analysis. Table 19 illustrates this analysis. Since the values of F_{685}/F_{695} listed in table 13 are all within approximately 20% of each other, regardless of the trend that they follow, these results may remain difficult to quantify in the current study. A nonlinear

relationship between the F_{685}/F_{695} measurement of LHCII association, and the excited state pigment dynamics may also be a factor in the poor quantification of these data. Nevertheless, consistent with the early research on spatial separation of two PSII species based on antenna size (Albertsson *et al.* 1990a; Albertsson *et al.* 1992; Anderson and Melis 1983; Thielen and Van Gorkom 1981a), among many other more recent papers, these results agree with a domain based separation of PSIIα and PSIIβ.

Table 19 - Hypothetical association of LHCIIb with each thylakoid membrane fraction based on the model for the pigment-protein distribution within the PSII complex in figure 9 (Thornber *et al.* 1991).

Fraction	Chlorophylls*	LHCIIb subunits†
Grana core (BS)	244	4
Grana (B3)	224	3-4
Grana Margins	202	3
Stroma lamellae (T3)	180	2-3

* calculated from the F685/F695 considering the grana core as the entire complex

† assuming that the loss of each subunit corresponds to 42 chlorophylls, consistent with the model suggesting a total of 4 subunits harbouring 168 chlorophylls.

The relative sizes of the light-harvesting antennae associated with PSII in different regions of the thylakoid membrane in relation to the spatial separation of PSIIα and PSIIβ is further explored upon examination of the PSII absorbance cross sections (figures 33 - 34). Larger chlorophyll antennae result in a large fluorescence yield at lower light intensities. The chlorophyll antenna associated with PSII centres in the grana core fraction render larger cross-sections relative to others, consistent with the idea that PSIIα centres with larger antennae dominate this fraction. The smallest PSII antenna, are found in purified stroma lamellae (the Y100 fraction), consistent with the proposed location PSIIβ centres harbouring small antennae. These findings are in agreement with Anderson and Melis, 1983, where differential antenna size among domain specific PSII centres was first described, and also agree with the findings based on the 77K fluorescence emission spectra analyses. These findings are illustrated by the δ values listed in table 11. The general trend of decreasing δ is followed by these values. However the degree to which this value decreases is much more than those suggested in the literature and what is reported in table 19. These data suggest that the PSII absorbance cross section measured from purified stroma lamellae is merely 20% of that measured from the grana core. This difference in antenna size is much larger than the popular 50% difference reported across the field. Fluorescence induction kinetics collected from grana partition membrane vesicles and stroma lamellae membrane vesicles, fit with Strasser's model (Strasser and Stirbet 1998; Strasser and Stirbet 2001), and agree with the wealth of spatial distribution data beginning as early as Jahns and Schweig 1995. Since the intensity and duration of the excitation flash remained constant from sample to sample, the differential rate constants undoubtedly due to the different antenna sizes (Thielen and Van Gorkom 1981a), are illustrated clearly as well in the PSII absorbance cross sections for the grana vesicles and stroma lamellae vesicles (figure 33).

It is reasonable now to suggest that the spatial separation of PSII and PSI between the stacked grana partition and the unstacked stroma lamellae (Albertsson *et al.* 1990b; Albertsson *et al.* 1992; Anderson and Melis 1983) and between the appressed grana core and the stroma exposed grana margins (Anderson *et al.* 1999; Webber *et al.* 1987; Webber *et al.* 1988;

Wollenberger *et al.* 1994; Wollenberger *et al.* 1995) is clearly demonstrated by the domain specific, nondetergent isolated thylakoid membrane fractions prepared by F. Mamedov and R. Danielsson under the direction of S. Styring of the Photosynthesis Group at Lunds Universitet, Lund, Sweden. It is also reasonable to accept the notion of PSIIα/β separation based on these data. For the purpose of analogous comparison the BS grana core fraction may be referred to as the α-fraction. Furthermore, the Y100 purified stroma lamellae may be referred to as the β-fraction.

In the last decade global target analysis of picosecond chlorophyll kinetics including an analysis of PSII heterogeneity has remained virtually untouched. Roelofs *et al.*, 1992 was the first study to examine the characteristics of the primary processes in PSIIα and PSIIβ centres to any appreciable degree. The results of their paper suggested the following. 1) PSIIα and PSIIβ centres exhibit a different molecular functioning. 2) Differential molecular structure of the reaction centres an/or relative local environment may give rise to these differences. 3) Spatial separation may have a role as well (Roelofs *et al.* 1992).

Data from Roelofs *et al.*, 1992, is summarized in table 20 and has been corrected to allow a valid comparison to the DAS rendered from this study. This was accomplished by considering only the plotted components of the DAS, leaving out the 10 ps decay. The uniqueness of the non-detergent thylakoid membrane preparations employed in this study, relative to Holzwarth's whole thylakoid analysis (Roelofs *et al.* 1992), is most likely the key determinant responsible for the differences that become apparent upon comparison of these kinetic data. Of course, variation among samples does exist to some degree, however, general trends among the DAS and their associated lifetimes and respective yields are usually maintained. Unlike the present study, Roelofs *et al.*, 1992, were not afforded the luxury of performing kinetic analyses on isolated, but intact, PSIIα and PSIIβ centres. DAS from Roelofs *et al.*, 1992 were scanned and redigitized in figures 52, F_M and figure 53, F_0, to aid in the comparison . For the purpose of this comparison table 21 describes the assignment of the novel DAS components using the same nomenclature as Roelofs *et al.*, 1992. In this case, DAS obtained from the grana core and purified stroma lamellae fractions represented the PSIIα population PSIIβ population respectively. This assignment is in

agreement with the overwhelming wealth of literature that suggests the existence of this spatial separation (Albertsson *et al.* 1990b; Albertsson *et al.* 1992; Anderson and Melis 1983).

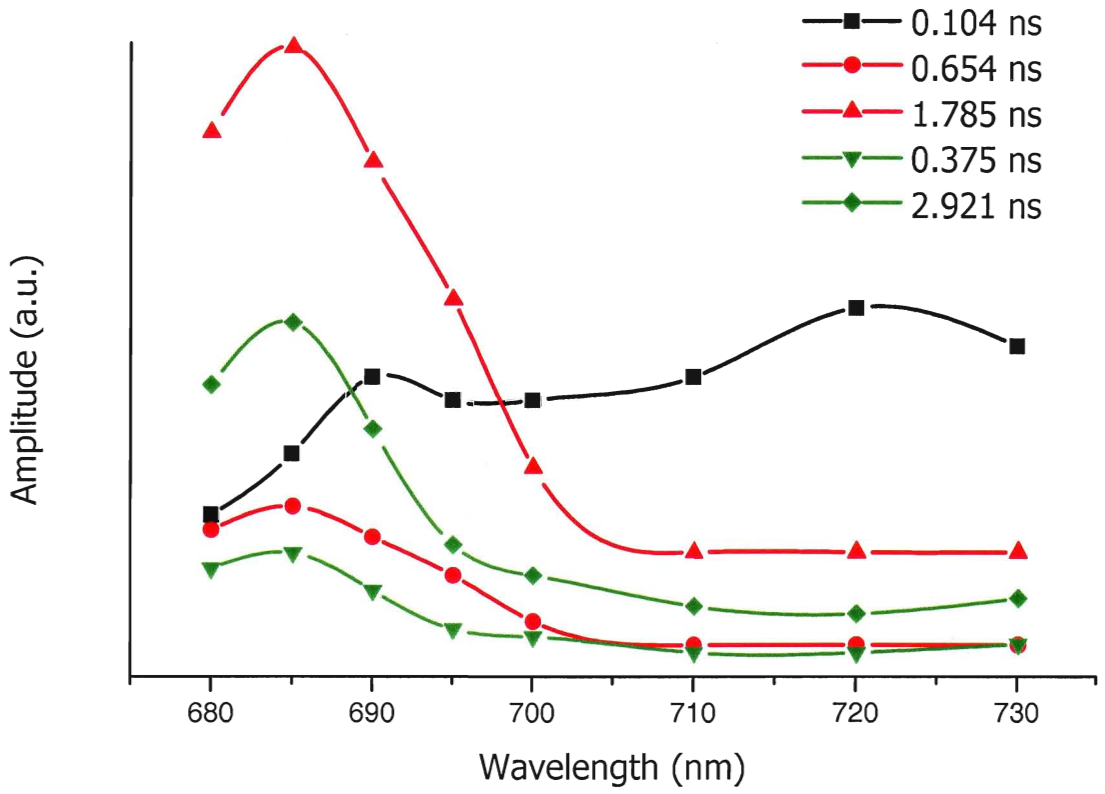

Figure 52 - DAS at F_M for whole thylakoid membranes from Roelofs *et al.*, 1992. The PSI component is plotted in black. Supposed PSIIα components are plotted in red. Supposed PSIIβ components are plotted in green. The 11 ps exciton equilibrium component has been omitted, as in the original document (Roelofs *et al.* 1992).

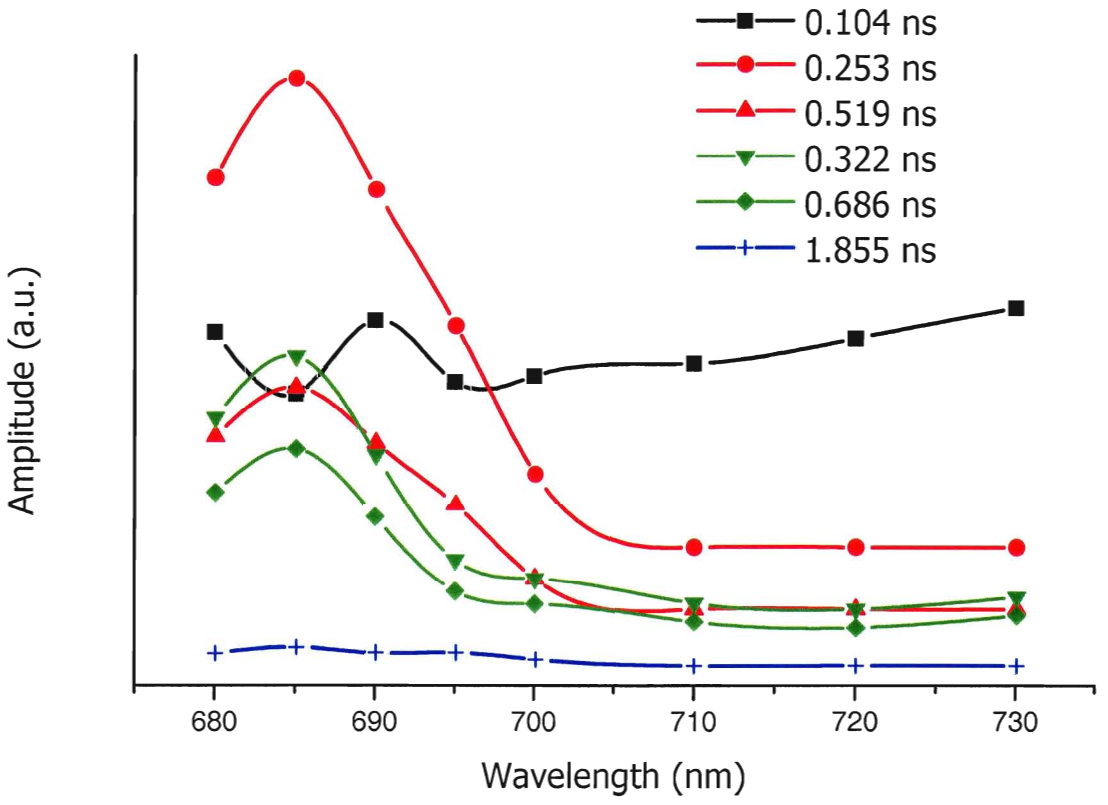

Figure 53 - DAS at F_0 for whole thylakoid membranes from Roelofs *et al.*, 1992. The PSI component is plotted in black. Supposed PSIIα components are plotted in red. Supposed PSIIβ components are plotted in green. The PSII closed component in plotted in blue. The 11 ps exciton equilibrium component has been omitted, as in the original document (Roelofs *et al.* 1992).

Table 20 - Results from the global target analyses of the fluorescence kinetics at F_0 and F_M from (Roelofs *et al.* 1992) employing whole thylakoid membranes. The reduced χ^2-value for the combined (F_M and F_0) global target analysis is 1.0662.

Case	Lifetimes (yield, %)*			
	PSI (ns)	PSIIα (ns)	PSIIβ (ns)	PSII closed (ns)
F_0	0.104 (30.5)	0.253, 0.519 (29.6, 14.2)	0.322, 0.686 (14.2, 10.2)	1.855 (1.3)
F_M	0.104 (30.3)	0.654, 1.785 (9.5, 35.8)	0.375, 2.921 (6.5, 18.0)	N.D.

* The lifetime component reflecting the exciton equilibrium process (34%-37%) appearing in the original paper is not reported to allow comparison to the present study. The yields reported here have been recalculated to allow this subtraction.

Table 21 - Comparison of the present study to Roelofs, *et al.*, 1992, at F_M and F_0 using assignments from Roelofs *et al.*, 1992. Fluorescence lifetimes, T_n, (ns) are obtained from the target global fitting procedure. The associated (%) yields are in parentheses. Fluorescent yields of deconvoluted components in the current study are assigned to either PSI or PSII.

		T_2, $PSI/PSII_{fast}$	T_3, $PSI_{slow}/PSII_1$	T_4, $PSII_2$	T_5, $PSII_3$
Roelofs et al., 1992					
F_M					
	PSIIα	0.104 (30.3)	0.654 (9.5)	1.785 (35.8)	N.D.
	PSIIβ		0.375 (6.5)	2.921 (18)	
F_0					
	PSIIα	0.104 (30.5)	0.253 (29.6)	0.519 (14.2)	1.855 (1.3)
	PSIIβ		0.322 (14.2)	0.686 (10.2)	
Present study					
F_M					
	PSIIα†	0.16 (4.4^{I}, 20.1^{II})	0.65 (26.6^{II})	1.74 (44)	3.76 (4.9)
	PSIIβ ‡	0.09 (80.8^{I})	0.26 (8.2^{I}, 3.5^{II})	0.88 (5.4)	2.28 (2.1)
F_0					
	PSIIα†	0.11 (2.4^{I}, 57.5^{II})	0.3 (38.2^{II})	0.67 (1.9)	7.98 (<1)
	PSIIβ ‡	0.04 (71.4^{I})	0.14 (18.3^{I}, 6.5^{II})	0.43 (3.3)	2.38 (<1)

† Other data in the current study suggest that the BS fraction is essentially a PSIIα preparation.

‡ Other data in the current study suggest that the Y100 fraction is essentially a PSIIβ preparation.

The results from global analysis reported by Roelofs *et al.*, 1992 in table 21 suggest alternative fluorescence decay lifetimes relative to those reported in the present study. Unlike the data presented in this paper at F_0, a low amplitude, long-lived fluorescence lifetime, usually about 2 ns or greater, is not reported for measurements taken at F_M. However, they do report a similar fluorescence decay component as the longer-lived of two PSII components associated with both α- and β-centres at this level of chlorophyll fluorescence.

The current study describes fluorescent lifetimes for PSIIβ centres that are shorter than those of PSIIα centres at F_M and F_0. This may be because of the structure and functionality of these PSII centres. Large, shared antenna PSIIα centres which are electron transport competent (capable of Q_B reduction) offer alternative fates of the excited state relative to the small, isolated antenna PSIIβ centres which cannot. Of the small absorption that the PSIIβ centres are capable of, more often than not, the result is probably some sort of quenching mechanism coupled with a fast release of low energy as heat, rather than moving towards charge stabilization. This explanation is supported by the PSII repair cycle (figures 12 and 13) where PSIIβ centres in stroma exposed regions of thylakoid membranes harbour a damaged, semi-repaired nonfunctional or no D1 reaction centre protein at all. In this state, photochemistry and the further reduction of PQ is not an option (Guenther and Melis 1990; Melis 1991). It may be advantageous for plants to protect damaged reaction centres during repair via quenching in order to reduce the production of dangerously reactive oxygen species that lead to proteolysis.

Holzwarth's group describe longer fluorescence lifetimes of PSIIα relative to those of PSIIβ in only one case. Table 21 lists the fluorescence lifetimes for Roelofs *et al.*, 1992, at F_M and F_0. Only at F_M, where the fastest of two PSII components is that of the β-centre, does this study agree with the current one. It is difficult to access the reasons for these differences among the relative lifetimes of PSIIα and PSIIβ since not all components have been resolved in Roelofs *et al.*, 1992.

The relative fluorescence yield of the two PSII components derived from the DAS at F_M of each fraction reports an interesting phenomenon. In cases where PSIIα is enriched, the faster decay component offers a lower yield relative to the slower decay component. This occurs in the

grana (T_3/T_4 = 0.78) and more-so in grana core (T_3/T_4 = 0.60). In fractions derived from stroma-exposed regions of thylakoid, the grana margins, the stroma lamellae fraction and the purified stroma fraction the T_3/T_4 ratios are 1.16, 1.9, 2.17 respectively.

6. Conclusions

Heterogeneity of PSII, related to its spatial distribution within the thylakoid membranes of higher plants is not a new concept (Albertsson *et al.* 1990b; Albertsson *et al.* 1992; Anderson and Melis 1983). However its understanding and significance have remained elusive over two decades of research. The present study aimed to offer insight on the biophysical properties of PSIIα and PSIIβ.

This study sought to address the notion of spatial separation within thylakoid membranes. The domain specific, nondetergent, thylakoid membrane fractions prepared by F. Mamedov and R. Danielsson under the direction of S. Styring from the Photosynthesis Group at Lunds Universitet. Lund, Sweden, offer an ideal candidate for this study. The first element of spatial heterogeneity is a product of the PSII/PSI distribution. This distribution was demonstrated clearly by the Gaussian decomposition of the absorption spectra. The red-shifted PSI absorption bands (Cramer and Butler 1968) were more dominant in the stroma exposed fractions of the thylakoid membrane. In addition, higher Chl *a/b* ratios are obtained from grana and more so from grana core. Since PSII is relatively rich in Chl *b*, compared to PSI, one can assume that these fractions agree with this trend. More evidence supporting the spatial separation of PSII and PSI was illustrated by the 77K fluorescence emission spectra. F_{695}/F_{730} was lowest in stroma exposed membrane fractions, known to be PSI-enriched. These include the stroma lamellae fraction (T3), purified stroma lamellae fraction (Y100), and the grana margin fraction.

The second element of spatial heterogeneity lies in the domain specific distribution of PSIIα and PSIIβ. The data presented here clearly demonstrate this distribution. First, further examination of the 77K fluorescence emission spectra via evaluation of the F_{685}/F_{695}, which reveals the relative association of LCHII, shows that this parameter is highest in grana (B3) and grana core (BS). These data coupled with the PSII absorption cross section agree with the notion of a separation of large PSIIα in grana and small PSIIβ in stroma (Anderson and Melis 1983; Thielen and Van Gorkom 1981a) and the PSII repair cycle where damaged PSII centres are stripped of the LHCII prior to migration towards the unstacked regions of the membrane (Aro *et al.* 1993; Guenther

and Melis 1990; Melis 1991). This study probed the differential antenna sizes of PSIIα and PSIIβ one other way. Proper analysis of fluorescence induction kinetics offers information about both antenna and reducing side heterogeneity of PSII centres; however, these enigmatic data are often difficult to describe (Holzwarth 1993). Arguably, PSII centres employing larger chlorophyll antennae may close their reaction centres (fully reduce Q_A) at greater rates than those employing smaller chlorophyll antennae under the same experimental conditions. Strasser's models for the theoretical yield of F_V based on PSII connectivity are useful in some respects upon measurement of these rates (Strasser and Stirbet 1998; Strasser and Stirbet 2001). PSIIα-rich grana vesicles and PSIIβ-rich stroma vesicles were valuable to this question. It was found that indeed, the rate of PSII closure was greater in the B3 fraction, relative to the T3 fraction. Another interesting finding was noted when the connectivity constants (equation 31) for domain specific PSIIα and PSIIβ were left free rather than fixing them at Strasser's theoretical values of 1.67 and 0 respectively for whole thylakoid membrane. For PSIIβ centres this value remained nil whereas, in PSIIα-rich grana membrane vesicles it remained relatively close to the model at 2.08. This may be interpreted as an indication of the vast exciton sharing that is reported upon description of the lake (or matrix) model of PSII units (Beauregard and Trissl 1999). It seems that in a relatively homogenous population the measurement of large shared PSII antennae is not clouded by the small isolated antenna of PSIIβ producing the typical biphasic kinetics see in many early papers on PSII heterogeneity (Black *et al.* 1986; Melis and Duysens 1979; Melis and Homann 1975; Melis and Homann 1976).

Spatial separation between photosystems I and II, and also between the two species of PSII, α- and β-centres have been established with these novel thylakoid membrane vesicles. Accordingly, an analysis of the relative picosecond fluorescence decay kinetics with respect to domain specific PSII heterogeneity was possible with the novel membrane fractions. Work on PSII heterogeneity with respect to TC-SPC on chlorophyll fluorescence decay kinetics on the sub-microsecond time scale has remained dormant since Roelofs *et al.,* 1992. The DAS from Holzwarth's paper were recreated in figure 52 at F_M and figure 53 at F_0 (Roelofs *et al.* 1992).

Unlike the current study, in only one case does the decay of the PSIIα component have a longer lifetime than the corresponding PSIIβ component reported by Roelofs *et al.*, 1992. At F_M, Roelofs *et al.*, 1992, describe fluorescence lifetimes of 0.654 ns and 0.375 ns for PSIIα and PSIIβ respectively. The current study describes a data set where all fluorescence lifetimes of PSIIα centres are longer lived than the respective PSIIβ centres. This fast chlorophyll fluorescence decay of PSIIβ centres may be a constituent of a rapid quenching mechanism that protects damaged PSII centres during their repair in unstacked stroma lamellae. Since long fluorescence lifetimes of $^3Chl^*$ enhance the generation of dangerously reactive $^1O_2$ when photochemistry is not an option, its rapid qN is the most advantageous way for a plant to recover the damaged PSII (Aro *et al.* 1993; Guenther and Melis 1990; Melis 1991).

7. Literature Cited

Ainbund MR, Buevich OE, Kamalov VF, Men'shikov GA, Toleutaev BN .1992. Simultaneous spectral and temporal resolution in a single photon counting technique. Review of Scientific Instruments. 63(6), 3274-3279.

Albertsson P-Å .1982. Interaction between the lumenal sides of the thylakoid membrane. FEBS Letters. 149, 186-190.

Albertsson P-Å (1986) 'Partition of cell particles and macromolecules.' (Wiley (Interscience): New York)

Albertsson P-Å .2001. A quantitative model of the domain strcuture of the photosynthetic membrane. Trends in Plant Science. 6, 349-354.

Albertsson P-Å, Andreasson E, Persson A, Svensson P (1990a) Organization of the thylakoid membrane with respect to the four photosystems, PSIα, PSIβ, PSIIα, PSIIβ. In 'Current Research in Photosynthesis'. (Ed. M Baltschefsky) pp. 923-926. (Kluwer Academic Publishers: Dordrecht)

Albertsson P-Å, Andreasson E, Stefánsson H, Wollenberger L .1994. Fractionation of thylakoid membrane. Methods in Enzymology. 228, 469-482.

Albertsson P-Å, Andreasson E, Svensson P .1990b. The domain organization of the plant thylakoid membrane. FEBS. 273, 36-40.

Albertsson P-Å, Andreasson E, Svensson P, Yu S-G (1992) The domains of the plant thylakoid membrane. In 'Trends in Photosynthesis Research'. (Eds J Barber, MG Guerrero, and H Medrano) pp. 45-57. (Intercept Limitied: Andover, U.K.)

Albertsson P-Å, Andreasson E, Svensson P, Yu S .1991. Location of cytochrome *f* in the thylakoid membrane: evidence for multiple domains. Biochimica et Biophysica Acta. 1098, 90-94.

Albertsson P-Å, Svensson P .1988. Counter-current distribution of sonicated inside-out thylakoid vesicles. Molecular and Cellular Biochemistry. 81, 155-163.

Albertsson P-Å, Yu S-G .1988. Heterogeneity among photosystem IIα. Isolation of thylakoid membrane vesicles with different functiona antenna size of photosystem IIα. Biochimica et Biophysica Acta. 936, 215-221.

Albertsson P-Å, Yu S-G, Larsson UK (1990c) Heterogeneity of PSIIα. In 'Current Research in Photosynthesis'. (Ed. M Baltschefsky) pp. 835-838. (Kluwer Academic Publishers: Dordrecht)

Albertsson P-Å, Yu S, Larsson UK .1990d. Heterogeneity in Photosystem II_{γ}. Evidence from fluorescence and gel electrophoresis experiments. Biochimica et Biophysica Acta. 1016, 137-140.

Allen JF .1992. Protein phosphorylation in regulation of photosynthesis. Biochimica et Biophysica Acta. 1098, 275-335.

Allen JF, Bennett J, Steinback KE, Arnzten C .1981. Chloroplast protein phosphorylation couples plastoquinone redox state to distribution of excitation energy between photosystems.

Nature. 291, 25.

Allen JF, Forsberg J .2001. Molecular recognition in thylakoid structure and function. Trends in Plant Science. 6, 317-326.

Allen JF, Holmes NG .1986. A general model for regulation of photosynthetic unit function by protein phosphorylation. FEBS Letters. 202, 175-181.

Anderson J .2001. Does functional photosystem II have an oxygen channel? FEBS Letters. 488, 1-4.

Anderson J, Melis A .1983. Localization of different photosystems in separate regions of chloroplast membranes. Proseedings of the National Academy of Sciences USA. 80, 745-749.

Anderson JM, Boardman NK .1966. Fractionation of the photochemical system of photosynthesis. I. Chlorophyll contents and photochemical activities of particles isolated from spinach chloroplasts. Biochimica et Biophysica Acta. 112, 403-421.

Anderson JM, Goodchild DJ (1987) Lateral distribution of the photosystem I complex between the appressed and non-appressed regions of spinach thylakoid membranes: An immunocytochemical study. In 'Progress in Photosynthesis Research'. (Ed. J Biggins) pp. 301-304. (Martinus Nijhoff Publishers: Dordrecht, The Netherlands)

Anderson JM, Goodchild DJ, Thomson WW (1999) The granal margins of plant thyalkoid membranes: An important nonappressed domain. In 'Current Research in Photosynthesis'. (Ed. M Baltschefsky) pp. 803-807. (Kluwer Academic Publishers: Dordrecht)

Anderson JM, Park Y-I, Soon WS .1998. Unifying model for the photoinactivation of photosystem II in vivo under steady-state photosynthesis. Photosynthesis Research. 56, 1-13.

Andreasson E, Svensson P, Weibull C, Albertsson P-Å .1988. Separation and characterization of stroma and grana membranes - evidence for heterogeneity in antenna size of both Photosystem I and Photosystem II. Biochimica et Biophysica Acta. 936, 339-350.

Andreeva A, Velitchkova M .1998. Mutual oreintation of absorbing chromophores and long wavelength pigments in photosystem I particles. Spectrochimica Acta Part A. 54, 639-644.

Arabidopsis Genome Initiative .2000. Analysis of the genome sequence ofthe flowering plant Arabidopsis thaliana. Nature. 408, 796-815.

Armond PA, Arnzten CJ, Briantais JM, Vernotte C .1976. Differentiation of chloroplast lamellae. Light harvesting efficiency and grana development. Archives of Biochemisrty and Biophysics. 175, 54-63.

Arnon DI, Tang GMS .1988. Cytochrome *b-559* and proton conductance in oxygenic photosynthesis. Proceedings of the National Academy of Sciences of the USA. 85, 9524-9528.

Arnzten CJ, Briantais J-M (1975) Chloroplast strcuture and function. In 'Bioenergetics and Photosynthesis'. (Ed. Govindjee) pp. 51-113. (Academic Press: New York)

Aro E-M, Virgin I, Andersson B .1993. Photoinhibition of Photosystem II. Inactivation, protein damage and turnover. Biochimica et Biophysica Acta. 1143, 113-134.

Arvidsson P-O, Sundby C .1999. A model for the topology of the chloroplast thylakoid membrane. Australian Journal of Plant Physiology. 26, 687-694.

Åkerlund H-E, Albertsson P-Å .1994. Thin-layer countercurrent distribution and centrifugal countercurrent disrtribution apparatus. Methods in Enzymology. 228, 87-99.

Barbato R, Friso G, Rigoni F, Frizzo A, Giacometti GM .1992. Characterization of a 41 kDa photoinhibition adduct in isolated photosystem II reaction centres. FEBS Letters. 309, 165-169.

Barber J (1990) The fluid-mosaic nature of the thylakoid membrane. In 'Current Research in Photosynthesis'. (Ed. M Baltschefsky) pp. 715-723. (Kluwer Academic Publishers: Dordrecht)

Barber J, Kühlbrandt W .2000. Photosystem II. Current Opinion in Structural Biology. 9, 469-475.

Barber J, Morris EP, Büchel C .2000. Revealing the structure of the photosystem II chlorophyll binding proteins, CP43 and CP47. Biochimica et Biophysica Acta. 1459, 239-247.

Barkan A .1998. Approaches to investigating nuclear genes that function in chloroplast biogenesis in land plants. Methods in Enzymology. 297, 38-57.

Bassi R, Høyer-Hansen G, Barbato R, Giacometti GM, Simpson D .1987a. Chlorophyll-proteins of the photosystem II antenna system. Jounal of Biological Chemistry. 262, 13333-13341.

Bassi R, Simpson D, Barbato R, Høyer-Hansen G, Hinz U, Giacometti GM (1987b) The role of LHCII in thylakoid membranes. In 'Progress in Photosynthesis Research'. (Ed. J Biggins) pp. 277-281. (Martinus Nijhoff Publishers: Dordrecht, The Netherlands)

Baymann F, Brugna M, Mühlenhoff U, Nitschke W .2001. Daddy, where did (PS)I come from? Biochimica et Biophysica Acta. 1507, 291-310.

Beauregard K, Trissl H-W .1999. Theories for kinetic and yields of fluorescenecand photochemistry: How, if at all, can different models of antenna organization be distinguished experimentally? Biochimica et Biophysica Acta. 1409, 125-142.

Beauregard M, Martin I, Holzwarth AR .1991. Kinetic modeling of exciton migration in photosynthetic systems. (1) Effects of pigment heterogeneity and antenna topography on exciton kinetics and charge separation yields. Biochimica et Biophysica Acta. 1060, 271-283.

Bennett J, Shaw EK, Michel H .1988. Cytochrome b6/f complex is required for phosphorylation of light harvesting chlorophyll a/b complex II in chloroplast photosynthetic membranes. European Journal of Biochemistry. 171, 95.

Berthold DA, Babcock GT, Yocum CF .1981. A highly resolved, oxygen-evolving photosystem II preparation from spinach thylakoid membranes. FEBS Letters. 134, 231-234.

Black MT, Brearley TH, Horton P .1986. Heterogeneity in chloroplast photosystem II. Photosynthesis Research. 89, 193-207.

Boardman NK, Anderson JM .1964. Isolation of spinach chloroplasts of particles containing different proportions of chlorophyll a and chlorophyll b and their possible role in the light reactions of photosynthesis. Nature. 206, 166-167.

Brearley TH, Horton P (1984) Properties of photosystem II-alpha and photosystem II-beta in spinach chloroplasts. In 'Advances in Photosynthesis Research'. (Ed. C Sybesma) pp. 433-436. (Martinis Nijhoff/Dr. W. Junk Publishers: Dordrecth, The Netherlands)

Breton J, Vermeglio A (1982) Orientation of photosynthetic pigments *in vivo.* In 'Photosynthesis, Energy Conversion by Plants and Bacteria'. (Ed. Govindjee) pp. 153-194. (Academic Press: New York)

Bricker TM, Prevost M, Vu V, Laborde S, Womack J, Frankel LK .2001. Isolation of lumenal proteins from spinach thylakoid membranes by Triton X-114 phase partitioning. Biochimica et Biophysica Acta. 1503, 350-356.

Bruce D, Miners J .1993. Use of pulsed laser diode to measure picosecond lifetimes. Photochemistry and Photobiology. 58, 464-468.

Canaani O, Havaux M .1990. Evidence for a biological role in photosynthesis for cytochrome *b-559* - a component of photosystem II reaction center. Proceedings of the National Academy of Sciences of the USA. 87, 9295-9299.

Cramer WP, Butler WL .1968. Further resolution of chlorophyll pigments in photosystem 1 and 2 of spinach chloroplasts by low-temperature derivative spectroscopy. Biochimica et Biophysica Acta. 153, 889-891.

Croce R, Cinque G, Holzwarth AR, Bassi R .2000. The Soret absorption properties of carotenoids and chlorophylls in antenna complexes of higher plants. Photosynthesis Research. 64, 221-231.

Dahlin C, Møller IM, Ryberg H, Sandelius AS (1990) Surface charge densities, lipid compositions and fluidities of thylakoid membranes showing different degrees of stacking. In 'Current Research in Photosynthesis'. (Ed. M Baltschefsky) pp. 813-816. (Kluwer Academic Publishers: Dordrecth)

Dean C, Leech RM .1982. Genome expression during normal leaf development: I. Cellular and chloroplast numbers and DNA, RNA and protein levels in tissues of different ages within seven-day old leaf. Plant Physiology. 69 , 904-910.

Debus RJ .1992. The manganese and calcium ions of photosynthetic oxygen evolution. Biochimica et Biophysica Acta. 1102, 269-352.

Dekker JP, van Roon H, Boekema EJ .1999. Heptameric association of light-harvesting complex II in partially solubilized photosystem II membranes. FEBS Letters. 449, 211-214.

Du H, Fuh A, Li J, Corkan A, Lindsey JS .1998. PhotochemCAD: A computer-aided design and research tool in photochemistry. Photochemistry and Photobiology. 68, 141-142.

Dubinskii AY, Tikhonov AN .1997. A mathamatical model of the thylacoid as a distributed heterogenous electron and proton transport system. Biophysics. 42, 639-655.

Durrant JR, Dekker JP, Kwa SLS, van Grondelle R, Barber J, Porter G, Klug DR .1995. Trapping of excitaiton energy bt photosystem two reaction centres: Is P680 a multimer? Solar Energy Materials and Solar Cells. 38, 135-138.

Durrant JR, Hastings G, Joseph DM, Barber J, Porter G, Clug DR. 1992. Subpicosecond equilibration of excitation energy in isolated photosystem II reaction centers. Proceedings of the National Academy of Science of the USA. 89, 11632-11636.

Ellis JR, Jellings AJ, Leech RM .1983. Nuclear DNA content and the control of chloroplast replication in wheat leaves. Planta. 157, 380.

Ellis JR, Leech RM .1985. Cell size and chloroplast size in realtion to chloroplast replication in light-grown wheat leaves. Planta. 165, 120-125.

Erickson JM (1998) Assembly of photosystem II. In 'The Molecular Biology of Chloroplasts and Mitochondria in Chlamydomonas'. (Eds J-D Rochaix, M Goldschmidt-Clermont, and S Merchant) pp. 261-285. (Kluwer Academic Publishers: Dordrecht, The Netherlands)

Erickson JM, Rochaix J-D (1992) The molecular biology of photosystem II. In 'The Photosystems: Structure, Function and Molecular Biology'. (Ed. J Barber) pp. 101-177. (Elsevier Science Publishers B.V.: Amsterdam, The Netherlands)

Fromme P, Jordan P, KrauB N .2001. Structure of photosystem I. Biochimica et Biophysica Acta. 1507, 5-31.

Funk C, Schröder WP, Green BR, Renger G, Andersson B .1994. The intrinsic 22 kDa protein is a chlorophyll-binding subunit of photosystem II. FEBS Letters. 342, 261-266.

Gadjieva R, Mamedov F, Albertsson P-Å .1999. Fractionation of thylakoid membranes from tobacco. A tentative isolation of 'end membrane' and purified 'stroma lamellae' membranes. Biochimica et Biophysica Acta. 1411, 92-100.

Gall B, Zehetner A, Scherz A, Scheer H .1998. Modification of pigment composition in the isolated reaction center of photosystem II. FEBS Letters. 434, 88-92.

Garab G, Mustárdy L .1999. Role of LHCII-containing macrodomains in the structure, function and dynamics of grana. Australian Journal of Plant Physiology. 26, 649-658.

Gierow JP .1994. Relative proximity of domains in plasma membrane and smooth nedoplasmic reticulum from rat liver. Methods in Enzymology. 228, 512-519.

Goodenough UW, Armstrong JJ, Levine RP .1969. Photosnythetic properties of ac-31, a mutant strain of *Chlamydomonas reinhardi* devoid of chloroplast membrane stacking. Plant Physiology. 44, 1001-1012.

Goodenough UW, Staehelin LA .1971. Structural differentiation of staked and unstacked chloroplast membranes. Freeze-etch electron microscopy of wild-type and mutant strains of *Chlamydomonas*. Journal of Cell Biology. 48, 594-619.

Graan T, Ort D .1986. Detection of oxygen-evolving photosystem II centers inactive in plastoquinone reduction. Biochimica et Biophysica Acta. 852, 320-330.

Graan T, Ort DR .1984. Quantificatioin of the rapid electron donors to P_{700}, the functional plastoquinone pool, and the ratio of the photosystems in spinach chloroplasts. Journal of Biological Chemisrty. 259, 14003-14010.

Gregory RPF (1989) 'Biochemistry of Photosynthesis.' (John Wiley & Sons: Chichester, U.K.)

Guenther JE, Melis A .1990. The physiological significance of photosystem II heterogeneity in chloroplasts. Photosynthesis Research. 23, 105-109.

Guenther JE, Nemson JA, Melis A .1988. Photosystem stoichiometry and chlorophyll antenna size in *Dunaliella salina* (green algae). Biochimica et Biophysica Acta. 934, 108-117.

Gunning BES, Schwartz OM .1999. Confocal mircoscopy of thylakoid autofluorescence in relation to origin of grana and phylogeny in the green algae. Australian Journal of Plant Physiology. 26, 695-708.

Hara H, Dzuba SA, Kawamori A, Akabori K, Tomo T, Satoh K, Iwaki M, Itoh S .1997. The distance between P680 and QA in photosystem II determined by ESEEM spectroscopy. Biochimica et Biophysica Acta. 1322, 77-85.

He Q, Schlich T, Paulsen H, Vermaas W .1999. Expression of higher plant light-harvesting chlorophyll *a/b* binding protein in *Synechocystis* sp. PCC 6803. European Journal of Biochemistry. 263, 561-570.

Heitz E .1936. Untersuchungen über den Bau der Plastiden. I. Die gericheten chlorophyllscheiben der chloroplasten. Planta. 26, 134-163.

Hemelrijk PW, Kwa SLS, van Grondelle R, Dekker JP .1992. Spectroscopic properties of LHC-II, the main light-harvesting chlorophyll a/b protein complex from chloroplast membranes. Biochimica et Biophysica Acta. 1098, 159-166.

Hemelrijk PW, Van Gorkom HJ .1996. Size-distributions of antenna and acceptor pool of photosystem II. Biochimica et Biophysica Acta. 1274, 31-38.

Henrysson T, Sundby C .1990. Characterization of photosystem II in stroma thyalkoid membranes. Photosynthesis Research. 25, 107-117.

Highkin HR, Boardman NK, Goodchild DJ .1969. Photosynthetic studies on a pea-mutant deficient in chlorophyll. Plant Physiology. 44, 1310-1320.

Hill R .1937. Oxygen evolved by isolated chloroplasts. Nature. 139, 881-882.

Hill R, Bendall F .1960. Function of the two cytochrome components in chloroplasts: A working hypothesis. Nature. 186, 136-137.

Hiratsuka J, Shimada H, Whitter R, Ishibashi T, Sakamoto M, Mori M, Kondo C, Honji Y, Sun CR, Meng BY, Li YQ, Kanno A, Nishizawa Y, Hirai A, Shinozaki K, Sugiura M .1989. The complete sequence of the rice (oryza-sativa) chloroplast genome - Intermolecular recombination between distinct transfer-RNA genes accounts for a major plastid DNA inversion during the evolution of the cereals. Molecular and General Genetics. 217, 185-194.

Hodges M, Barber J .1986. Analysis of chlorophyll fluorescence induction kinetics exhibited by DCMU-inhibited thylakoids and the origin of α and β centres. Biochimica et Biophysica Acta. 848, 239-246.

Holzwarth AR .1993. Is it time to throw away your apparatus for chlorophyll fluorescence induction? Biophysical Journal. 64, 1280-1281.

Holzwarth AR (1996) Data analysis of time-resolved measurements. In 'Biophysical Techniques in Photosynthesis'. (Eds J Amesz and AJ Hoff) pp. 75-92. (Kluwer Academic Publishers: Dordrecht, The Netherlands)

Holzwarth AR, Wendler J, Suter GW .1987. Studies on chromophore coupling in isolated phycobiliproteins. II. Picosecond energy transfer kinetics and time-resolved fluorescence spectra of C-phycocyanin from *Synechococcus* 6301 as as function of the aggregation state. Biophysical Journal. 51, 1-12.

Horton P .1981. The effect of redox potential on the kinetics of fluorescence induction in pea chloroplasts. I. Removal of the slow phase. Biochimica et Biophysica Acta. 635, 105-110.

Horton P .1999. Are grana necessary for regulation of light harvesting? Australian Journal of Plant Physiology. 26, 659-669.

Horváth G, Droppa M, Melis A .1984. Herbicide action on photosystem II in spinach chloroplasts: Concentration effect on PS IIα and PS IIβ. Photobiochemistry and Photobiophysics. 7, 249-256.

Ikegami I, Itoh S .1988. Absorption spectroscopy of P-700-enriched particles isolated from spinach. Is P-700 a dimer or a monomer? Biochimica et Biophysica Acta. 934, 39-46.

Jahns P, Schweig S .1995. Energy dependent fluorescence quenching in thylakoids from intermittent light grown pea plants: evidence for an interaction of zeaxanthin and the chlorophyll a/b binding protein CP26. Plant Physiology and Biochemistry. 33, 683-687.

Jansson S .1999. A guide to the Lhc genes and their relatives in *Arabidopsis*. Trends in Plant Science. 4, 236-240.

Jansson S, Stefánsson H, Nyström U, Gustafsson P, Albertsson P-Å .1997. Antenna protein composition of PS I and PS II in thylakoid sub-domains. Biochimica et Biophysica Acta. 1320, 297-309.

Jennings RC, Bassi R, Garlaschi FM, Dainese P, Zucchelli G .1993. Distribution of the chlorophyll forms in the chlorophyll-protein complexes of photosystem II antenna. Biochemistry. 32, 3203-3210.

Jeong WJ, Park Y-I, Suh K, Raven JA, Yoo OJ, Liu JR .2002. A large population of small chloroplasts in tobacco leaf cells allows more effective chloroplasts movemnet than a few enlarged chloroplasts. Plant Physiology. 129, 112-121.

Juhler RK, Andreasson E, Yu S, Albertsson P-Å .1993. Composition of photosynthetic pigments in thylakoid membrane vesicles from spinach. Photosynthesis Research. 35, 171-178.

Kaneko T, Sato S, Kotani H, Tanaka A, Asamizu E, Nakamura Y, Miyajima N, Hirosawa M, Sugiura M, Sasamoto M, Kimura T, Hosouchi T, Matsuno A, Muraki A, Nakazaki N, Narou K, Okumura S, Shimpo S, Takeuchi C, Wada T, Watanabe A, Yamada M, Yasuda M, Tabata S .1996. Sequence analysis of the genome of the unicellular cyanobacterium Synechocystis sp. strain PCC6803. II. Sequence determination of the entire genome and assignment of potential protein-coding regions. DNA Research. 3, 109-136.

Karukstis K, Berliner M, Jewell C, Kuwata K .1990. Chlorophyll fluorescence measurements to assess the competition of substituted anthraquinones for the Q_B binding site. Biochimica et Biophysica Acta. 1020, 163-168.

Keck RW, Dilley RA, Ke B .1970. Photochemical characteristics in a soybean mutant. Plant Physiology. 46, 699-704.

Kieselbach T, Hagman Å, Andersson B, Schröder WP .1998. The thylakoid lumen of chloroplasts. Isolation and characterization. Jounal of Biological Chemistry. 273, 6710-6716.

Kindle KL (1998) Nuclear transformation: Technology and Applications. In 'The Molecular Biology of Chloroplasts and Mitochondria in Clamydomonas'. (Eds J-D Rochaix, M Goldschmidt-Clermont, and S Merchant) pp. 41-61. (Kluwer Academic Publishers: The Netherlands)

Kirchhoff H, Horstmann S, Weis E .2000. Control of photosynthetic electron transport by PQ diffusion microdomains in thylakoids of higher plants. Biochimica et Biophysica Acta. 1459, 148-168.

Knorr FJ, Harris JM .1981. Resolution of multicomponent fluorescence spectra by an emission wavelength-decay time data matrix. Analytical Chemistry. 53, 272-276.

Kobayashi M, Watanabe T, Nakazato M, Ikegami I, Hiyama T, Matsunaga T, Murata N .1988. Chlorophyll a'/P-700 and pheophytin a/P-680 stoichiometries in higher plants and cyanobacteria determined by HPLC analysis. Biochimica et Biophysica Acta. 936, 81-89.

Kochubey SM, Samokhval EG .2000. Long-wavelength chlorophyll forms in photosystem I from pea thylakoids. Photosynthesis Research. 63, 281-290.

Kok B, Forbush B, McGloin M .1970. Cooperation of charges in photosynthetic O_2 evolution - 1. A linear four step mechanism. Photochemistry and Photobiology. 11, 457-475.

Krause G .1988. Photoinhibition of photosynthesis: An evaluation of damaging and protective mechanisms. Physiologia Plantarum. 74, 566-574.

Kuroiwa S, Tonaka M, Kawamori A, Akabori K .2000. The position of cytochrome b_{559} relative to Q_A in photosystem II studied by electron-electron double resonance (ELDOR). Biochimica et Biophysica Acta. 1460, 330-337.

Lam E, Baltimore B, Ortiz W, Chollar S, Melis A, Malkin R .1983. Characterization of a resolved oxygen-evolving photosystem II preparation from spinach thylakoids. Biochimica et Biophysica Acta. 724, 201-211.

Lazár D .1999. Chlorophyll *a* fluorescence induction. Biochimica et Biophysica Acta. 1412, 1-28.

Lazár D, Tomek P, Ilík P, Nauš J .2001. Determination of the antenna heterogeneity of photosystem II by direct simultaneous fitting of several fluorescence rise curves measured with DCMU at different light intensities. Photosynthesis Research. 68, 247-257.

Leech RM (1976) The replication of plastids in higher plants. In 'Cell Division in Higher Plants'. (Ed. MM Yeoman) pp. 135-139. (Academic Press: London)

Leibl W, Breton J, Deprez J, Trissl H-W .1989. Photoelectric study on the kinetics of trapping and charge stabilization in oriented PSII membranes. Photosynthesis Research. 22, 257-275.

Li X-P, Björkman O, Shih C, Grossman AR, Rosenquist M, Jansson S, Niyogi KK .2000. A pigment-binding protein essential for regualtion of photosynthetic light harvesting. Nature. 403, 391-395.

López-Pérez MJ, París G, Larsson C .1981. Highly puriifed mitochondria from rat brain prepared by phase partition. Biochimica et Biophysica Acta. 635, 359-368.

Lyon MK .1998. Multiple crystal types reveal PSII to be a dimer. Biochimica et Biophysica Acta. 1364, 403-419.

Mamedov F, Stefánsson H, Albertsson P-Å, Styring S .2000. Photosystem II in different parts of the thylakoid membrane: A functional comparison between different domains. Biochemistry. 39, 10478-10486.

Marr KM, Mastronarde DN, Lyon MK .1996. Two dimensional crystals of photosystem II: Biochemical characterisation, cryoelectron microscopy and localisation of the D1 and cytochrome b559 ploypeptides. Journal of Cell Biology. 132, 823-833.

Mauzerall D, Greenbaum NL .1989. The absolute size of a photosynthetic unit. Biochimica et Biophysica Acta. 974, 119-140.

Mayanagi K, Ishikawa T, Toyoshima C, Inoue Y, Nakazato K .1998. Three dimensional electron microscopy of photosystem II core complex. Journal of Structural Biology. 123, 221-224.

McCauley SW, Bittersmann E, Mueller M, Holzwarth AR (1990) Picosecond chlorophyll fluorescence from higher plants. In 'Current Research in Photosynthesis'. (Ed. M Baltschefsky) pp. 297-300. (Kluwer Academic Publishers: Dordrecht)

McDonnel A, Staehelin LA .1980. Adhesion between liposomes mediated br the chlorophyll a/b light-harvesting protein complex from the chloroplast membrane. The Journal of Cell Biology. 84, 40.

Mehta M, Sarafis V, Critchley C .1999. Thylakoid membrane architecture. Australian Journal of Plant Physiology. 26, 709-716.

Melis A .1985. Functional properties of photosystem II_{β} in spinach chloroplasts. Biochimica et Biophysica Acta. 808, 334-342.

Melis A .1991. Dynamics of photosynthetic membrane composition and function. Biochimica et Biophysica Acta. 1058, 87-106.

Melis A .1999. Photosystem-II damage and repair cycle in chloroplasts: what modulates the rate of photodamage *in vivo*? Trends in Plant Science. 4, 130-135.

Melis A, Anderson J .1983. Structural and functional organization of the photosystems in spinach chloroplasts. Antenna size, relative electron-transport capacity, and chlorophyll composition. Biochimica et Biophysica Acta. 724, 473-484.

Melis A, Duysens LNM .1979. Biphasic energy conversion kinetics and absorbance difference spectra of PSII of chloroplasts. Evidence for two different photosystem II reaction centers. Photochemistry and Photobiology. 29, 373-382.

Melis A, Homann PH .1975. Kinetic analysis of the fluorescence induction in 3-(3,4-dichlorophenyl)-1,1-dimethyurea poisoned chloroplasts. Photochemistry and Photobiology. 21, 431-437.

Melis A, Homann PH .1976. Heterogeneity of the photochemical centers in system II of chloroplasts. Photochemistry and Photobiology. 23, 343-350.

Melis A, Ow RA .1982. Photoconversion kinetics of chloroplast photosystems I and II: Effect of Mg^{2+}. Biochimica et Biophysica Acta. 682, 1-10.

Menke W .1962. Structure and chemistry of plastids. Annual Review of Plant Physiology. 13, 27-44.

Metzner P .1954. Ünterscuhungen zur kenntnis der plastiden. Flora. 142, 81-108.

Miller KR, Staehelin LA .1976. Analysis of the thylakoid outer space. Coupling factor is limited to unstacked membrane. The Journal of Cell Biology. 68, 30-47.

Mullet JE, Arnzten CJ .1980. Stimulation of grana stacking in a model membrane system. Mediation by a purified light-harvesting complex from chloroplasts. Biochimica et Biophysica Acta. 589, 100.

Nakazato K, Toyoshima C, Enami I, Inoue Y .1996. Two-dimensional crystallisation and cryo-electron microscopy of photosystem II. Journal of Molecular Biology. 257, 225-232.

Nedelcu AM, Lee RW (1998) Modes and tempos of mitochondrial and chloroplast genome evolution in *Chlamydomonas*: A comparative analysis. In 'The Molecular Biology of Chloroplasts and Mitochondria in Chlamydonomas'. (Eds J-D Rochaix, M Goldschmidt-Clermont, and S Merchant) pp. 63-91. (Kluwer Academic Publishers: The Netherlands)

Newell WR, Zara SJ, Barber J (1987) An analysis of the salt-induced rise of chlorophyll fluorescence to investigate ion-specific effects between and within valency groups. In 'Progress in Photosynthesis Research'. (Ed. J Biggins) pp. 269-272. (Martinus Nijhoff Publishers: Dordrecht, The Netherlands)

Nugent JHA, Rich AM, Evans MCW .2001. Photosynthetic water oxidation: towards a mechanism. Biochimica et Biophysica Acta. 1503, 138-146.

O'Connor DV, Phillip D (1984) 'Time-Correlated Single Photon Counting.' (Academic Press Inc.: London, UK)

Pascal AA, Peterman EJG, Gradinaru CC, van Amerongen H, van Grondelle R, Robert B .2000. Structure and interactions of the chlorophyll a molecules in the higher plant lhcb4 antenna protein. Journal of Physical Chemistry, B. 104, 9317-9321.

Pålsson LO, Gillbro T, Svensson P, Albertsson P-Å (1990) Interaction between LHC-II antenna and PS 2 core in thylakoid vesicles. In 'Current Research in Photosynthesis'. (Ed. M Baltschefsky) pp. 301-304. (Kluwer Academic Publishers: Dordrecht)

Pesaresi P, Sandonà D, Giuffra E, Bassi R .1997. A single point mutation (E166Q) prevents dicyclohexylcarbodiimide binding to the photosystem II subunit CP29. FEBS Letters. 402, 151-156.

Renger G (1992) Energy transfer and trapping in photosystem II. In 'The Photosystems: Structure, Function and Molecular Biology'. (Ed. J Barber) pp. 45-99. (Elsevier Science Publishers B.V.: Amsterdam, The Netherlands)

Renger G .1993. Water cleavage by solar radiation--An inspiring challenge of photosynthesis research. Photosynthesis Research. 38, 229-247.

Rhee K-H, Morris EP, Barber J, Kuhlbrandt W .1998. Three-dimensional structure of the plant

photosystem II reaction centre at 8 Å resolution. Nature. 396, 283-286.

Rhee K-H, Morris EP, Zheleva D, Hankamer B, Barber J .1997. Two-dimensional structure of plant photosystem II at 8 Å resolution. Nature. 389, 522-526.

Rochaix J-D, Dron M, Rahire M, Malone P .1984. Plant Molecular Biology. 3, 363-370.

Roelofs TA, Lee C-H, Holzwarth AR .1992. Global target analysis of picosecond chlorophyll fluorescence kinetics from pea chloroplasts. Biophysical Journal. 61, 1147-1163.

Ryrie IJ, Anderson J, Goodchild DJ .1980. The role of the light-harvesting chlorophyll a/b-protein complex in chloroplast membrane stacking. Cation-induced aggregation of reconsituted proteoliposomes. European Journal of Biochemistry. 107, 345.

Salisbury FB, Ross CW (1992) 'Plant physiology.' (Wadsworth Publishing Conpany: Belmont, CA)

Sauer K (1975) Primary events in the trapping of energy. In 'Bioenergetics of Photosynthesis'. (Ed. Govindjee) pp. 115-181. (Academic Press, Inc.: New York)

Sauer K, Debreczeny M (1996) Fluorescence. In 'Biophysical Techniques in Photosynthesis'. (Eds J Amesz and AJ Hoff) pp. 41-61. (Kluwer Academic Publishers: Dordrecht, The Netherlands)

Schatz GH, Brock H, Holzwarth AR .1988. Kinetic and energetic model for the primary processes in photosystem II. Biophysical Journal. 54, 397-405.

Scheller HV, Jensen PE, Haldrup A, Lunde C, Knoetzel J .2001. Role of subunits in eukaryotic photosystem I. Biochimica et Biophysica Acta. 1507, 41-60.

Schluchter WM, Shen G, Zhoa J, Bryant DA .1996. Characterization of pasI and psaL mutants of Synechococcus sp. strain PCC 7002: A new model for stat transitions in cyanobacteria. Photochemistry and Photobiology. 64, 53-66.

Schmid VHR, Thomê P, Rühle W, Paulsen H, Kühlbrandt W, Rogl H .2001. Chlorophyll *b* is Involved in long-wavelength spectral properties of light-harvesting complexes LHC I and LHC II. FEBS Letters. 499, 27-31.

Seaton GGR, Walker DA (1992) Measuring photosynthesis by measuring fluorescence. In 'Trends in Photosynthesis Research'. (Eds J Barber, MG Guerrero, and H Medrano) pp. 289-304. (Intercept Limited: Andover, U.K.)

Sétif P (1992) Energy transfer and trapping in photosystem I. In 'The Photosystems: Structure, Function, and Molecular Biology'. (Ed. J Barber) pp. 471-499. (Elsevier Science Publishers B.V.: Amsterdam)

Silflow CD (1998) Organization of the nuclear genome. In 'The Molecular Biology of Chloroplasts and Mitochondria in Clamydomonas'. (Eds J-D Rochaix, M Goldschmidt-Clermont, and S Merchant) pp. 25-40. (Kluwer Academic Publishers: The Netherlands)

Singer SJ, Nicolson GL .1972. The fluid mosaic model of the structure of cell membranes. Science. 175, 720-731.

Staehelin LA (1986) Chloroplast structure and supramolecular organization of photosynthetic

membranes. In 'Photosynthesis III: Photosynthetic Membranes and Light Harvesting Systems'. (Eds LA Staehelin and CJ Arnzten) pp. 1-84. (Springer-Verlag: Berlin)

Staehelin LA, van der Staay GWM (1996) Structure, composition, functional organization and dynamic properties of thylakoid membranes. In 'Oxygenic Photosynthesis: The Light Reactions'. (Eds DR Ort and CF Yocum) pp. 11-30. (Kluwer Academic Publishers: Dordrecht, The Netherlands)

Stefánsson H, Andreasson E, Weibull C, Albertsson P-Å .1997. Fractionation of the thylakoid membrane from *Dunaliella salina* - heterogeneity is found in photosystem I over a broad range of growth irradiance. Biochimica et Biophysica Acta. 1320, 235-246.

Stewart DH, Brudvig GW .1998. Cytochrome b_{559} of photosystem II. Biochimica et Biophysica Acta. 1367, 63-87.

Stirbet AD, Strasser RJ .1996. Numerical simulation of the *in vivo* fluorescence in plants. Mathamatics and Computers in Simulation. 42, 245-253.

Strasser RJ, Stirbet AD .1998. Heterogeneity of photosystem II probed by the numerically simulated chlorophyll *a* fluorescence rise (O-J-I-P). Mathamatics and Computers in Simulation. 48, 3-9.

Strasser RJ, Stirbet AD .2001. Estimation of the energitic connectivity of PSII centres in plants using the fluorescence rise O-J-I-P. Fitting of experimental data to three different PSII models. Mathamatics and Computers in Simulation. 56, 451-461.

Svensson P, Albertsson P-Å .1989. Preparation of highly enriched photosystem II membrane vesicles by a non-detergent method. Photosynthesis Research. 20, 249-259.

Svensson P, Andreasson E, Albertsson P-Å .1991. Heterogeneity of photosystem I. Biochimica et Biophysica Acta. 1060, 45-50.

Svensson P, Yu S-G, Larsson UK, Andreasson E, Albertsson P-Å (1990) Properties of a non-detergent PS II membrane prepartion. In 'Current Research in Photosynthesis'. (Ed. M Baltschefsky) pp. 839-842. (Kluwer Academic Publishers: Dordrecht)

Tabata S, Ikeuchi M .2001. *Synechocystis* sp. PCC 6803 - a useful too in the study of the genetics of cyanobacteria. Photosynthesis Research. 70, 73-83.

Thielen APGM, Van Gorkom HJ .1981a. Energy transfer and quantum yield in photosystem II. Biochimica et Biophysica Acta. 637, 439-446.

Thielen APGM, Van Gorkom HJ .1981b. Quantum efficiency and antenna size of photosystem IIα, IIβ and I in tobacco chloroplasts. Biochimica et Biophysica Acta. 635, 111-120.

Thielen APGM, van Grokum HJ (1981) Electron transport properties of the photosystems IIα and IIβ. In 'Electron Transport and Photophosphorylation'. (Ed. G Akoyunoglou) pp. 57-64. (Balaban International Science Services: Philadelphia, PA)

Thompson LK, Brudvig GW .1988. Cytochrome b_{559} may function to protect photosystem II from photoinhibition. Biochemistry. 27, 6653-6658.

Thornber JP, Morishige DT, Anandan S, Peter GF (1991) Chlorophyll-caroteniod proteins of higher plant thylakoids. In 'Chlorophylls'. (Ed. H Sheer) pp. 554-586. (CRC Press, Inc.: Boca

Raton, FL)

Timmerhaus M, Weis E (1990) Regulation of photosynthesis: α- to β- conversion of photosystem *II* and thylakoid protein phosphorylation. In 'Current Research in Photosynthesis'. (Ed. M Baltschefsky) pp. 771-774. (Kluwer Academic Publishers: Dordrecht)

van Grondelle R .1985. Excitation energy transfer, trapping and annihilation in photosynthetic systems. Biochimica et Biophysica Acta. 811 , 147-195.

van Roon H, van Breemen JFL, de Weerd FL, Dekker JP, Boekema EJ .2000. Solubilization of green plant thylakoid membrane with *n*-dodecyl-α,D-maloside. Implications for the structural organization of the photosystem II, photosystem I, ATP synthase and cytochrome b_6f complexes. Photosynthesis Research. 64, 155-166.

van Spronsen EA, Sarafis V, Brakenhoff GJ, van der Voort HTM, Nanninga N .1989. Three-dimensional structure of living chloroplasts as visualized by confocal scanning laser microscopy. Protoplasma. 148, 8-14.

van Wijk KJ, Schnettger B, Graf M, Krause GH .1993. Photoinhibition and recovery in relation to heterogeneity of photosystem II. Biochimica et Biophysica Acta. 1142, 59-68.

Vasil'ev S, Orth P, Zouni A, Owens TG, Bruce D .2001. Excited-state dynamics in photosystem II: Insights for the x-ray crystal structure. Proseedings of the National Academy of Sciences USA. 98, 8602-8607.

Vasil'ev S, Wiebe S, Bruce D .1998. Non-photochemical quenching of chlorophyll fluorescence in photosynthesis. 5-hydroxy-1,4-naphthoquinone in spinach thylakoids as a model for antenna based quenching mechanisms . Biochimica et Biophysica Acta. 1363, 147-156.

Vermaas WFJ .1998. Gene modification and mutation mapping to study the function of photosystem II. Methods in Enzymology. 297, 293-310.

Voet D, Voet JG (1995) Photosynthesis. In 'Biochemistry'. pp. 626-661. (John Wiley & Sons, Inc.: New York)

Wakasugi T, Tsudzuki T, Sugiura M .2001. The genomics of land plant chloroplasts: Gene content and alteration of genomic information by RNA editing. Photosynthesis Research. 70, 107-118.

Waller RF, Keeling PJ, Donald RG, Striepen B, Handman E, Lang-Unnasch N, Cowman AF, Besra GS, Roos DS, McFadden GI .1998. Nuclear-encoded proteins target to the plastid in *Toxoplasma gondii* and *Plasmodium falciparum*. Proceedings of the National Academy of Sciences of the USA. 95, 12352-12357.

Webber AN, Lubitz W .2001. P700: The primary electron donor of photosystem I. Biochimica et Biophysica Acta. 1507, 61-79.

Webber AN, Platt-Aloia KA, Heath RL, Thomson WW .1988. The marginal regions of thylakoid membranes: A partial characterization by polyoxyethylene sorbitan monolaurate (Tween 20) solubilization of spinach thylakoids. Physiologia Plantarum. 72, 288-297.

Webber AN, Platt-Aloia KA, Thomson WW, Heath RL (1987) Composition of marginal regions of thylakoid membranes. In 'Progress in Photosynthesis Research'. (Ed. J Biggins) pp. 285-288. (Matinus Nijhoff Publishers: Dordretcht, The Netherlands)

Weis E, Ball JT, Berry J (1987) Photosynthetic control of electron transport in leaves of Phaseolus vulgaris: Evidence for regulation of photosystem 2 by the proton gradient. In 'Progress in Photosynthesis Research'. (Ed. J Biggins) pp. 553-556. (Nartinus Nijhoff Publishers: Dordrecht, The Netherlands)

Wendler J, Holzwarth AR .1987. State transitions in the green alga *Scenedesmus obliquus* probed by time-resolved chlorophyll fluorescence spectroscopy and global data analysis. Biophysical Journal. 52, 717-728.

Wendler J, John W, Scheer J, Holzwarth AR .1986. Energy transfer kinetics in trimeric C-phycocyanin studied by picosecond fluorescence kinetics. Photochemistry and Photobiology. 44, 79-85.

Whatley JM (1988) Mechanisms and morphology of plastid division. In 'Division and Segregation of Organells'. (Eds SA Boffey and D Lloyd) pp. 63-84. (Cambridge University Press: Cambridge, UK)

Wollenberger L, Stefánsson H, Yu S, Albertsson P-Å .1994. Isolation and characterization of vesicles originating from the chloroplast grana margins. Biochimica et Biophysica Acta. 1184, 93-102.

Wollenberger L, Weibull C, Albertsson P-Å .1995. Further characterization of the chloroplast grana margins: the non-detergent preparation of granal Photosystem I cannot reduce ferrodoxin in the absence of $NADP^+$ reduction. Biochimica et Biophysica Acta. 1230, 10-22.

Wollman FA .2001. State transitions reveal the dynamics and flexability of the photosynthetic apparatus. EMBO. 20, 3623-3630.

Yakovlev AG, Taisova AS, Fetisova ZG. 2002. Light control over the size of an antenna unit building block as an efficient strategy for light harvesting in photosynthesis. FEBS Letters. 512, 129-132.

Youvan D, Bylina E, Alberti M, Begusch H, Hearst J .1984. Cell. 37, 949-957.

Yu S, Albertsson P-Å .1993. Characterization of a non-detergent PSII - cytochrome *b/f* preparation (BS). Photosynthesis Research. 37, 227-236.

Zouni A, Witt H-T, Kern J, Fromme P, KrauB N, Saenger W, Orth P .2001. Crystal structure of photosystem II from *Synechococcus elongatus* at 3.8 Å resolution. Nature. 409 , 739-743.

Zubay G (1993) 'Biochemsitry.' (Wm. C. Brown Publishers: Dubuque, Iowa)

Zucchelli G, Dainese P, Jennings RC, Breton J, Garlaschi F, Bassi R .1994. Gaussian decomposition of absorption and linear dichroism spectra of outer antenna complexes of photosystem II. Biochemistry. 33, 8982-8990.

8. Appendices

Nondetergent Fractionation of Thylakoid Membranes

Reagents

Preparation Medium
- 50 mM sodium phosphate buffer (pH 7.4)
- 5 mM $MgCl_2$
- 300 mM sucrose

Washing Medium I
- 10 mM tricine (pH 7.4)
- 5 mM $MgCl_2$
- 300 mM sucrose

Washing Medium II
- 10 mM sodium phosphate buffer (pH 7.4)
- 5 mM NaCl
- 1 mM $MgCl_2$
- 100 mM sucrose

Polymer Mixture
- 3.32 g of 20% (w/w) dextran T500
- 1.66 g of 40% (w/w) PEG 3350 (4000)
- 0.53 g 0.2 M sodium phosphate buffer (pH 7.4)
- 0.30 g of 0.1 M NaCl
- 1.07 g of 10 mM $MgCl_2$
- 1.33 g of 0.1 M sucrose
- 2.45 g ddH_2O

Fractionation I
- 2 g of thylakoid suspension to 9.66 g of *Polymer Mixture* to give the following final concentrations:
  - 5.7% dextran T500
  - 5.7% PEG 3350 (4000)
  - 10mM sodium phosphate buffer (pH 7.4)
  - 20 mM sucrose
  - 3 mM NaCl
  - 1 mM $MgCl_2$
- Sonicate with ½-inch horn in six 30s bursts with 60s between bursts in a cylindrical aluminum tube immersed in ice and water.
  - The ultrasonic intensity output setting is 7,
  - with 20% duty pulses
- 6.43 g of pure lower phase and 5 g of pure top phase are added to:
  - 5.7% dextran T500
  - 5.7% PEG 3350 (4000)
  - 10mM sodium phosphate buffer (pH 7.4)
  - 20 mM sucrose
  - 5 mM NaCl
- mixed at 4 °C
- centrifuged at 2000 g for 3 min to achieve separation
- upper and lower phases are separated and washed twice in 10 mlof fresh upper and lower phase respectively
- the final upper phase following wash with fresh lower phase constitutes the T3 fraction
- the final lower phase following wash with fresh upper phase constitutes the B3 fraction

Fractionation II

- grana cores and margins were separated from within the B3 fraction
  - Sonicate with ½-inch horn in twelve 30s bursts with 60s between bursts in a cylindrical aluminum tube immersed in ice and water.
  - The ultrasonic intensity output setting is 7,
  - with 20% duty pulses
- upper and lower phases are diluted three times in:
  - 10 mM sodium phosphate buffer (pH 7.4)
  - 5 mM NaCl
  - 100 mM sucrose
- centrifuged at 100000 g for 90 min.

Fractionation III

- Y100 in a buffer similar to Washing Medium II (except 5 mM $MgCl_2$) are disintegrated in a Yeda press at 10 MPa nitrogen pressure
- homogenate is diluted 5x in $MgCl_2$-free buffer and centrifuged at 40000x g for 30 min.
- membrane vesicles in supernatant are sedimented at 100000x g for 45 min.

<u>Resuspension Buffer</u>

0.33 M	Sorbitol
10 mM	HEPES (pH 7.8)
15 mM	$MgCl_2$
10 mM	NaCl
3 mM	Ascorbic Acid
0.5 g/L	B.S.A. (only when noted)

Table 22 - Parameters (Par) of the global Gaussian decomposition of the low-temperature absorption spectra. Peak centers (xc) half-widths (w) and amplitudes are fixed with the exception of xc7.

Fraction	Par.	1	2	3	4	5	6	7	8	9	10
BS	xc	620	633.74797	640.69468	649.74823	664.08294	670.69474	676.4956	681.77687	695	710
		± 2.07458	± 2.24115	± 0.23617	± 0.41182	± 0.27332	± 0.09671	± 0.05019	± 0.43553	±0.6323	± 1.04854
	w	11.47054	15.6277	7.15577	9.80214	12.76675	5.65299	6.02294	9.13889	11.09081±	11.79803
		± 2.83359	± 14.0538	± 0.81117	± 0.95668	±1.35369	± 0.18886	± 0.14246	± 0.55699	1.21996	± 1.71128
	A	1.06719	1.47673	0.46119	2.24253	4.50411	1.83646	3.2508	2.52745	0.43273	0.11024
		± 0.9616	± 1.68532	± 0.30806	± 0.72396	± 0.56583	± 0.258	± 0.29244	± 0.31217	± 0.06423	± 0.02122
B3	xc	620	633.74797	640.69468	649.74823	664.08294	670.69474	676.56555	681.77687	695	710
		± 2.07458	± 2.24115	± 0.23617	± 0.41182	± 0.27332	± 0.09671	± 0.05968	± 0.43553	±0.6323	± 1.04854
	w	11.67113	15.22403	6.80506	10.23449	12.33027	5.54941	6.14731	10.00207	10.6995	15.83155
		± 3.089	± 11.9988	± 0.94714	± 0.91799	± 1.27825	± 0.21557	± .15605	± 0.58447	± 1.01257	± 2.03051
	A	0.92585	1.24587	0.33232	2.09841	3.76746	1.53689	2.75619	2.46592	0.35498	0.15791
		± 0.77134	± 1.27581	± 0.23101	± 0.56275	± 0.48172	± 0.23522	± 0.24959	± 0.2787	± 0.05894	± 0.02349
Ma	xc	620	633.74797	640.69468	649.74823	664.08294	670.69474	676.68679	681.77687	695	710
		± 2.07458	± 2.24115	± 0.23617	± 0.41182	± 0.27332	± 0.09671	± 0.08089	± 0.43553	±0.6323	± 1.04854
	w	12.71792±	14.04992±	6.55154	10.27785±	12	6.35416	6.69345	11.54893±	14.29706±	13.73827
		3.15696	7.78694	± 0.97734	0.68053	± 0.97246	± 0.19368	± 0.22472	0.63445	1.73477	± 0.86779
	A	1.44104	1.46	0.40638	2.56698	4.61218	2.07097	3.00874	6.10689	1.73477	0.595
		± 0.80348	± 1.18006	± 0.29182	± 0.39599	± 0.49637	± 0.29109	± 0.48436	± 0.73339	± 0.29764	± 0.10855
T3	xc	620	633.74797	640.69468	649.74823	664.08294	670.69474	676.94604	681.77687	695	710
		± 2.07458	± 2.24115	± 0.23617	± 0.41182	± 0.27332	± 0.09671	± 0.14737	± 0.43553	±0.6323	± 1.04854
	w	14.79864±	14.49524±	7.14029	10.60261	11.55852	6.94731	7.03409	13.27189	19	15.42797
		4.3339	5.97677	± 1.30284	± 0.71266	± 0.77065	± 0.23405	± 0.35704	± 0.58064	± 3.02683	± 0.7333
	A	1.26882	1.11457	0.27426	1.71072	3.42697	1.47127	1.42797	6.66107	2.19778	0.69833
		± 0.64292	± 0.80359	± 0.23584	± 0.23322	± 0.33224	± 0.24028	± 0.36141	± 0.71532	± 0.5486	± 0.24881
Y100	xc	620	633.74797	640.69468	649.74823	664.08294	670.69474	677.50234	681.77687	695	710
		± 2.07458	± 2.24115	± 0.23617	± 0.41182	± 0.27332	± 0.09671	± 0.21552	± 0.43553	±0.6323	± 1.04854
	w	16.44248±	13.16579±	7.65789	12.61952±	10.66721±	7.50237	7.45664	12.71242	21.88148±	15.02179
		5.65177	3.81989	± 2.32097	1.90809	0.88292	± 0.28929	± 0.39606	± 0.48574	7.96583	± 2.84138
	A	2.39991	1.5249	0.29165	2.5278	3.90308	2.45729	2.0665	3.43548	3.17268	0.59421
		±1.10816	± 1.01897	± 0.50283	± 0.45729	± 0.61402	± 0.4322	± 0.56198	± 1.12321	± 1.65602	± 0.79836

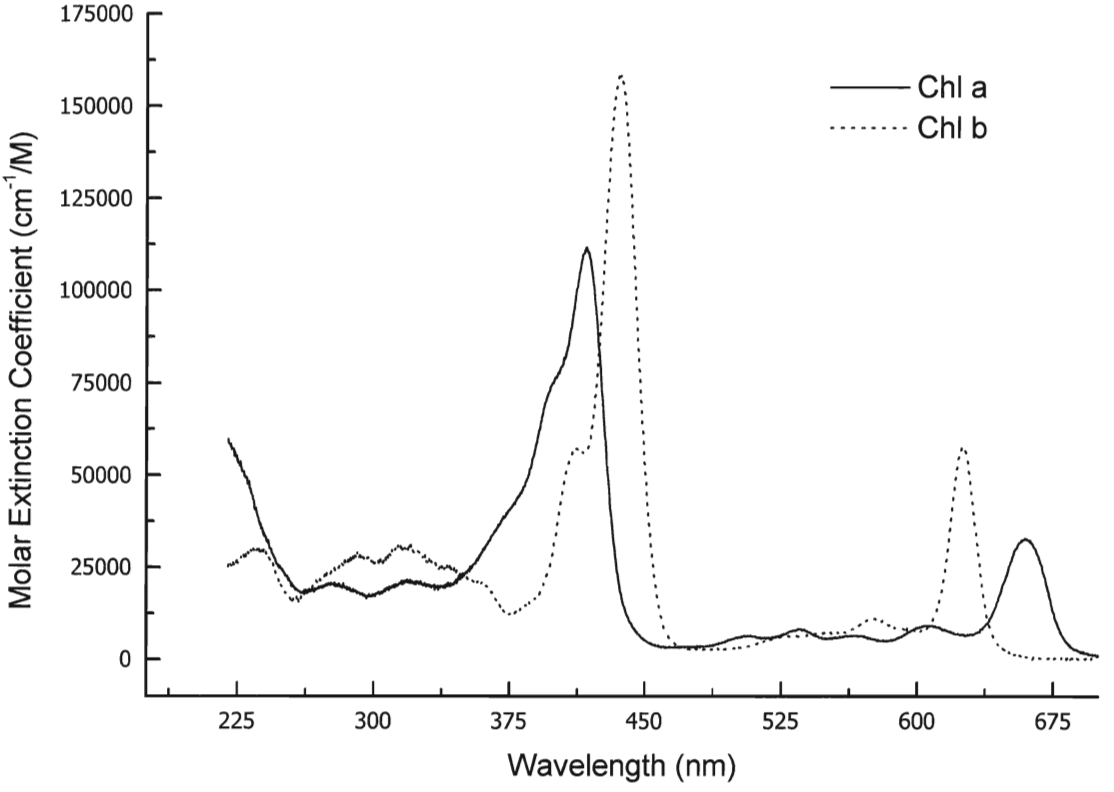

Figure - 54 - Molar extinction coefficients of Chls *a* and *b* (Du *et al.* 1998).

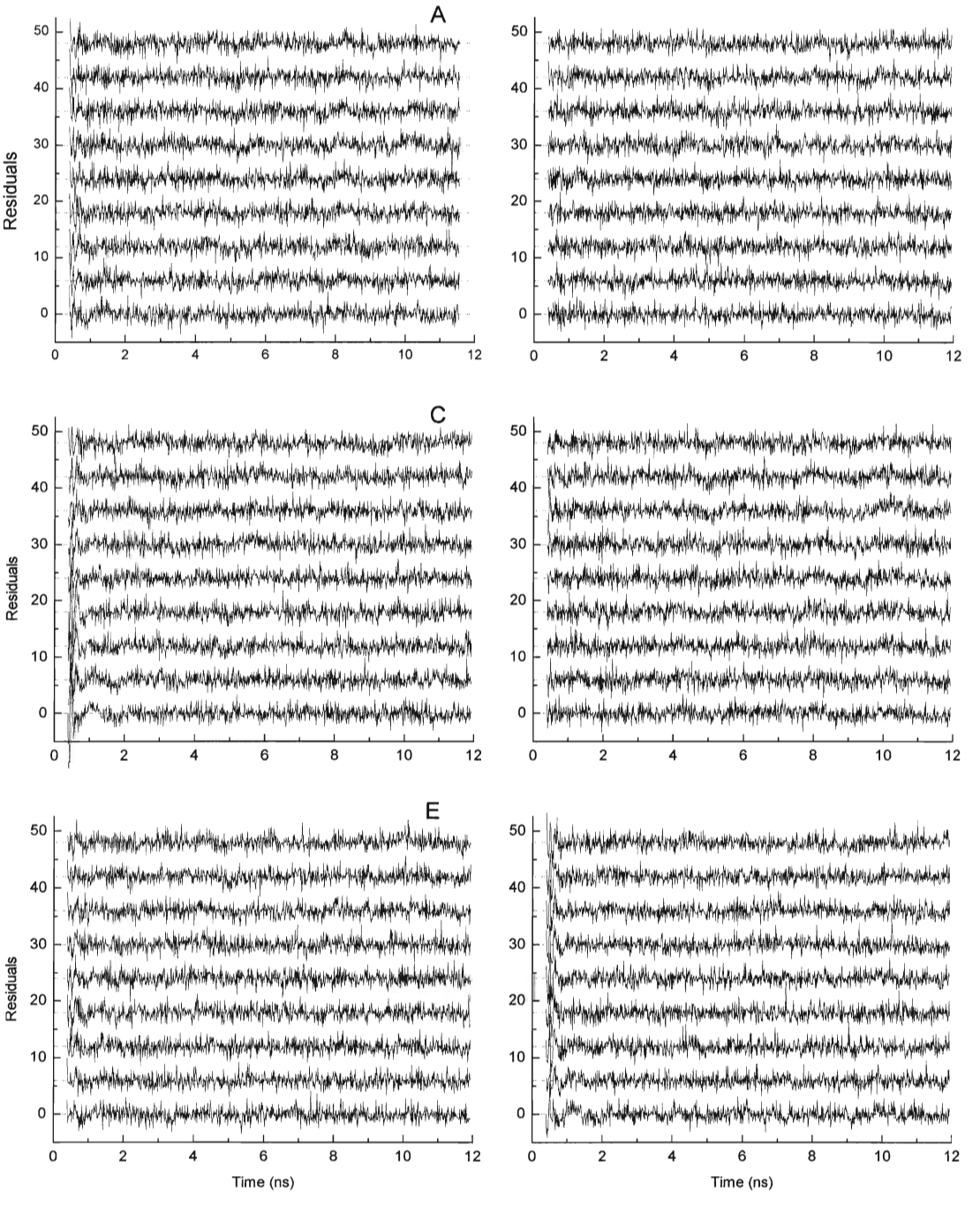

Figure 55- Residuals generated from global analysis of decay kinetics of thylakoid membrane fractions at F_M. χ^2 values for each plot are A) whole thylakoid - 1.216, B) B3 fraction - 1.10, C) T3 fraction - 1.25, D) BS fraction - 1.162, E) Ma fraction - 1.135 and F) Y100 - 1.191. Each residual represents the distribution about the median for each of nine emission wavelengths collected from 675 nm (top) to 730 nm (bottom).

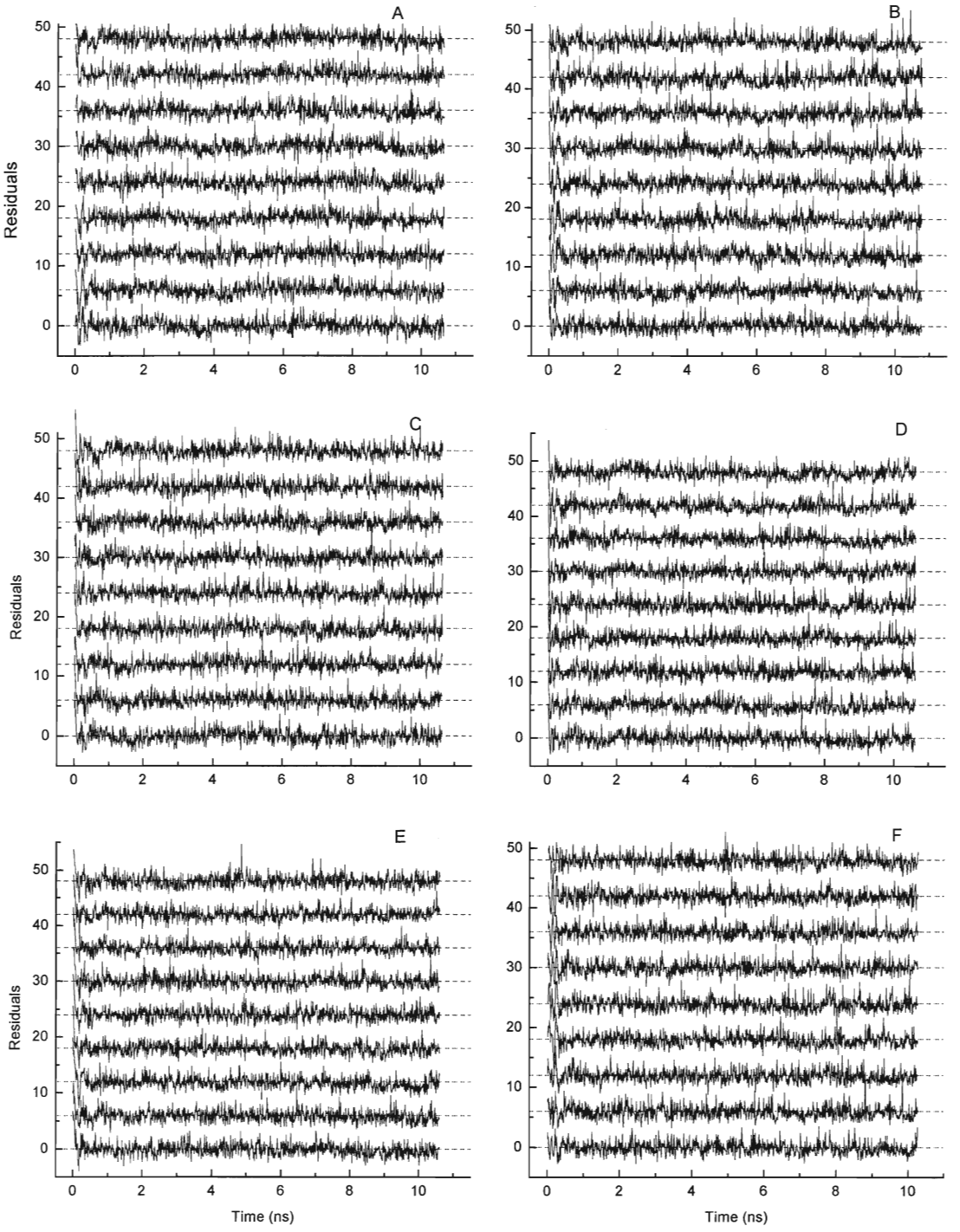

Figure 56- Residuals generated from global analysis of decay kinetics of thylakoid membrane fractions at F_0. χ^2 values for each plot are A) whole thylakoid - 1.18, B) B3 fraction - 1.293, C) T3 fraction - 1.259, D) BS fraction - 1.446, E) Ma fraction - 1.281 and F) Y100 - 1.316. Each residual represents the distribution about the median for each of nine emission wavelengths collected from 675 nm (top) to 730 nm (bottom).